USE OF CREEP COMPLIANCE AND DYNAMIC MODULUS INTERCONVERSION TO EVALUATE FLEXIBLE PAVEMENT PERFORMANCE IN MECHANISTIC EMPIRICAL PAVEMENT DESIGN GUIDE

by

HAMPTON WORTHEY

(Under the Direction of S. Sonny Kim)

ABSTRACT

Response functions of linear viscoelastic (LVE) materials, dynamic modulus (|E*|) and creep compliance (D(t)) are considered primary mechanical property inputs for flexible pavement in the Mechanistic-Empirical Pavement Design Guide (MEPDG). The contents of this thesis investigate the impact of these mechanical properties on the performance of hot-mix asphalt (HMA) pavement layers in Georgia. Tree-based methods are used to predict |E*| using an existing library of HMA mixtures of differing material properties. Subsequently, an LVE interconversion model is developed to determine D(t) estimates using |E*| in favor of laboratory testing. A performance analysis is provided to determine the most sensitive distress outputs associated with these inputs and to identify the potential necessity for a Level 1 creep compliance library. Ultimately, it is found that such design considerations will significantly impact the international roughness index (IRI), rutting, and thermal cracking performance on long-term flexible pavement sections.

INDEX WORDS: flexible pavement, creep compliance, dynamic modulus, tree analysis, LVE interconversion, sensitivity analysis, Pavement ME Design, MEPDG

USE OF CREEP COMPLIANCE AND DYNAMIC MODULUS INTERCONVERSION TO EVALUATE FLEXIBLE PAVEMENT PERFORMANCE IN MECHANISTIC EMPIRICAL PAVEMENT DESIGN GUIDE

by

HAMPTON WORTHEY

B.S., The University of Georgia, 2019

A Thesis Submitted to the Graduate Faculty of The University of Georgia in Partial Fulfillment of the Requirements for the Degree

MASTER OF SCIENCE

ATHENS, GEORGIA

2020

USE OF CREEP COMPLIANCE AND DYNAMIC MODULUS INTERCONVERSION TO EVALUATE FLEXIBLE PAVEMENT PERFORMANCE IN MECHANISTIC EMPIRICAL PAVEMENT DESIGN GUIDE

by

HAMPTON WORTHEY

Major Professor: S. Sonny Kim

Committee: Stephan A. Durham

Mi Geum Chorzepa

Jidong J. Yang

Electronic Version Approved:

Ron Walcott

Interim Dean of the Graduate School

The University of Georgia

May 2020

ACKNOWLEDGEMENT

The author would like to acknowledge those who provided valuable contributions towards the completion of this report. Dr. S. Sonny Kim acted as mentor to the author, providing guidance and expertise throughout the duration of the project. Committee members, Dr. Stephan A. Durham, Dr. Jidong Yang, and Dr. Mi Geum Chorzepa deserve special recognition for their valuable input and support towards the project's completion. Dr. Hyung Suk Lee for assisting the author and associates with viscoelastic theory application. Special thanks are owed to Ryan Romeo, without whose efforts the interconversion would not have been possible. Finally, on behalf of the University of Georgia, the author would like to acknowledge the Georgia Department of Transportation for the opportunity and financial support required to develop this thesis.

TABLE OF CONTENTS

LIST OF TABLES

LIST OF FIGURES

1.0 INTRODUCTION

Current pavement design methodology for many state Department of Transportation agencies is conducted under the 1972 AASHTO Interim Guide for Design of Pavement Structures. While this guide has been in use for over 20 years, the empirical data used to develop the software were derived from procedures conducted during the 1950's.

In an effort to improve these dated guidelines, the Mechanistic Empirical Pavement Design Guide (MEPDG) was developed. The MEPDG aims to provide a more complete pavement design methodology by implementing mechanistic-empirical based inputs for pavement layers, material properties, traffic loadings, climate conditions, and more. These inputs are structured on a basis of hierarchical levels (1, 2, and 3) that provide the engineer with flexibility over the accuracy of their design. Among these inputs are dynamic modulus and creep compliance, the primary mechanical properties of asphalt materials and characterizations of hot mix asphalt (HMA) viscoelastic behavior.

Dynamic modulus is defined as the stress/strain response under dynamic loading and is considered the principal stiffness measurement of HMA. As a result, it a highly regarded performance metric for pavement design applications and remains a premier input in all three design input levels of the MEPDG. Specifically, dynamic modulus is relied upon to determine load-induced distresses such as longitudinal cracking, alligator cracking, and pavement rutting.

Conducted under AASHTO TP107, dynamic modulus determination may be a difficult and expensive procedure to perform in the laboratory. Overtime an abundance of historic laboratory-tested dynamic modulus has led to the generation of a variety of accurate prediction models. These models often prove sufficient for global applications, but the wide array of asphalt material properties limits their precision when evaluating project-specific samples. Therefore, among the objectives of this study is the development of a tree-based regression model for dynamic modulus prediction using an existing library of Georgia-specific asphalt mixtures. These efforts intend to provide supplemental value to the existing materials library utilized in pavement design practices in Georgia.

Creep compliance is the ratio of time-dependent strain to the applied constant stress. It is a material property that illustrates low temperature cracking behavior of asphalt mixtures and is a primary input to predict the thermal/transverse cracking of flexible pavement in Pavement ME Design (PMED). Creep compliance is determined in the laboratory through AASHTO T322, "Standard Method of Test for Determining the Creep Compliance and Strength of Hot Mix Asphalt (HMA) Using the Indirect Tensile Test Device (IDT)".

Creep compliance is used to predict HMA thermal cracking at low temperatures and permanent deformation at high temperatures. The prediction of thermal cracks is important because the predicted transverse cracks have an impact on the International Roughness Index (IRI) calculation in PMED. PMED predicts transverse cracks based on a thermal event or mechanism (i.e., shrinkage). However, using the previous global calibration values derived under the NCHRP 1-40D project, PMED never predicts any transverse cracks although Georgia exhibits transverse cracks in flexible pavements.

Recently, new calibration coefficients were derived under the Mean Annual Air Temperature (MAAT) dependent global calibration process. To use the MAAT-dependent calibration coefficients in PMED, creep compliance for asphalt mixture is essential. With MAAT-dependent calibration coefficients and creep compliance of asphalt mixtures, transverse cracking can be predicted for use in the IRI regression equation.

Determining the creep compliance provides valuable information in regard to long-term pavement performance and expected permanent deformations. As a result, it remains a valuable input for flexible pavement design in the MEPDG. However, due to the complexity of laboratory testing and expense of required equipment, it is advantageous to instead determine creep compliance from other material properties using viscoelastic models. In this study, mathematic processes are utilized to convert a pre-existing library of dynamic modulus (|E*|) values to creep compliance values (D(t)) for a set of Georgia asphalt mixtures. This method permits the use of converted creep compliance values as a Level 2 input for pavement design using MEPDG. To determine the effectiveness of this approach, a PMED performance analysis is also conducted. The predicted distress outputs for a design incorporating measured dynamic modulus values (Level 1) are analyzed against designs using converted creep compliance values (Level 2) and global default values (Level 3) using PMED.

The results of this investigation aim to provide state highway agencies with valuable resources necessary for MEPDG implementation. Conversion to the MEPDG from the empirical pavement design guide represents a paradigm shift in modern pavement design, opening the door for superior pavement development across the United States.

2.0 BACKGROUND IN GEORGIA

Implementation of the MEPDG for state DOT agencies is a lengthy, multi-step process that requires local calibration, operational processes integration, traffic and climate data collection, material database development, and more. GDOT is among the state highway agenies conducting such efforts to improve their current practices, conducted under the 1972 AASHTO Interim Guide for Design of Pavement Structures. These efforts were supported by several cooperating agencies such as Applied Research Associates (ARA) and local universities including the University of Georgia (UGA). The following sections summarize relevant work currently developed for Georgia MEPDG implementation, with respect to flexible pavement design.

A significant GDOT implementation milestone involved local calibration of MEPDG analysis parameters. The standard MEPDG distress transfer functions and prediction methodologies were calibrated using data from the Long Term Pavement Performance (LTPP) program under the National Cooperative Highway Research Program (NCHRP). In a report submitted by ARA, the transfer functions were validated, or in some cases, re-calibrated to more accurately represent the performance of Georgia roadways (Von Quintus et al., 2016). The study investigated 32 LTPP flexible pavement sections with full time series data and 15 without. To further populate the sampling templates and include roadways that exhibited high distress levels, an additional 19 non-LTPP sections were included in the analysis. Soil class is more important relative to flexible pavement performance in comparison to rigid pavement performance, so a variety of soil class types above and below the “fall line” were also included in the flexible testing matrix (Von Quintus et al., 2016).

The results of ARA’s investigation suggest a sufficient number of test sections were available and used to derive the calibration coefficients of the fatigue cracking, rut depth, and transverse cracking transfer functions, as well as the IRI regression equation for new flexible pavements and HMA overlays (Von Quintus et al., 2016). Table 2.1 summarizes the modified calibration factors proposed to GDOT based on their results. After calibration, ARA provided additional resources, such as *The GDOT Pavement ME Design User Input Guide* to promote further implementation efforts (ARA, 2015). This document guides new pavement engineers through the PMED input selection process for both flexible and rigid new and overlay designs.

The expansion of GDOT’s pavement materials library is another primary contribution to MEPDG implementation in Georgia. Under GDOT Research Project (RP) 12-07 conducted by Kim (2013), the dynamic moduli of Georgia asphalt mixtures were measured using Job Mix Formulas from 2 GDOT Highway Contractor plants with 3 different nominal maximum aggregate sizes (NMAS) (25mm, 19mm, and 12.5mm) and 2 types of binder grades (PG 64-22 and PG 67-22). This combination yielded 36 asphalt mixtures with varying air void percentages and bulk specific gravities. A summary of the mixture properties is listed in Table 2.2.

Dynamic modulus (|E*|) testing was conducted for each mixture combination and the master curves were developed. A typical increase in |E*| as loading frequency increases and decrease in |E*| as temperature increases was observed during analysis (Kim, 2013). Figure 2.1 shows an example master curve generated from this data for a Plant A mixture with PG 64-22. The resulting dynamic modulus database was compiled for the GDOT material testing library and can be imported into the MEPDG software in accordance with the MEPDG Software Manual (ARA, 2015).

Table 2.1. Transfer Function Coefficients (Von Quintus et al., 2016)

Asphalt Concrete Rut Depth			
Transfer Function Coefficient	**Global Value**	**GDOT Value**	
		Neat Mixtures	**PMA Mixtures**
K1	-3.35412	-2.45	-2.55
K2	1.5606	1.5606	1.5606
K3	0.4791	0.30	0.30
Std. Deviation	0.24*Pow(RD,0.80519)+0.001	0.20*Pow(RD,0.55)+0.001	
RD = Average rut depth predicted by the Pavement ME Design software.			
Unbound Layer Rut Depth			
Transfer Function Coefficient	**Global Value**	**GDOT Value**	
Coarse-Grained, Bs1	1.00	0.50	
Fine-Grained, Bs1	1.00	0.30	
Flexible Pavement Bottom-Up Faigue Cracking			
Transfer Function Coefficient	**Global Value**	**GDOT Value**	
		Typ. HMA Mixtures	**High RAP; Older Mixes**
K1	0.007566	0.00151	0.000757
K2	3.9492	3.9492	3.9492
K3	1.281	1.281	1.281
C1	1.00	2.20	2.20
C2	1.00	2.20	2.20
C3	6,000	6,000	6,000
Std. Deviation	$1.13 + \frac{10}{(1 + Exp(7.57 - 15.5 * Log10(DI_{Bottom} + 0.0001))}$	$1.0 + \frac{10}{(1 + Exp(7.5 - 6.5 * Log10(DI_{Bottom} + 0.0001))}$	
DI_Bottom = Damage index for bottom up fatigue or alligator cracking.			

Table 2.2. RP 12-07 HMA Mixture ID and Volumetric Characteristics (Kim, 2013)

	Mix ID	%AV	Gmb
Plant A	12.5mm_PG64_SP1	4.28	2.44
	12.5mm_PG64_SP2	3.81	2.45
	12.5mm_PG64_SP3	4.21	2.44
	12.5mm_PG67_SP1	4.36	2.45
	12.5mm_PG67_SP2	3.93	2.46
	12.5mm_PG67_SP3	4.09	2.46
	19mm_PG64_SP1	4.06	2.48
	19mm_PG64_SP2	3.72	2.49
	19mm_PG64_SP3	3.99	2.48
	19mm_PG67_SP1	4.18	2.49
	19mm_PG67_SP2	4.17	2.49
	19mm_PG67_SP3	3.60	2.50
	25mm_PG64_SP1	4.45	2.47
	25mm_PG64_SP2	4.25	2.48
	25mm_PG64_SP3	3.91	2.49
	25mm_PG67_SP1	4.47	2.49
	25mm_PG67_SP2	3.56	2.51
	25mm_PG67_SP3	3.93	2.50
Plant B	12.5mm_PG64_SP1	4.47	2.41
	12.5mm_PG64_SP2	4.47	2.41
	12.5mm_PG64_SP3	4.40	2.41
	12.5mm_PG67_SP1	4.42	2.41
	12.5mm_PG67_SP2	4.36	2.41
	12.5mm_PG67_SP3	4.36	2.41
	19mm_PG64_SP1	4.49	2.42
	19mm_PG64_SP2	4.29	2.42
	19mm_PG64_SP3	4.10	2.43
	19mm_PG67_SP1	4.06	2.43
	19mm_PG67_SP2	4.08	2.43
	19mm_PG67_SP3	4.11	2.43
	25mm_PG64_SP1	3.73	2.45
	25mm_PG64_SP2	4.34	2.44
	25mm_PG64_SP3	4.20	2.44
	25mm_PG67_SP1	3.93	2.45
	25mm_PG67_SP2	3.58	2.46
	25mm_PG67_SP3	3.59	2.46

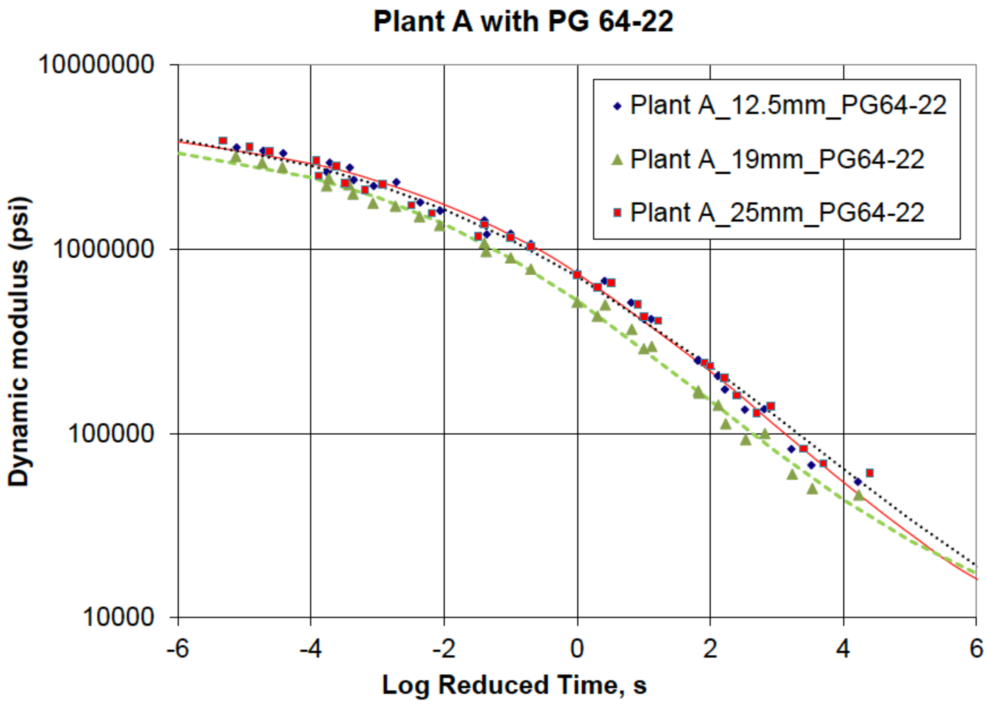

Figure 2.1. RP 12-07 Master Curve (Plant A JMF with PG 64-22) (Kim, 2013)

Kim (2013) also recorded the resilient modulus (M_R) for 11 sources of graded aggregate base (GAB) material and 9 sources of subgrade soil gathered from varying counties across Georgia. The material properties for both the GAB and subgrade samples are found in Tables 2.3 and 2.4, respectively. Repeated load triaxial test was performed on the GAB and subgrade specimens to investigate the factors affecting M_R and correctly characterize material behavior. The results suggest a correlation between improved stiffness properties and increased stress magnitude for GAB, possibly attributed to the reduction in air voids and thus greater friction forces between aggregate particles (Kim, 2013). Further, Kim (2013) showed a decrease in subgrade M_R as fine content (passing #200 sieve) increased along with the expected decrease in M_R at high deviatoric stress and low confining stress.

Table 2.3. RP 12-07 Aggregate Sources and Physical Properties (Kim, 2013)

QPL ID	Aggregate Group	Source Location	GAB Character	W_{opt} (%)	Max. γ_d (pcf)	W_{actual} (%)	Actual γ_d (pcf)	Percent Compaction	LA Abrasion (%)	Bulk Specify Gravity
011C	II	Lithonia	Granite Gneiss	5.7	133.9	4.3	133	99	50	2.614
013C	I	Dalton	Limestone	6.6	142.5	4.7	139	98	25	2.702
024C	II	Gainesville	Mylonitic Gneiss	6	136.6	6.7	134	98	39	2.605
028C	II	Hitchcock	Mylonitic Gneiss	6.2	141.2	5.6	138	98	18	2.697
050C	II	Stockbridge	Granite Gneiss	5.9	134.2	5.9	134	100	42	2.611
101C	II	Demorest	Meta-sandstone	5.3	137.4	5	137	100	32	2.642
108T	I	Mayo Mine	Lime rock	13.6	112.6	11.5	110	98	N/A	N/A
118C	II	Columbus	Granite Gneiss	6	137.2	6.5	135	98	33	2.677
141C	II	Dahlonega	Granite Gneiss	5.6	135.2	4	132	98	34	2.646
158C	II	Walton County	Biotite Gneiss	6.4	135	4.5	132	98	41	2.64
165T	II	I-75 Unadilla	Recycled Concrete	7	134	8.5	131	98	N/A	N/A

Table 2.4. RP 12-07 Subgrade Sources and Physical Properties (Kim, 2013)

Subgrade No.	Location (County)	Percent Passing (%)				% Clay	% Volume Change	% Swell	% Shrink	Max. Dry Density (pcf)	Opt. Moisture Content (%)	LL (%)	PI (%)	Eros Index	GA Soil Class	USCS Soil Class	AASHTO Soil Class
		#10	#40	#60	#200												
1	Lincoln	99.3	96.8	93.8	48.9	40.7	24.5	20.5	4.0	93.4	23.5	39.9	8.6	4.23	IIB4	SC	A-4
2	Washington	99.8	84.6	56.1	23.8	20.6	4.7	4.5	0.2	117.8	11.0	23.0	6.6	7.30	IIB2	SM	A-2-4
3	Coweta	89.5	64.6	48.9	28.3	24.0	12.2	11.2	1.0	105.3	16.7	42.5	11.0	6.69	IIB3	SC	A-2-7
4	Walton	89.4	61.5	50.5	36.3	28.3	4.0	1.0	3.0	104.8	16.8	40.5	12.7	5.71	IIB4	SC	A-7-6
5	Chatham	99.9	97.4	93.5	3.6	1.8	0.0	3.6	0.0	97.4	12.7	0.0	0.0	9.76	IIB4	SM	A-2-4
6	Lowndes	99.0	74.9	52.9	12.2	4.5	0.0	0.0	0.0	113.1	4.7	0.0	0.0	8.65	IA2	SP	A-2-4
7	Franklin	97.3	89.4	70.9	31.1	19.6	5.2	3.0	2.2	105.1	22.6	39.3	9.8	6.32	IIB3	SC	A-2-4
8	Cook	79.9	66.4	46.6	25.0	18.4	0.6	0.6	0.0	113.1	9.9	0.0	0.0	7.06	IIB2	SM	A-2-4
9	Toombs	84.2	37.8	17.6	6.2	4.6	1.1	0.1	1.0	119.3	11.9	0.0	0.0	9.39	IA1	SP	A-1-b

The results of RP 12-07 confirmed an expected discrepancy between the global default values for MEPDG unbound aggregate and subgrade soil properties and those observed in the Georgia specimens. Included in Kim's (2013) research are artificial neural networks (ANN) models that present more accurate estimations of resilient modulus for GAB and subgrade given their basic physical properties. The database developed for this report was later adopted by GDOT for inclusion in *The GDOT Pavement ME Design User Input Guide* (ARA, 2015).

Following the efforts of RP 12-07, additional research was conducted under RP 14-12 to investigate the effect of recycled asphalt pavement (RAP) contents and sources on the dynamic modulus and the performance of Georgia asphalt concrete mixtures (Kim et al., 2016). This topic was investigated on the basis of NCHRP's claim that RAP content and source significantly affect |E*| and pavement performance, proving significant for MEPDG designs. To verify this claim, asphalt mixtures were developed using two Georgia mixing plants with 12.5mm NMAS and three types of binder grades (PG 64-22, PG 67-22, and PG 76-22). The associated asphalt mixture summary is found in Table 2.5, where COAC refers to corrected optimum asphalt content.

Several conclusions were drawn from the dynamic modulus results and master curves for these specimens. Mainly, it was observed that |E*| tends to increase as RAP % increases (up to 30%) due to the added stiffness provided by the recycled materials. It was also seen that |E*| increases as binder grade increases. This held true for all temperatures and frequencies. The observations were verified through statistical analyses and the RAP % and binder grade were considered significant influencers on asphalt dynamic modulus (Kim et al., 2016).

Table 2.5. RP 14-12 COAC Summary (Kim et al., 2016)

Mixture	%RAP	Binder	OAC(%)	RAP AC(%)	COAC(%)
Superpave	0%	PG64-22	5.30	N/A	5.30
		PG67-22	**5.30**	**N/A**	**5.30**
		PG76-22	5.30	N/A	5.30
	15%	PG64-22	5.10	5.05	5.30
		PG67-22	5.10	5.05	5.30
		PG76-22	5.10	5.05	5.30
	25%	PG64-22	4.96	5.05	5.52
		PG67-22	**4.96**	**5.05**	**5.52**
		PG76-22	**4.92**	**5.05**	**5.52**
	30%	PG64-22	**5.03**	**5.09**	**5.41**
		PG67-22	5.03	5.09	5.41
		PG76-22	**5.03**	**5.09**	**5.41**
SMA	0%	PG76-22	**6.20**	**N/A**	**6.20**
	15%	PG76-22	**6.45**	**5.28**	**6.65**
Superpave	0%	PG64-22	5.10	N/A	5.10
		PG67-22	**5.10**	**N/A**	**5.10**
		PG76-22	**5.27**	**N/A**	**5.27**
	15%	PG64-22	4.84	4.46	5.20
		PG67-22	**4.84**	**4.46**	**5.20**
		PG76-22	**5.30**	**4.46**	**5.47**
	25%	PG64-22	**5.00**	**4.80**	**5.30**
		PG67-22	5.00	4.80	5.30
		PG76-22	**5.07**	**4.98**	**5.38**
SMA	10%	PG76-22	**6.35**	**4.46**	**6.46**

The RP 14-12 research group also conducted fatigue performance and performance evaluation procedures to determine the effect of RAP on pavement durability. The results indicate that the addition of RAP up to 25% using GDOT's COAC method significantly improve the fatigue resistance (Kim et al., 2016). No difference in fatigue resistance was seen across PG 64-22 and PG 67-22 binder grades but improvements over both were seen with PG 76-22. Using PMED, the distress predictions across PG 64-22 and PG 67-22 designs remained largely unchanged with the exception of rut depth (Kim et al., 2016).

More recently, Kim et al. (2019) broadened the dynamic modulus database for Georgia MEPDG through RP 16-19. This project looked to enhance the work established in RP 12-07 and RP 14-12 by adding polymer-modified asphalt (PMA) mixtures and additional aggregate resources to the dynamic modulus database. Table 2.6 provides a list of the studied asphalt mixtures and their physical properties. This report also included an examination of material characteristics effects on dynamic modulus and fatigue cracking. Three fatigue test methods were performed for comparison—the cyclic direct tension test based on the simplified-viscoelastic continuum damage (S-VECD) model, the semicircular bend (SCB) test, and the modified overlay test (OT) (Kim, et al., 2019).

Consistent with the results achieved by Kim et al. (2016), the dynamic modulus increased as the RAP % increased for the mixtures found in Table 2.6. And once again, |E*| gathered from PG 76-22 mixtures was greater than those gathered from PG 64-22 and PG 67-22, but no difference was seen between the latter. New conclusions showed dynamic modulus was not significantly different between NMAS of 9.5mm and 12.5mm or 19mm and 25mm, but variation was evident between 12.5mm and both 19mm and 25mm (Kim et al., 2019). Per the fatigue cracking analysis, the SCB and S-VECD methods are both recommended over the modified overlay test. Though they show conflicting results on the effect of PMA binders—SCB suggesting it lowers fatigue resistance and S-VECD suggesting it increases. One would expect to see PMA improve fatigue resistance, thus, the cyclic direct tension test with S-VECD model is preferred for future pavement performance evaluation.

The work developed under RP 14-12 and RP 16-19 have yet to be integrated into *The GDOT Pavement ME Design User Input Guide*. Efforts to adopt these results are currently ongoing.

Table 2.6. RP 16-19 Plant Produced Mixture Properties (Kim et al., 2019)

Specimen_ID	NMAS (mm)	Binder Grade	RAP (%)	Binder (%)	G_{mm}	Air Void (%)	VMA (%)	VFA (%)	Effective Binder (%)	Test Performed
A 19_64_N1	19	PG 64-22	25	4.6	2.545	5.5	14.7	68.8	10.1	$\|E^*\|$
A 25_64_N1	25	PG 64-22	25	4.3	2.542	5.5	15.0	65.1	9.8	$\|E^*\|$
A 12.5_67_N	12.5	PG 67-22	30	5.52	2.466	6.3	18.0	65.3	11.8	$\|E^*\|$, OT
A 12.5_76_N	12.5	PG 76-22	30	5.41	2.549	5.7	18.4	68.7	12.6	$\|E^*\|$, SVECD, SCB
A 19_64_N2	19	PG 64-22	30	5.25	2.501	5.5	17.1	68.0	11.6	$\|E^*\|$, SVECD
A 25_64_N2	25	PG 64-22	30	5.20	2.513	5.5	16.7	67.3	11.2	$\|E^*\|$
B 9.5_64_M1	9.5	PG 64-22	30	5.90	2.447	6.5	19.3	65.2	12.6	$\|E^*\|$, OT
B 9.5_64_M2	9.5	PG 64-22	30	5.60	2.498	6.4	18.1	64.3	11.6	$\|E^*\|$, SVECD
C 9.5_67_M	9.5	PG 67-22	30	5.63	2.494	5.5	17.8	72.9	12.9	$\|E^*\|$, SCB, OT
A 12.5_64_M2	12.5	PG 64-22	30	5.40	2.468	5.6	17.7	68.7	12.2	$\|E^*\|$, SVECD, SCB, OT
A 12.5_64_M1	12.5	PG 64-22	30	5.50	2.459	5.5	17.7	70.7	12.5	$\|E^*\|$, SVECD, SCB
B 12.5_64_M	12.5	PG 64-22	30	5.50	2.463	5.6	18.0	69.2	12.5	$\|E^*\|$
C 12.5_67_M	12.5	PG 67-22	30	5.68	2.526	5.8	17.3	66.3	11.5	$\|E^*\|$, SVECD, OT
C 12.5_76_M	12.5	PG 76-22	15	5.10	2.477	5.5	16.8	68.6	11.5	$\|E^*\|$, OT
B 19_64_M	19	PG 64-22	30	4.70	2.529	5.5	15.8	66.3	10.5	$\|E^*\|$, SVECD
B 25_64_M	25	PG 64-22	30	4.40	2.554	5.9	15.3	61.4	9.4	$\|E^*\|$
B 9.5_67_S	9.5	PG 67-22	25	5.84	2.454	5.6	18.4	69.4	12.8	$\|E^*\|$, SCB, OT
B 12.5_67_S	12.5	PG 67-22	25	5.40	2.468	6.0	18.1	66.8	12.1	$\|E^*\|$, SVECD, SCB
D 12.5_76_S	12.5	PG 76-22	25	5.37	2.483	5.6	17.5	68.1	11.9	$\|E^*\|$. SVECD, SCB OT

Note: Specimen ID labeled as X ##_##_X denotes Plant Source, NMAS, Binder Type, and Location.

3.0 LITERATURE REVIEW

3.1 History of AASHTO Pavement Design Guides

The American Association of State Highway Officials (AASHO) was founded in 1914 with the goal of shaping highway legislation, policy, and standards for the growing U.S. transportation network. In 1958, under the administration of the Highway Research Board (HRB), AASHO began what would become the largest road experiment of its time, the AASHO Road Test. The objective of this study was to evaluate the performance of pavement and bridge structures of known characteristics under moving loads of known magnitude and frequency (HRB, 1961). Located in Ottawa, Illinois, the test facility housed 6 two-lane loops that experienced more than 1,114,000 axle loads over the course of the two-year experiment. The results of the test provided AASHO with a catalog of design materials, pavement thicknesses, load applications, traffic rates, construction techniques, and climatic conditions, along with a new unit of measurement for vehicle loads, the equivalent single axle load (ESAL) (HRB, 1961).

Following the events of the AASHO Road Test, a subcommittee of the AASHO Operating Committee on Design used the experiment's findings to develop the *AASHO Interim Guide for the Design of Flexible Pavement Structures* in 1961 and the *AASHO Interim Guide for the Design of Rigid Pavement Structures* in 1962. These guides, issued as separate documents, were to be tested alongside existing state procedures for a 1-year trial. Following this period, the documents did not experience major revisions until a decade later when they were published together as the *AASHO Interim Guide for the Design of Pavements (1972)*. Although the pavement design methods for this document did not change from 1962 to 1972, additional material was added to facilitate implementation (TRB, 2007).

In 1973, AASHO changed its name to the American Association of State Highway and Transportation Officials (AASHTO), reflecting its desire to represent all modes of U.S. transportation. The design guide experienced minor revisions to the rigid pavement design sections in 1981 and major revisions to both rigid and flexible designs in 1986. These additions implemented or improved upon the topics of pavement reliability, resilient modulus testing procedures, function of environmental factors, subbase erosion, load equivalency values, pavement rehabilitation, traffic data, pavement management, and more (AASHTO, 2015b). Subsequent revisions were made to the overlay design procedure and were incorporated in the development of the *AASHTO Guide for the Design of Pavements (1993)*. This guide features a new set of pavement design equations that reflect the inclusion of subgrade resilient modulus and reliability as design criteria. Equation 3.1 and represents the 1993 design equation for asphalt concrete pavements.

$$\log(W_{18}) = Z_R \times S_0 + 9.36\log(SN+1) - 0.20 + \frac{\log\left(\frac{\Delta PSI}{4.2-1.5}\right)}{0.40+\frac{1094}{(SN+1)^{5.19}}} + 2.32\log(M_R) - 8.07 \quad (3.1)$$

where:

W_{18}	=	predicted number of 18-kip equivalent single axle load applications
Z_R	=	standard normal deviate
S_0	=	combined standard error of the traffic prediction and performance prediction
ΔPSI	=	difference between the initial design serviceability index, p_0, and the design terminal serviceability index, p_t
M_R	=	resilient modulus (psi)

a_i = i^{th} layer coefficient

D_i = i^{th} layer thickness (in.)

m_i = i^{th} layer drainage coefficient

k = modulus of subgrade reaction (pci)

Since 1993, the design guide has remained relatively unchanged with the exception of the 1998 *Supplement to the AASHTO Guide for Design of Pavement Structures*. The 1998 supplement was developed using data gathered from the National Cooperative Highway Research Program (NCHRP) Project 1-30 and the long-term pavement performance (LTPP) program to improve the rigid pavement design process (AASHTO, 2015b). Table 3.1 presents a summary of the AASHTO pavement design publications between 1961 and 1998. After 1998, efforts to improve the pavement design guide have largely focused on the utilization of a mechanistic-empirical approach. Although the idea of a mechanistic-empirical based approach existed much earlier, technology, data collection, data analysis, and pavement testing has limited its feasibility. For these reasons, many state DOTs continue to practice under the 1993 AASHTO Design Guide.

Table 3.1. Summary of AASHTO Publications (GDOT Pavement Design Guide, 2005)

Date	Publication	Major Advancement
1961	Interim Guide for the Design of Rigid and Flexible Pavement Structures	Established a modern, consistent pavement design system
1972	AASHTO Interim Guide for Design of Pavement Structures	Added information based on subsequent research and experience
1981	AASHTO Interim Guide for Design of Pavement Structures	Revision of the Portland Cement Concrete Pavement Design
1986	AASHTO Guide for Design of Pavement Structures	Guide Officially Adopted by AASHTO including a new section on rehabilitation

Date	Publication	Major Advancement
1993	AASHTO Guide for Design of Pavement Structures	Changes to the Overlay Design Procedure and the addition of 14 new design considerations
1998	Supplement to the AASHTO Guide for Design of Pavement Structures	Improvement to the Rigid Pavement Design performance models

3.2 Mechanistic-Empirical Pavement Design Guide

While the 1958 AASHO Road Test and subsequent Pavement Design Guides were a significant breakthrough for pavement design within the U.S., they are not without their limitations. The effectiveness of these guides is called into question when considering their deficiencies in areas such as traffic loading, rehabilitation, climatic effects, subgrade variability, material database, drainage effects, design life, and reliability (NCHRP, 2004). To improve these practices, the AASHTO Joint Technical Committee on Pavements introduced a mechanistic-empirical based approach to pavement design in 1998 under NCHRP Project 1-37A. The result was the development of the *Guide for the Design of New and Rehabilitated Pavement Structures (1998-2004)* and related software. In an effort to facilitate implementation, AASHTO published an interim version of the design guide entitled, *AASHTO Mechanistic-Empirical Pavement Design Guide (MEPDG), A Manual of Practice (2008)* a few years later.

The MEPDG and related software provide a new, theoretically more grounded methodology for the analysis and performance prediction of different types of pavements. The design process includes a more robust system of input parameters that define the pavement materials, layers, and design features as well as traffic loads and climate conditions. Pavement performance is evaluated based on outputs such as terminal IRI, deformation, cracking, rutting, and other distresses predicted by the MEPDG. Advancements also include procedures for evaluating existing pavements and recommendations for rehabilitation treatments, drainage, and foundation improvements (Li, et al. 2007).

The most recent product of NCHRP Project 1-37A and MEPDG development was the introduction of AASHTOWare® Pavement ME Design™ software in 2011. The purpose of this software is to provide pavement engineers with a design platform that incorporates the mechanistic-empirical approach. This is accomplished by using a hierarchical series of detailed traffic, environmental, and material inputs in conjunction with nationally or locally calibrated models to assess the predicted performance of the pavement over the desired lifetime (AASHTO, 2015b). To highlight some of the most important input parameters, the following sections contain a brief overview of relevant design considerations for a flexible pavement within PMED.

3.2.1 PMED Input Level Hierarchy

The MEPDG and PMED software provide a fundamental input hierarchy that is not utilized in the previous AASHTO design guides (NCHRP, 2004). Inputs are structured on a basis of three levels (1, 2, and 3) that provide the engineer with flexibility over the accuracy and conservatism of their design. A brief outline of the input levels is depicted in Table 3.2. Inputs considered under this hierarchy include traffic, materials, and environmental factors.

Level 1 inputs represent values gathered from site-specific or laboratory conducted tests. This may include procedures such as resilient modulus, dynamic modulus, elastic modulus, compressive strength, falling weight deflectometer (FWD), etc. The values used in Level 1 designs are directly indicative of the in-situ conditions and, thus, contain the highest level of accuracy and the lowest level of uncertainty. However, Level 1 inputs also require the most time and resources to collect.

Level 2 inputs represent values determined through limited testing, correlation, or database selection. Examples of a Level 2 input may include the use of estimated values (e.g. modulus or strength properties) using predictive equations or using locally accumulated traffic volume data in conjunction with agency-specific axle load spectra. The values used in Level 2 designs are considered less accurate than Level 1, but generally require less time and resources to obtain.

Level 3 inputs represent values determined by typical averages for a region or nationally accepted values. This may include quantities such as the default unbound materials resilient modulus or typical void ratio values for a specific binder-grade. Level 3 inputs provide the lowest level of design accuracy and the highest level of uncertainty but are the most efficient inputs to determine.

Although a design consisting of all Level 1 inputs theoretically provides the most accurate and effective estimation of pavement performance, it is often not feasible to do so. Therefore, it is possible for an MEPDG pavement design to include inputs from across different levels.

Table 3.2. MEPDG Input Hierarchy

Input	Accuracy	Requirements
Level 1	High	Site Specific Laboratory/Field Tested Values
Level 2	Intermediate	Relevant Local Database Correlated/Predicted Values
Level 3	Low	Regional or National Default Values

3.2.2 Flexible Pavement Structure

Flexible pavements are pavements that experience flex under the actions of traffic and rebound when traffic loads are removed (GDOT, 2019). Most often, flexible pavements are defined by the presence of hot-mix asphalt (HMA) material on the surface layer. A typical GDOT flexible pavement consists of the following structure: an infinite or bedrock layer, subbase or subgrade material layer, base course layer, and HMA layers. A visual of this pavement profile is depicted in Figure 3.1. Common base course materials include graded aggregate base (GAB), cement stabilized base, or soil cement depending on the level of traffic loading. Cement stabilized base or soil cement are commonly used in areas that lack quality aggregate sources or experience heavy load applications (Mohammad, Raghavandra, & Huang, 2000). The HMA surface of a flexible pavement generally contains a series of different HMA mixtures—base, binder, and surface. The discrepancy between mixtures is mostly attributed to the NMAS, in which the base mixture contains the largest NMAS and the surface mix contains the smallest.

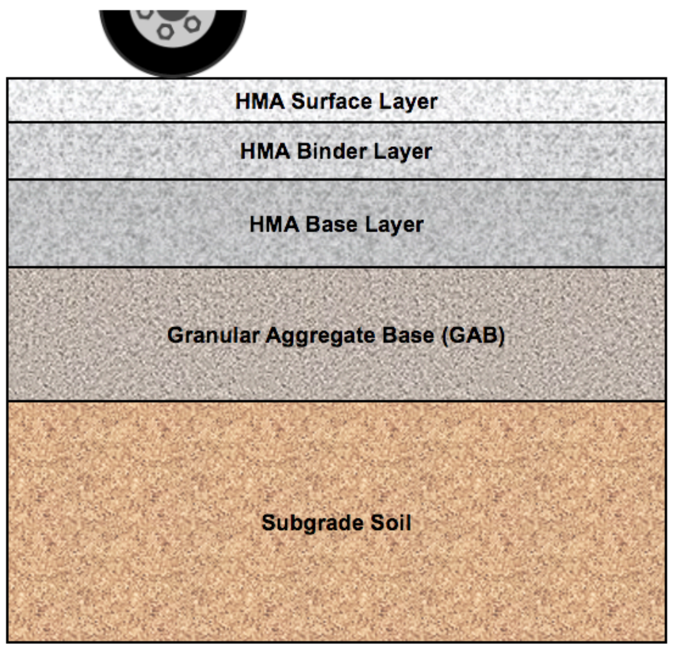

Figure 3.1. Typical GDOT Flexible Pavement Profile

As all pavement layers are considered infinite in the lateral direction, vertical thickness is the primary structural input for pavement designs. In fact, a study conducted by the LTPP program suggests that pavement thickness is the most influential design feature when evaluating the overall performance of rehabilitated flexible pavements when considering other factors such as mixture types and virgin vs. recycled materials (Carvalho et al., 2011).

3.2.3 Mixture Volumetrics

Mixture volume characteristics, or volumetrics, for MEPDG flexible pavement design include air void percentage, effective binder content, Poisson's ratio, and unit weight. Air voids are pockets of air that exist as part of the homogeny of an HMA mixture. The percentage of air voids plays a key role in HMA durability. Properly designed mixtures must contain a high enough air void percentage to prevent permanent deformation due to plastic flow, but not too high so as to prevent permeability (Brown, 2000). Equation 3.2 is used to determine air voids of a compacted HMA specimen.

$$\text{Air Voids } (V_a) = \left(1 - \frac{G_{mb}}{G_{mm}}\right) \times 100 \tag{3.2}$$

where:

G_{mb} = bulk specific gravity

G_{mm} = theoretical maximum specific gravity'

Effective binder content refers to the percentage of bituminous material present in an HMA sample. It is often determined using the ignition method (AASHTO T 308) in which the binder content is calculated as the difference between the initial mass of HMA and the mass of the residual aggregate, moisture content, and a correction factor. Similar to air voids, binder content effects the long-term performance and permanent deformation experience by flexible pavements. An increase in binder content has shown to decrease HMA cracking, while reducing the dynamic modulus and rutting resistance (Sreedhar & Coleri, 2018).

Poisson's ratio is defined as the ratio of transverse to longitudinal strains of a loaded specimen (PI, 2011). This elastic material constant is one of two material properties required to determine the stress, strain, and displacement response of the pavement system within MEPDG (Maher & Bennert, 2008). The equation for Poisson's ratio is presented below.

$$\text{Poisson's Ratio } (\mu) = -\frac{\varepsilon_D}{\varepsilon_L} \tag{3.3}$$

where:

ε_D = strain along the diametrical (horizontal) axis

ε_L = strain along the longitudinal (vertical) axis

Unit Weight is a measure of specific weight for HMA, usually in units of lbs/ft^3. The unit weight of an asphalt sample is a product of its aggregate, binder, air voids, and compaction level. It can be seen with some variability that an increase in asphalt unit weight improves the dynamic modulus and fatigue potential of flexible pavements (del Pilar Vivar & Haddock, 2006; Sreedhar & Coleri, 2018).

3.2.4 Mechanical Properties

The primary mechanical properties inputs for MEPDG flexible pavement design are creep compliance and dynamic modulus. Creep compliance is a measure of asphalt durability defined as the rate of strain increase for a constant applied stress over a given time. For Level 3 designs, creep compliance is predicted using a linear regression equation developed by the NCHRP. This model generates creep compliance as a function of coefficients, D_1 and m, based on the asphalt temperature and volumetric properties. The model is represented below using Equations 3.4 through 3.6. (AASHTO, 2015a).

$$D(t) = D_1 t^m \tag{3.4}$$

$$\log(D_1)_T = -8.5241 + 0.01306T + 0.7957\log(V_a) + 2.0103\log(VFA) - 1.923\log(A_{RTFO}) \tag{3.5}$$

$$m = 1.1628 - 0.00185T - 0.04596V_a - 0.01126VFA + 0.00247Pen_{77} + 0.001683Pen_{77}^{0.4605}T. \tag{3.6}$$

where:

t	=	time (months)
T	=	test temperature (°C) (i.e., -20°C, -10°C, and 0°C)
V_a	=	air voids (%)
VFA	=	void filled with asphalt (%)
A_{RTFO}	=	intercept of binder viscosity-temperature relationship for RTFO condition
Pen_{77}	=	asphalt penetration at 77°F (mm/10)

Recent evaluations of this model imply that it tends to inaccurately predict localized D(t) values without regional calibration efforts. A study conducted by Yin et al. (2010) found that the Level 3 creep compliance estimates using MEPDG were overpredicted when compared to both laboratory measured and LVE interconverted creep compliance values. Esfandiapour and Shalaby (2017) developed similar conclusions when conducting creep compliance calibration, adding that the model is particularly less reliable when predicting D(t) at low temperatures. Inconsistencies with the model resulted in bias of the thermal cracking performance and IRI predictions. As a result, relying on Level 3 creep compliance may result in variable service life and life cycle cost estimates.

Dynamic modulus (|E*|) is a stiffness metric represented by the stress/strain response under dynamic loading. Current versions of the PMED software include two models for |E*| prediction, the NCHRP 1-37A viscosity-based model and the NCHRP 1-40D binder shear modulus-based model (AASHTO, 2015a). These models are useful when Level 1 data in unavailable for design. Also referred as the original Witczak equation, the NCHRP 1-37A model has been nationally calibrated for use in the MEPDG and is primarily a function of asphalt aggregate gradation, volumetric properties, loading frequency, and binder viscosity. A more in-depth overview of these models and their performance is discussed in a later section.

As the primary stiffness property for the characterization of HMA in MEPDG, the dynamic modulus is considered the most influential variable when determining the structural response of a flexible pavement. Specifically, |E*| is one of the key parameters used to evaluate both rutting and fatigue cracking distress predictions within the MEPDG (NCHRP, 2004).

3.2.5 Binder Grade

New mechanical property inputs for flexible pavement in the MEPDG also include binder grade. Asphalt binder grades effect the deformation characteristics of asphalt pavements, particularly in the early stages of their lifetime. Specifically, higher binder grades typically decrease susceptibility to rutting (Gogula, Hossain, Boyer, & Romanoschi, 2003). Typical binder grades used in Georgia include PG64-22, PG67-22, and PG76-23. The PG76-23 binder is considered polymer modified. Polymer modified binders have shown to produce greater elastic recovery, higher softening points, greater viscosity, greater cohesive strength, and greater ductility than standard binders (Yildirim, 2007).

3.2.6 Thermal Properties

Thermal properties affect the distribution of temperature and moisture within a pavement system by controlling the flow of heat. As a result, thermal properties influence proliferation of pavement distresses such as thermal cracking. Heat capacity and thermal conductivity are considered thermal property inputs for flexible pavements in the MEPDG. Overall, flexible pavements tend to have lower heat capacity and thermal conductivities than rigid pavements, resulting in greater temperature variations.

3.2.7 Failure Mechanisms and Performance Criteria

Failure mechanisms are used within the MEPDG to provide long term pavement distress predictions. Pavement response models are used to determine the structural response of the pavement system due to traffic loads and environmental influences. Each response variable is evaluated at the critical location within the pavement layer where the parameter is at its most extreme value (NCHRP, 2004). The existence of a distress prediction summary is an advantage to using the MEPDG over the 1993 AASHTO Guide for Pavement Design Structures. Descriptions of the measurable failure mechanisms for flexible pavement in PMED are listed below.

The rut depth of a pavement is defined as the plastic or permanent deformation in PMED. Pavement deformation or rutting is a surface depression of the wheel path that occurs due to sustain traffic loading. Due to the flexible nature of asphalt materials, consolidation of the pavement profile may occur overtime and across seasonal temperature changes .Within the software, rutting is calculated as the incremental deformation within each sublayer and the plastic deformation for a given season is found through the sum of the vertical deformations within each layer (AAASHTO, 2015a). The associated equations for permanent deformation prediction are highlighted below.

$$\Delta_{p(HMA)} = \varepsilon_{p(HMA)} h_{HMA} = \beta_{1r} k_z \varepsilon_{r(HMA)} 10^{k_{1r}} n^{k_2 \beta_{2r}} T^{k_{3r} \beta_{3r}} \tag{3.7}$$

$$k_z = [(-0.1039(H_{HMA})^2 + 2.4868 H_{HMA} - 17.342) + (0.0172(H_{HMA})^2 - 1.733 H_{HMA} + 27.428)] \times 0.328196^D \tag{3.8}$$

where:

$\Delta_{p(HMA)}$	=	accumulated permanent vertical deformation in the HMA layer (in.)
$\varepsilon_{p(HMA)}$	=	accumulated permanent axial strain in the HMA layer (in.)
$\varepsilon_{r(HMA)}$	=	resilient or elastic strain calculated by the structural response model at the mid-depth of each HMA sublayer (in./in.)
h_{HMA}	=	thickness of the HMA layer (in.)
n	=	number of axle-load repetitions
T	=	mix or pavement temperature (°F)
k_z	=	depth confinement factor
$k_{1r,2r,3r}$	=	global field calibration parameters; k_{1r}= -3.35412, k_{12}= 0.4791, k_{3r}= 1.5606
β_{1r}, β_{2r}, β_{3r}	=	local or mixture field calibration constants
D	=	depth below the surface (in.)
H_{HMA}	=	total HMA thickness (in.)

Both alligator and longitudinal cracking are model in PMED as load-related or fatigue cracks. Fatigue cracking is a traditional form of pavement cracking that develops as a series of interconnected cracks caused by fatigue failure of the HMA surface under repeated traffic loading. PMED includes both top-down and bottom-up fatigue cracking distress predictions, however, top-down cracking is a largely unstudied form of fatigue cracking that is not considered an accurate indicator of pavement performance by GDOT (ARA, 2015). In thin pavements, cracking initiates at the bottom of the HMA layer where the tensile stress is the highest then propagates to the surface as one or more longitudinal cracks. It is more common for fatigue cracking to be modeled in this way. There are two models available for bottom-up fatigue cracking prediction in the MEPDG, the Shell Oil Model and the Asphalt Institute (MS-1) Model. The MS-1 Model is expressed in the same mathematical form as the Shell Oil Model but contains fewer coefficients. The mathematical form for estimating the number of repetitions to fatigue cracking (N_f) using these models is expressed in Equations 3.9 and 3.10 (AASHTO, 2015a).

$$N_f = k_{f1}(C)(C_H)\beta_{f1}(\varepsilon_t)^{k_{f2}\beta_{f2}}(E_{HMA})^{k_{f3}\beta_{f3}} \tag{3.9}$$

$$C = 10^{4.84\left(\frac{V_{beff}}{V_{beff}+V_a}-0.69\right)} \tag{3.10}$$

where:

ε_t	=	tensile strain at the critical location (in./in.)
E_{HMA}	=	dynamic modulus of the HMA measured in compression (psi)
k_{f1}, k_{f2}, k_{f3}	=	global field calibration coefficients (k_{f1} = 0.007566, k_{f2} = 3.9492, k_{f3} = 1.281)
β_{1r}, β_{2r}, β_{3r}	=	local or mixture specific field calibration constants
C	=	laboratory to field adjustment factor
V_a	=	air voids (%)
V_{beff}	=	effective asphalt content (%)

Non-load related cracks are considered transverse or thermal cracks within the PMED software. Although not all transverse cracking is a result of thermal cracking, current distress outputs do not differentiate the two as both are considered cracking that propagates perpendicular to the traffic lane. These distresses are generally caused by low temperatures and contraction of asphalt binders leading to stresses in the pavement surface. The preferred model for AC thermal cracking in PMED is highlighted in Equations 3.11 through 3.13. Currently, transverse cracking caused by low temperature events is considered not prevalent for Georgia roadways (ARA, 2015). As seen from below equations, the distress model for AC thermal cracking is correlated to fracture parameters, *A* and *n*, which are affected by the asphalt mechanical properties. As a result, it is a primary performance output for investigation within this study.

$$\Delta C = A(\Delta K)^n \tag{3.11}$$

$$A = k_t \beta_t 10^{[4.389 - 2.52 \log(E_{HMA} \sigma_m \eta)} \tag{3.12}$$

$$K = \sigma_{tip}[0.45 + 1.99(C_0)^{\ 0.56} \tag{3.13}$$

where:

ΔC	=	change in crack depth due to a cooling cycle
ΔK	=	change in the stress intensity factor due to a cooling cycle
A, n	=	fracture parameters
k_t	=	coefficient determine through global calibration (level 1 = 1.5; level 2 = 0.5; level 3 = 1.5)
E_{HMA}	=	indirect tensile modulus (psi)
σ_m	=	mixture tensile strength (psi)
m	=	the *m*-value derived from the IDT creep compliance curve
β_t	=	local or mixture calibration factor
σ_{tip}	=	far-field stress from pavement response model at depth of crack tip (psi)
C_0	=	current crack length (ft)

Evaluation of a pavement's smoothness in PMED is determined via terminal IRI. The International Roughness Index (IRI) is used to define a characteristic of the roadway profile and constitutes a standardized roughness measurement. Pavement roughness is generally defined as an expression of irregularities in the pavement surface that adversely affect the ride quality of a vehicle. The terminal IRI is the point at which the pavement is considered too rough and requires some type of rehabilitation. The prediction model for terminal IRI of new flexible pavements in PMED is presented in Equations 3.14 and 3.15 (AASHTO, 2015a). It can be seen that IRI is a product of transverse cracking and fatigue cracking, among other factors, making it a principal output for this investigation.

$$IRI = IRI_0 + C_1(RD) + C_2(FC_{Total}) + C_2(TC) + C_4(SF) \tag{3.14}$$

$$SF = Age^{1.5}\{\ln[(Precip + 1)(FI + 1)p_{02}]\} + \{\ln[(Precip + 1)(PI + 1)p_{200}]\} \tag{3.15}$$

where:

IRI_0	=	initial IRI after construction (in./mi)
FC_{Total}	=	area of fatigue cracking (% of total lane area)
TC	=	length of transverse cracking (ft/mi)
RD	=	average rut depth (in.)
$C_{1,2,3,4}$	=	calibration factors; C_1= 40.0, C_2= 0.400, C_3= 0.008, C_4= 0.015
Age	=	pavement age (years)
PI	=	percent plasticity index of the soil
FI	=	average annual freezing index (°F days)
Precip	=	average annual precipitation or rainfall (in.)
p_{02}	=	percent passing the 0.02 mm sieve
p_{200}	=	percent passing the 0.075 mm sieve

3.2.8 Sensitivity Studies on Flexible Pavement

Sensitivity analysis of MEPDG flexible pavement input parameters has been a topic of research as early as the release of MEPDG in 2004 and is a valuable practice for developing regional PMED design strategies (Masad & Litte, 2004). While the results of individual sensitivity studies may vary based on factors such as climate, traffic, pavement structure, material types, and calibration factors, it is still advantageous to review the conclusions drawn through these investigations. As a complete sensitivity analysis is beyond the scope of this study, the following discussion is limited to the mechanical property inputs of interest in this report.

Several studies noted that HMA dynamic modulus values significantly affect the MEPDG performance predictions for rutting and fatigue cracking (longitudinal and alligator cracking) (Li et al., 2009; El-Badawy et al., 2011; El-Badawy et al., 2012). Further, an investigation of the impact of asphalt binder input level on pavement performance found that rutting predictions increased significantly at higher design levels (El-Badawy et al., 2012). Due to the relationship between binder input levels and dynamic modulus input levels, an influence on PMED rutting predictions may also be expected when varying |E*| input levels.

While varying creep compliance input strategies, Yin et al. (2010) and Esfandiapour and Shalaby (2017) found that Level 3 default D(t) values significantly underpredict the intensity of thermal cracking predictions when compared to Level 1 or 2 inputs. These conclusions suggest a sensitive relationship exists between the creep compliance and non-fatigue related distress predictions.

A comprehensive global sensitivity analysis of flexible pavement predictions was conducted by Schwartz et al. (2013) in which material properties, among other inputs, were evaluated under five climatic conditions and three traffic levels. Using a combination of multivariate linear regression and artificial neural network analysis, the study found that HMA |E*| parameters were among the most highly sensitive inputs. Consequently, the variability of distress predictions associated with fatigue cracking and pavement rutting were substantially greater than the values for IRI and thermal cracking (Schwartz et al., 2013). However, creep compliance parameters were still found to be very sensitive, maintaining the largest influence on thermal cracking performance. Table 3.3 includes their input sensitivity ranking using a normalized sensitivity index (NSI) approach. Supported by the conclusions drawn by previous researchers, these discoveries become the motivation for the mechanical property sensitivity analysis performed within this thesis.

Table 3.3. HMA Design Inputs by Maximum $NSI_{\mu+2\sigma}$ Values (Schwartz et al., 2013)

Design Input	Long. Crack	Alligator Crack	Thermal Crack	AC Rut Depth	Total Rut Depth	IRI	Max.
	Maximum $NSI_{\mu\pm2\sigma}$ Values (ANN RSMs)[a]						
Hypersensitive ($NSI_{\mu\pm2\sigma}$ > 5)							
HMA E^* alpha parameter[b]	−29.52	−15.94	−0.58	−24.40	−8.98	−3.58	−29.52
HMA E^* delta parameter[b]	−23.87	−13.18	2.41	−24.43	−8.99	−2.80	−24.43
HMA thickness	−10.31	−7.46	−0.86	−4.21	−1.58	−1.11	−10.31
Very Sensitive (1 < $NSI_{\mu\pm2\sigma}$ < 5)							
HMA creep compliance m exponent	na	na	−4.85	na	na	na	−4.85
Base resilient modulus	−4.72	−2.73	−0.17	0.14	−0.15	−0.36	−4.72
Surface shortwave absorptivity	4.32	1.28	−0.20	4.65	1.67	0.67	4.65
HMA air voids	4.47	3.39	1.33	−0.05	0.03	0.29	4.47
HMA Poisson's ratio	−2.38	−1.01	0.23	−4.33	−1.46	−0.43	−4.33
Traffic volume (AADTT)	3.72	3.94	0.02	1.87	0.66	0.51	3.94
HMA effective binder volume	−3.88	−2.93	−0.17	0.05	0.06	−0.24	−3.88
Subgrade resilient modulus	−2.07	−3.41	0.15	0.08	−0.28	−0.44	−3.41
Base thickness	−2.40	−1.02	−0.03	0.22	0.04	−0.09	−2.40
Subgrade percent passing No. 200	−1.71	−0.68	0.08	−0.10	−0.10	−0.12	−1.71
HMA tensile strength at 14°F	na	na	−1.59	na	na	na	−1.59
Operational speed	−1.26	−0.83	−0.04	−1.06	−0.39	−0.15	−1.26
HMA creep compliance D parameter	na	na	−1.03	na	na	na	−1.03
Sensitive (0.1 < $NSI_{\mu\pm2\sigma}$ < 1)							
HMA unit weight	−0.88	0.97	−0.76	−0.88	−0.30	−0.08	0.97
Base Poisson's ratio	0.91	0.90	0.18	−0.19	−0.05	0.09	0.91
HMA heat capacity	−0.76	−0.55	−0.77	−0.81	−0.28	−0.14	−0.81
Subgrade liquid limit	−0.67	−0.79	−0.10	−0.10	0.07	0.03	−0.79
Binder low-temperature PG	0.56	0.09	−0.74	0.25	0.09	0.02	−0.74
HMA thermal conductivity	−0.53	−0.40	−0.67	0.20	0.04	0.02	−0.67
Binder high-temperature PG	−0.60	−0.48	0.00	−0.66	−0.25	−0.09	−0.66
Subgrade Poisson's ratio	0.44	−0.59	0.16	0.08	0.07	0.04	−0.59
Groundwater depth	0.20	−0.16	0.08	0.01	−0.02	−0.02	0.20
Subgrade plasticity index	−0.15	0.11	0.03	0.01	0.02	0.00	−0.15
Insensitive ($NSI_{\mu\pm2\sigma}$ < 0.1)							
Aggregate coefficient thermal contraction	na	na	−0.07	na	na	na	−0.07

NOTE: long. = longitudinal; max. = maximum.
[a]Maximum sensitivity (in absolute value sense) over all baseline cases and distresses.
[b]See Equation 1.

3.3 Dynamic Modulus Prediction Methods

Level 1 inputs in PMED require the entry of discrete, laboratory-measured |E*| quantities at a range of temperature and frequency values. As a result, pavement design agencies often rely on the usage of dynamic modulus prediction models to complete their designs under ME practices.

The following sections outline the most relevant |E*| prediction models and justification for the Georgia HMA regression analysis generated within this report.

3.3.1 Witczak Models

Currently, the Witczak model is considered the most widely used and accepted method for predicting dynamic modulus of asphalt materials. Two forms of the model exist today, the original 1999 model (Witczak 1-37A), found in older versions of the MEPDG, and the revised 2006 model (Witczak 1-40D), utilized in the modern MEPDG (Andrei et al., 1999; Bari & Witczak, 2006). Both Witczak equations were obtained using linear multivariate regression analysis and are represented by Equations 3.16 and 3.17. The 1999 Witczak |E*| prediction model was developed using a large database of 205 HMA mixtures containing 2,750 data points where the primary inputs include binder viscosity, loading frequency, aggregate gradation, and mixture volumetric properties (Andrei et al., 1999). Revisions made for the 2006 Witczak model began with a more robust database of 346 HMA mixtures and 7,400 measured data values. However, the primary improvement of the 2006 model is the recharacterization of asphalt binder using dynamic shear modulus and phase angle inputs (Bari & Witczak, 2006).

$$\log_{10} E^* = -1.249937 + 0.02923\rho_{200} - 0.001767(\rho_{200})^2 - 0.002841\rho_4 - 0.058097V_a - 0.82208 \cdot \frac{V_{beff}}{V_{beff}+V_a} + \frac{3.871977 - 0.0021\rho_4 + 0.003958\rho_{38} - 0.000017(\rho_{38})^2 + 0.00547\rho_{34}}{1+e^{(-0.603313-0.313351\log f - 0.393532\log\eta}} \quad (3.16)$$

where:

E*	=	dynamic modulus (10^5 psi)
ρ_{200}	=	percent passing #200 sieve
ρ_4	=	percent passing #4 sieve
ρ_{38}	=	percent retained on 3/8 in. sieve
ρ_{34}	=	percent retained on ¾ in. sieve

V_a = air voids (%)

V_{beff} = effective asphalt content (%)

f = loading frequency (Hz)

η = binder viscosity at temperature of interest (10^6 poise)

$$\log_{10} E^* = -0.349 + 0.754(|G_b^*|^{-0.0050}) \times (6.65 - 0.032\rho_{200} + 0.0027(\rho_{200})^2 + 0.011\rho_4 - 0.0001(\rho_4)^2 + 0.006\rho_{38} - 0.00014(\rho_{38})^2 - 0.08V_a - 1.06\left(\frac{V_{beff}}{V_{beff}+V_a}\right)\Bigg) + \frac{2.56+0.03V_a+0.71\left(\frac{V_{beff}}{V_{beff}+V_a}\right)+0.012\rho_{38}-0.0001(\rho_{38})^2-0.01\rho_{34}}{1+e^{(-0.7814-0.5785\log\left|G_b^*\right|+0.8834\log\delta_b)}} \tag{3.17}$$

where:

E^* = dynamic modulus (psi)

ρ_{200} = percent passing #200 sieve

ρ_4 = percent passing #4 sieve

ρ_{38} = percent retained on 3/8 in. sieve

ρ_{34} = percent retained on ¾ in. sieve

V_a = air voids (%)

V_{beff} = effective asphalt content (%)

$|G_b^*|$ = dynamic shear modulus of binder (psi)

δ_b = phase angle of binder associated with $|G_b^*|$ (degree)

Although these models have proven successful for universal applications, such as the MEPDG and associated software, deficiencies may exist under localized or project-specific conditions. Noticeable bias in the Witczak model at the lower and upper |E*| extremes has been well documented (Bari & Witczak, 2006; Schwartz, 2005; Ceylan et al., 2009).

3.3.2 Machine Learning Models

More recently, as alternatives to the linear multivariable approach of the Witczak model, machine learning techniques such as artificial neural networks or kernel methods have been developed for |E*| prediction in localized regions. Ceylan et al. (2007) are credited with developing an advanced ANN model using the same input parameters as the Witczak equations. A four-layered feed forward error-back propagation architecture (Figure 3.2) was used to develop the model using the same dataset as Bari and Witczak (2006). The 7,400 measured values were randomly divided into two subsets—a training subset comprised of 6,900 data points and a testing subset containing the other 500 data points (Ceylan et al., 2007). The results of the study suggest the ANN model is not only more accurate than the Witczak models using the same dataset, but do a more balanced job of capturing temperature and other mixture influences (Ceylan et al. 2007; Ceylan et al., 2009)

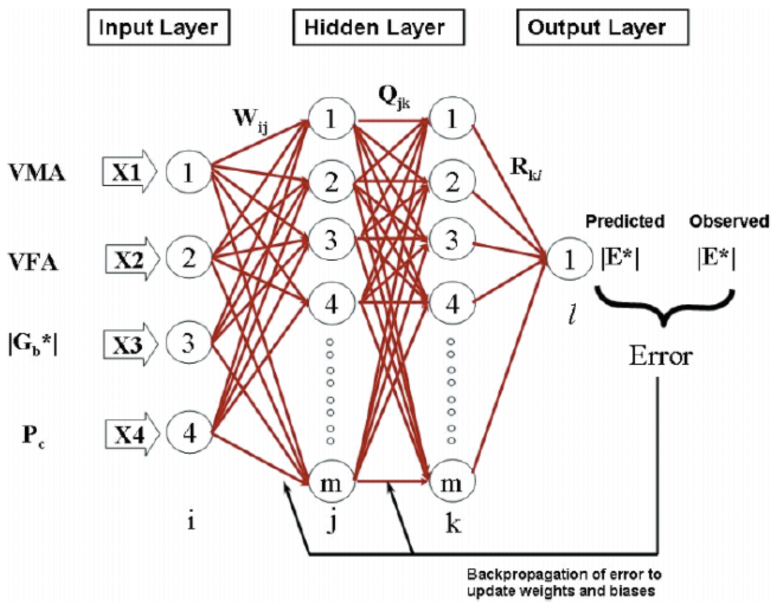

Figure 3.2. Four-layered Neural Network Architecture employed by Ceylan et al. 2007

A subsequent study performed by Gopalakrishnan et al. (2009) explored the feasibility of employing another machine learning technique for |E*| prediction using support vector regression (SVR). The SVR model architecture applied to this study is referenced in Figure 3.3. Once again, the Bari and Witczak (2006) data set was used and divided into training and testing subsets of the same proportions. However, the inputs for the SVR model developed by Gopalakrishnan et al. (2009) only included the eight original inputs from the 1999 Witczak model. The Gaussian function was selected as the SVR Kernel function and the model was evaluated. Similar to the previous study, a comparison of the models found that the SVR model exhibited smaller bias than that of the Witczak models.

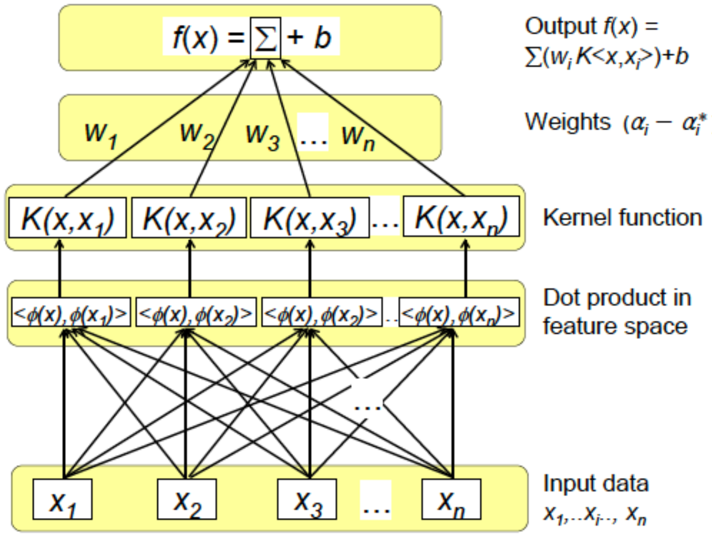

Figure 3.3. Support Vector Regression Architecture of Gopalakrishnan et al. (2009)

Conversely, tree-based or model tree (MT) approaches to regression analysis are rarely conducted for asphalt moduli. A variety of sources may be found on the subject of MT analysis of concrete strength properties, for example, in which researchers found it a useful and accurate prediction tool (Deepa et al., 2010; Deshpande et al., 2014; Gholampour et al., 2018). However, none such resources are available for flexible pavement materials and their associate mechanical properties. Though often not considered as accurate as ANN models, tree-based methods provide advantages in their simple geometric structure and the ability to efficiently handle a large number of datasets with different attributes. Based on the existing literature, it is found that tree regression is among the superior regression methods that exhibit greater prediction accuracy than that of generic models. As a result, it is may be a valuable approach for predicting HMA dynamic modulus under project-specific conditions in Georgia.

3.4 Viscoelastic Theory and Interconversion Methods

Known as a linear viscoelastic (LVE) material, asphalt can be characterized by a series of response functions. Among the most fundamental response functions used for HMA characterization are creep compliance, relaxation modulus, and complex modulus (Kim, 2009). It is well documented that all LVE material functions are considered mathematically equivalent and contain the same information on the mechanical properties of a material. This is true for both shear and uniaxial loading (Park & Schapery, 1999). As a result, it is possible to obtain an unknown response function using a known response function for an LVE material through a series mathematical interconversion techniques. Extensive literature on this subject has been developed in detail by Ferry (1980), Tschoegl (1989), and others. Therefore, the following sections provide a brief overview of the relevant viscoelastic theory and its application in the interconversion process.

3.4.1 Creep Compliance

As previously mentioned, the creep compliance, D(t), is the ratio of strain response to a constant stress input for an LVE material. In equation form, the creep compliance response function is represented by the following.

$$D(t) = \frac{\varepsilon(t)}{\sigma_0} \tag{3.18}$$

where:

$\varepsilon(t)$ = strain at given time, t

σ_0 = constant stress

Using the Boltzmann convolution integral, the stress-strain relationship for creep compliance can be represented by Equation 3.19 for uniaxial loading and nonaging conditions.

$$\varepsilon = \int_0^t D(t-\tau)\frac{d\sigma}{d\tau}d\tau \tag{3.19}$$

where:

τ = integration variable

3.4.2 Relaxation Modulus

Conversely, the relaxation modulus, E(t), is the ratio of stress response to a constant strain input as depicted by Equation 3.20.

$$E(t) = \frac{\sigma(t)}{\varepsilon_0} \tag{3.20}$$

where:

$\sigma(t)$ = stress at given time, t

ε_0 = constant strain

The stress-strain relationship for relaxation modulus using the Boltzmann convolution integral under uniaxial loading and nonaging conditions in depicted in the equation below.

$$\sigma = \int_0^t E(t-\tau)\frac{d\varepsilon}{d\tau}d\tau \tag{3.21}$$

where:

τ = integration variable

In the Laplace transform domain, the creep compliance and relaxation modulus can be evaluated as reciprocals. In the time domain, the material must exhibit perfectly elastic behavior for D(t) and E(t) to be characterized in this way. Instead, the exact relationship between E(t) and

D(t) in the time domain is determined using convolution integrals. The convolution integral in Equation 3.22 relates the functions by substituting Equation 3.19 for ε in Equation 3.21.

$$1 = \int_0^t E(t-\tau)\frac{dD(t)}{d\tau}d\tau \quad (3.22)$$

3.4.3 Complex Modulus

The complex modulus, E*, is a response function of LVE materials defined by the stress-strain ratio under sinusoidal loading. This function is characterized by the dynamic modulus (|E*|) and phase angle (ϕ) represented by the following equations.

$$|E^*| = \frac{\sigma_{amp}}{\varepsilon_{amp}} \quad (3.23)$$

$$\varphi = 2\pi f \Delta t \quad (3.24)$$

where:

σ_{amp}	=	stress amplitude
ε_{amp}	=	strain amplitude
f	=	loading frequency
Δt	=	time lag between stress and strain response

The phase angle acts as an indicator of the material's viscosity and elastic behavior. As the viscosity of a material increases, so does the phase angle. Therefore, a material is considered perfectly elastic when the phase angle is equal to 0 and perfectly viscous when the phase angle is equal to 1.

As a complex function, E* can be represented by real and imaginary components as shown in Equation 3.25. These components are referred to as the storage modulus (E') and loss modulus

(E”), respectively. Figure 3.4 depicts the complex plane in which E’ is plotted to the real axis and E” is plotted to the imaginary axis.

$$E^* = E' + iE" \tag{3.25}$$

where:

E’	=	$\lvert E^*\rvert \cos(\phi)$
E”	=	$\lvert E^*\rvert \sin(\phi)$
i	=	$\sqrt{-1}$

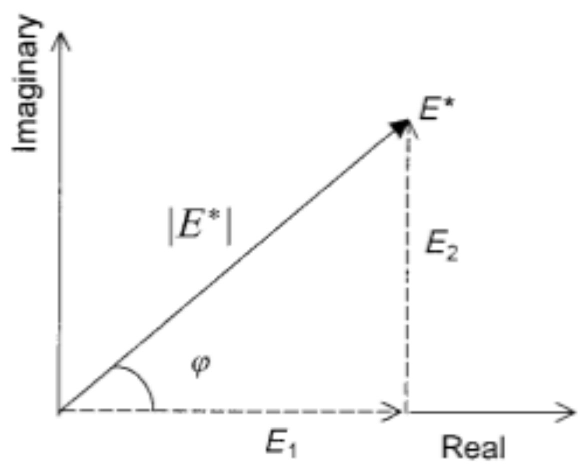

Figure 3.4. Complex Plane (Kim, 2009)

3.4.4 Interconversion between Relaxation Modulus and Creep Compliance

There are several approaches to LVE response function interconversion that have been refined by researchers in recent years. In most instances, an approximate interconversion using numerical methods is recommended when experimental data is available for the source, or known, function. This is because experimental data does not typically cover the complete range of time or frequency. For this reason, exact analytical interconversions can be challenging and time consuming. Among the first to document LVE interconversion processes, Ferry (1980) introduced an exact relationship between E(t) and D(t) seen in Equation 3.26. To perform the interconversion near-exactly, a numerical integration technique is applied to the convolution integral.

$$\int_0^t E(t-\tau)D(\tau)d\tau = t\,, \qquad for\ t > 0 \tag{3.26}$$

where:

E(t)	=	relaxation modulus
D(t)	=	creep compliance
t	=	time
τ	=	integration variable

A number of approximate interrelationship methods have been developed and validated by other researchers as well (Denby, E.F., 1975; Christensen, 1982; and Jeong, 2005). Specifically, Park and Kim (1999) developed a technique that modifies the exact relationships from the Pure Power Law (PPL) method and applies a logarithmic time shift to approximately convert between relaxation modulus and creep compliance. In this study, the new technique outperformed previously developed approximate methods and was shown to match the accuracy of exact techniques. By the PPL, Park and Kim (1999) represent the relaxation modulus and creep compliance using the below power law fits.

$$E(t) = E_1 t^{-n} \tag{3.27}$$

$$D(t) = D_1 t^{n} \tag{3.28}$$

where:

E_1	=	positive relaxation modulus constant
D_1	=	positive creep compliance constant

n = magnitude of the slope of the response function, R_H, on the log scale

$$n = \left| \frac{d \log_{10}(R_H(t))}{d \log_{10}(t)} \right|$$

From Equations 3.27 and 3.28, the following power law interrelationship between relaxation modulus and creep compliance was obtained.

$$E(t) \cdot D(t) = \frac{\sin(n\pi)}{n\pi} \quad (3.29)$$

A new expression for creep compliance was then be determined by substituting Equation 3.27 into Equation 3.29, yielding the relationship below.

$$D(t) = \frac{\sin(n\pi)}{E_1 n\pi} t^n \quad (3.30)$$

A new expression for the interrelationship is then proposed as the following.

$$E(t^*) \cdot D(t) = 1 \quad (3.31)$$

where:

t^* = "equivalent time" of t

Whereby substituting Equations 3.27 and 3.30 into Equation 3.31, the subsequent expression for equivalent time was defined.

$$t^* = \frac{\sin(n\pi)^{\frac{1}{n}}}{n\pi} t \quad (3.32)$$

Finally, the response functions were approximately related by the below equations.

$$E(t) = \frac{1}{D(\frac{t}{\propto})} \tag{3.33}$$

$$D(t) = \frac{1}{E(\propto t)} \tag{3.34}$$

where:

$$\propto = \left(\frac{\sin n\pi}{n\pi}\right)^{\frac{1}{n}}$$

4.0 PROBLEM STATEMENT

The MEPDG marks a measurable improvement over the current standard design methodologies employed by the Georgia Department of Transportation. However, a greater quantity of complex inputs is required for design. In order to achieve full implementation of the MEPDG, GDOT must develop a comprehensive library of empirical data related to Georgia traffic, climate, materials, pavement performance, and more. The contents of this report look to enhance this library in two significant ways.

First, a dynamic modulus prediction model is to be developed utilizing the library of asphalt material properties acquired by Kim et al. (2019). Using a tree-based method, this model will provide insight into which asphalt mixture characteristics have significant impact on the dynamic modulus of the material. If validated, this model will prove a useful resource for dynamic modulus estimation in favor of laboratory testing. Second, the effects of creep compliance as a flexible pavement mechanical input in the PMED software are to be investigated. Specifically, this paper examines the use of converted creep compliance values from the existing dynamic modulus library developed for Georgia MEPDG. Due to the required time, expense, and expertise necessary for creep compliance laboratory testing, it may be advantageous for agencies to use interconverted values in place of experimental data. This approach is possible due to the linear viscoelastic behavior of asphalt.

Therefore, the primary objectives of this research are to: (1) Develop a regression tree model for predicting dynamic modulus ($|E^*|$) provided basic asphalt material properties; (2) Formulate an effective method for |E*| to creep compliance (D(t)) interconversion; (3) Successfully generate a D(t) library using the existing |E*| library produced by Kim et al. (2019); (4) Evaluate the effects |E*| and D(t) at differing inputs levels in the PMED software through analysis of the pavement performance output; and (5) Update existing GDOT MEPDG resources to reflect the findings of this study and provide recommendations for future flexible pavement design. Ultimately, these efforts look to accelerate the implementation of MEPDG in Georgia. Furthermore, the associated conclusions may provide pavement engineers with a more accurate and efficient approach to modern pavement design.

5.0 TREE ANALYSIS OF ASPHALT PROPERTIES ON DYNAMIC MODULUS

5.1 Preparation of Model Database

To effectively evaluate the use of tree regression as an alternative method for dynamic modulus prediction, the input parameters must contain only readily available properties for all current and future GDOT asphalt mixtures. The library of asphalt material properties utilized for this study were drawn from the results of Kim et al. (2019). The testing conducted therein resulted in the laboratory-acquired |E*| for a variety of asphalt mixtures, but standard material property inputs were only recorded for 11 of the 18 mixtures. Consequently, the database utilized for the following tree analysis includes 198 discrete |E*| datapoints at varying combinations of temperatures and frequencies. The complete predictor space available for the model includes 17 mixture-defining properties and the temperature and frequency of testing for each |E*| output. The naming convention used to reference these mixtures is defined by Kim et al. (2019) and described in Table 2.6.

The Witczak 1-37A model (Andrei et al., 1999) requires the input of binder viscosity (η) for dynamic modulus prediction. Since modern models rely on the use of dynamic shear modulus (G_b^*) and phase angle (δ) measurements as a replacement, η was not explicitly recorded under the direction of Kim et al. (2019). The binder viscosity is instead derived from existing laboratory measurements using the ASTM A_i-VTS_i relationship defined in Equation 5.1 (ASTM, 1998) and the "Witczak-Sybilski $\eta - G_b^*$ Model" in Equation 5.2 (Bari & Witczak, 2006). Regression parameters, *A* and *VTS*, represent the intercept and slope of the linear line of Equation 5.1, respectively. Figure 5.1 provides an example of this relationship by plotting the binder properties of mixture A_12.5_64_M2 from the dataset.

$$\log\log\eta = A + VTS\log T_R \tag{5.1}$$

where:

η	=	viscosity of binder (centipoise)
A, VTS	=	regression parameters
T_R	=	temperature (ºRankine)

$$\eta = \frac{|G_b^*|}{10}\left(\frac{1}{\sin\delta_b}\right)^{4.8628} \tag{5.2}$$

where:

G_b^*	=	dynamic shear modulus of binder (psi)
δ_b	=	phase angle of G_b^* (degrees)

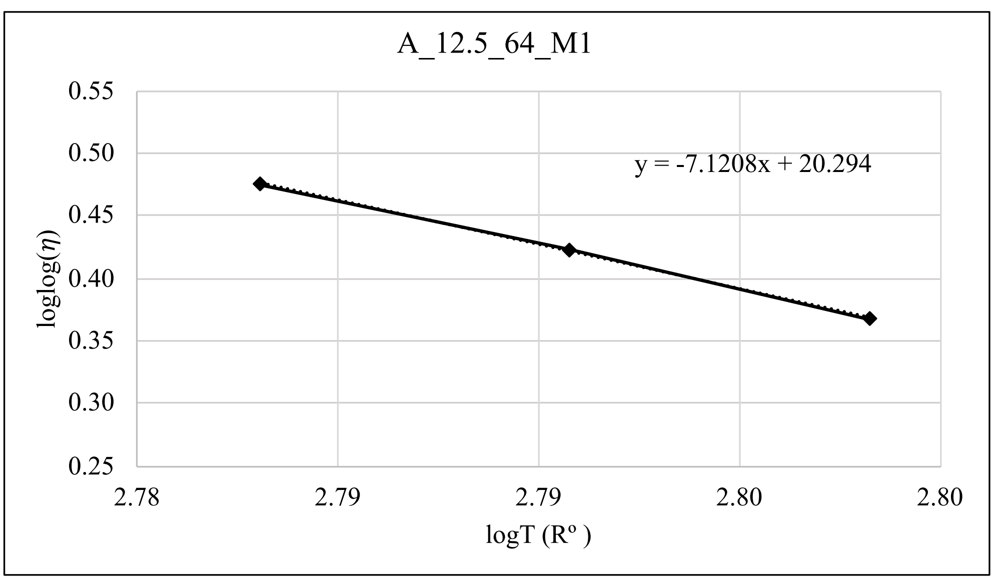

Figure 5.1. Asphalt Binder Relationship using ASTM A-VTS

The resulting list of input parameters available for model development is summarized in Table 5.1. Although the number of available inputs is substantially greater than the Witczak model, each parameter is readily available through the Georgia HMA library established for GDOT and thus a justifiable benefit to the localized prediction. The numerical values of every parameter listed is recorded in Appendix A for each of the 11 HMA mixtures.

Table 5.1. Dynamic Modulus Prediction Model Input Parameters

Parameter ID		Description	Model Integration	
			Witczak 1-37A	GDOT
region	north	Regional location of binder plant source delineated by North, Middle, and South Georgia		✓
	middle			✓
	south			✓
binder_gr	pg64	Asphalt binder Superpave performance grading identification: PG-64, PG-67, and PG-76		✓
	pg67			✓
	pg76			✓
nmas		Nominal maximum aggregate size (in.)		✓
rap		Recycled asphalt pavement content (%)		✓
binder		Binder content (%)		✓
gmm		Maximum theoretical specific gravity (%)		✓
av		Air voids in asphalt mixture (%)	✓	✓
vma		Voids in mineral aggregate (%)		✓
vfa		Effective asphalt content (%)	✓	✓
eff_binder		Effective binder content (%)		✓
pp200		Percent passing No. 200 sieve (%)	✓	✓
pp4		Percent passing No. 4 sieve (%)	✓	✓
pr38		Percent retained on 3/8" sieve (%)	✓	✓
pr34		Percent retained on 3/4" sieve (%)	✓	✓
eta		Loading Frequency (Hz)	✓	✓
temp_f		Loading Temperature (◦F)		✓
freq		Loading Frequency (Hz)	✓	✓

5.2 Model Development

Tree-based methods for regression involve the segmenting of the predictor space into distinct, non-overlapping regions. Predictions are then made for each observation within a region using the mean or mode of the training observations in that region. As a result of this segmentation, the final predictor space may be represented as a tree. Tree-based methods are generally regarded for their simplicity and efficient interpretation of large datasets and are not considered competitive with more advanced machine learning techniques. Thus, the use of bagging, random forests, and boosting techniques are utilized to improve the regression model.

Bagging, random forests, and boosting are sophisticated algorithms within tree-regression that each involve the production of multiple trees which are combined to yield a single consensus prediction. The expected outcome is a dramatic increase in prediction accuracy at the expense of some loss in interpretation. The unique methodology of the three approaches is best summarized in Table 5.2.

Table 5.2. Tree-Based Algorithms

Algorithm	Generalized Approach	Relevant Equations
Bagging	Take many training sets from the population. Build a separate prediction model for each training set. Average the resulting predictions.	$\hat{f}_{bag}(x) = \frac{1}{B}\sum_{b=1}^{B} \hat{f}^{*b}(x)$
Random Forest	Type of bagging where a random sample of m predictors is chosen as split candidates instead of the complete training set.	$m \approx \sqrt{p}$
Boosting	Fit a regression tree using a modified version of the original dataset. Grow a set of sequential trees using information from previously grown trees.	$\hat{f}(x) = \sum_{b=1}^{B} \lambda \hat{f}^{b}(x)$

To perform a direct comparison to the nationally calibrated |E*| prediction model employed by the MEPDG, the first set of tree regression models were generated using only the predictors found in the Witczak 1-37A equation. When combined, the available variables include aggregate gradation, mixture volumetric properties, binder viscosity, and loading frequency. The data was partitioned into 80% training set and 20% testing set and the tree in Figure 5.2 was generated. To determine which of the three techniques described in Table 5.2 enhance this model the most, each algorithm was used to predict |E*| one at a time using the same dataset. The results of this comparison are highlighted in Figure 5.3, where it is found that the boosted regression tree produced the most accurate prediction model with the lowest mean-square error (MSE) and an R^2 = 0.982.

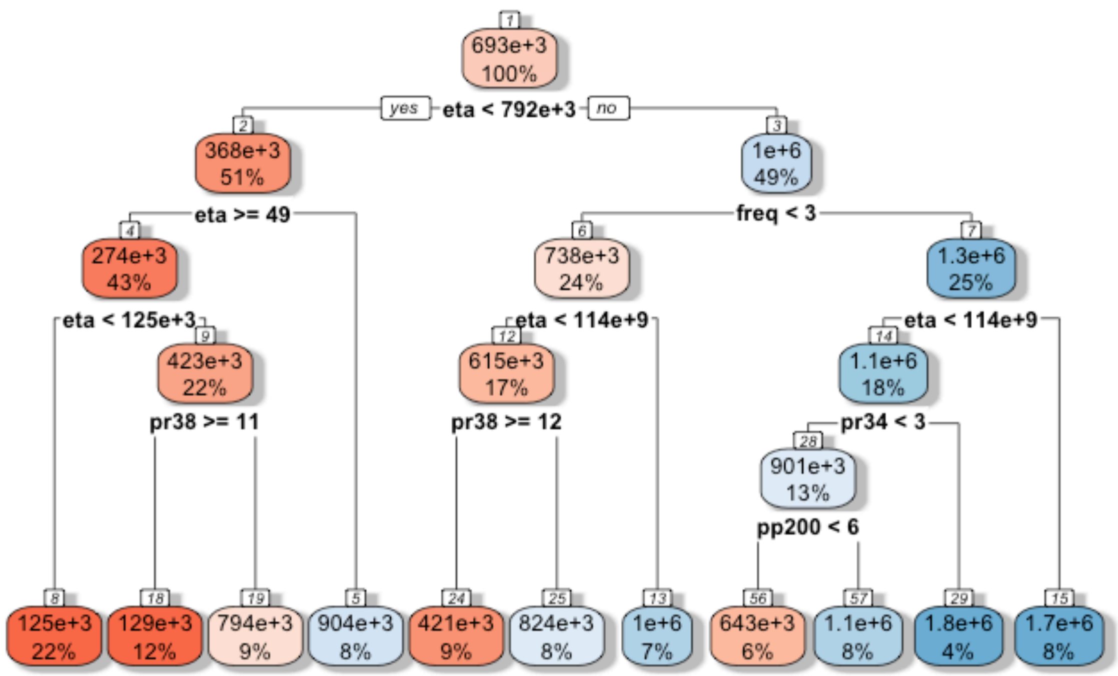

Figure 5.2. Model Tree Using 1-37A Witczak Predictors

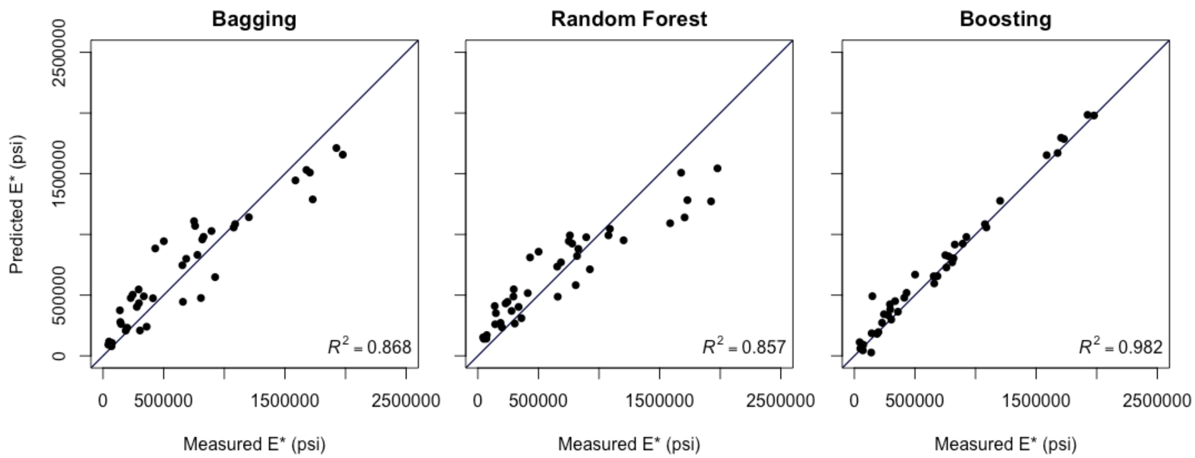

Figure 5.3. Method Comparison Using Witczak Predictors

Knowing that a model tree approach is capable of producing highly accurate |E*| estimates, the same methods were performed to develop a regression tree using the complete list of inputs found in the GDOT materials library. The predictor space for these models expand to include binder source location, binger grade, additional volumetric properties, and loading temperature. As seen in Figure 5.4, the inclusion of these variables altered the original model, reducing the total number of branches and leaves. Bagging, random forest, and boosting algorithms were used once again to determine the most suitable approach for improving the model. The results, found in Figure 5.5, suggest the boosted tree remains the preferred method.

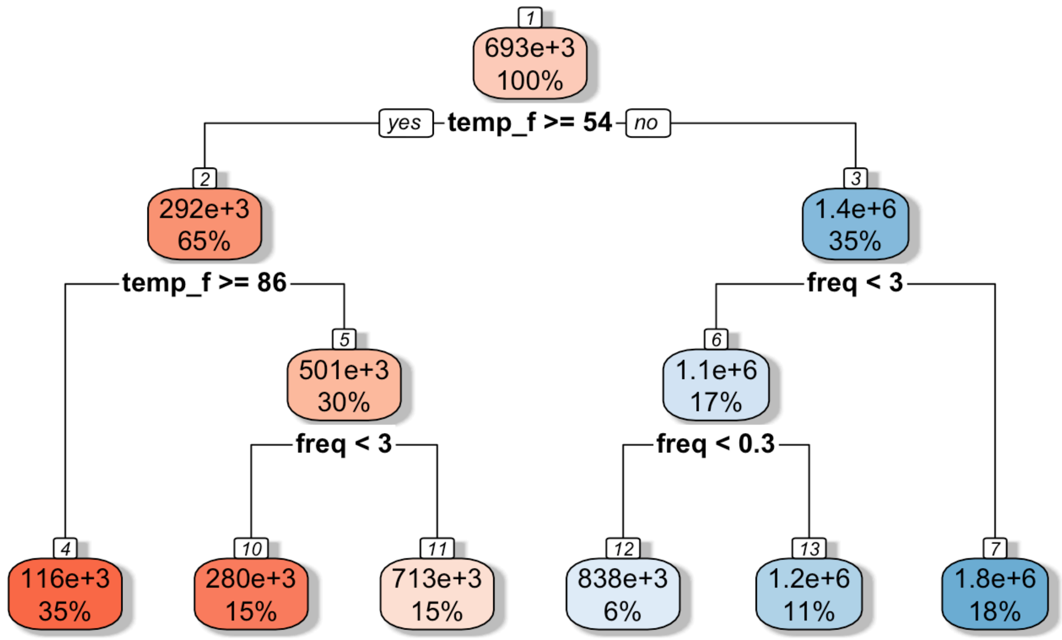

Figure 5.4. Model Tree Using GDOT Predictors

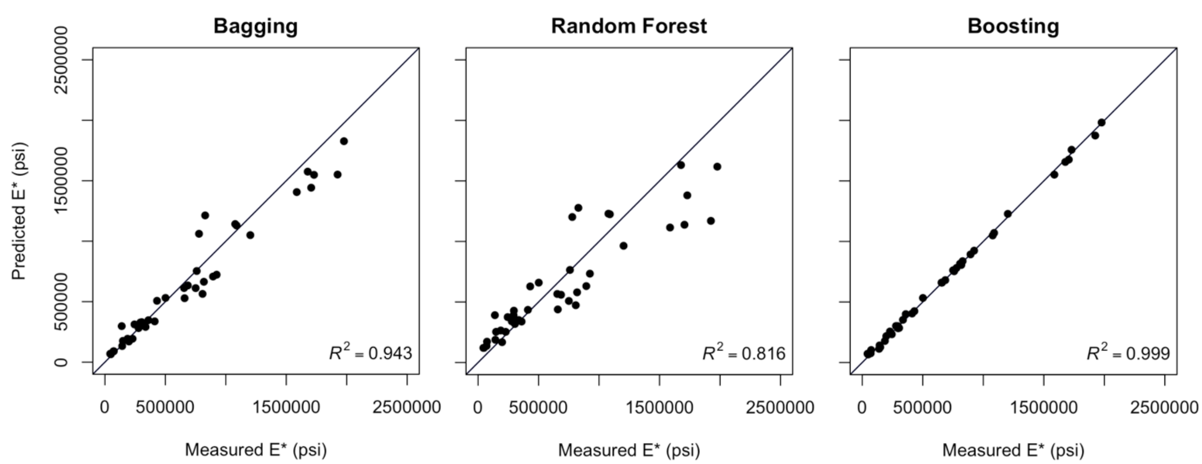

Figure 5.5. Method Comparison Using GDOT Predictors

5.3 Results and Discussion

Two highly accurate boosted regression tree models were developed as a result of the above |E*| prediction methods. The model generated using all applicable variables in the GDOT HMA materials library is considered slightly more accurate than the model generated using only the variables found in the original Witczak equation with R^2-values of 0.999 and 0.983, respectively. To determine which additional variables attributed to the increased accuracy of the second model, the relative influence of each input parameter was plotted for both model trees in Figure 5.6.

Relative influence is the measure of a variable's contribution to the output of the model. To simplify the comparison, only the 8 most influential variables among the 17 GDOT predictors are included in the plot. By a substantial margin, the loading temperature (temp_f) is considered the most important variable in the second model, accounting for over 75% of the total influence. Whereas binder viscosity (eta) drops to the fourth most valuable input, behind loading frequency (freq) and binder content (binder). Therefore, the inclusion of loading temperature as a predictor has a noticeable impact on model accuracy and should remain a primary variable of interest when considering future applications of the model.

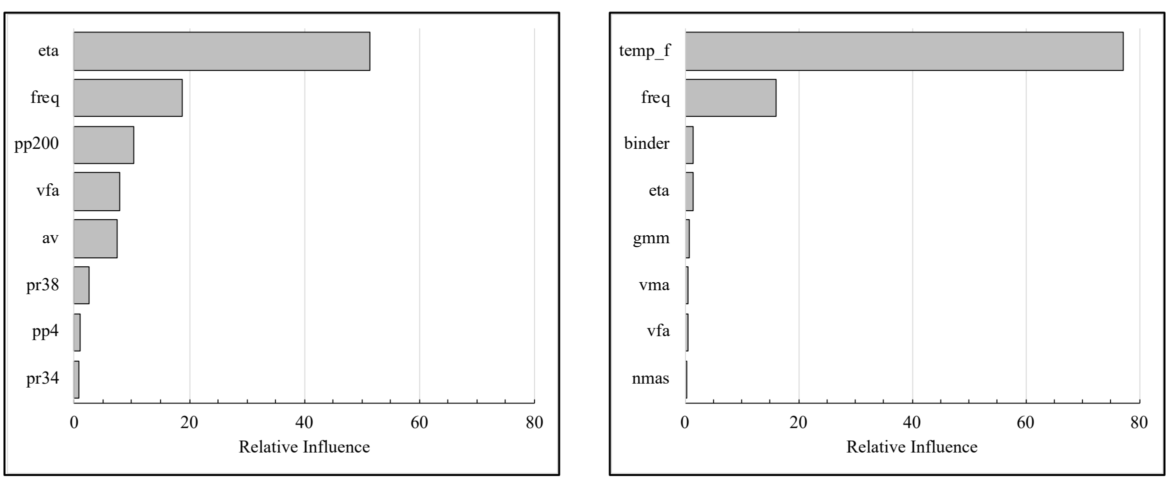

(a) Witczak 1-37A Predictors (b) GDOT Predictors

Figure 5.6. Relative Influence of Module Predictors

To compare the first regression tree model to the nationally calibrated PMED model, the measured versus predicted values were plotted against the output of the Witczak 1-37A equation for the same testing set (Figure 5.7). Analyzing this figure, the performance of the boosted regression tree far exceeds the PMED model when considering their |E*| estimation accuracy. An R^2-value of 0.392 for the original Witczak equation suggests the boosted tree model is far superior when applied to the HMA library developed by Kim et al. (2019). Consequently, tree-based methods are among the many other machine learning approaches to recommend as alternatives to the current MEPDG characterization models of dynamic modulus.

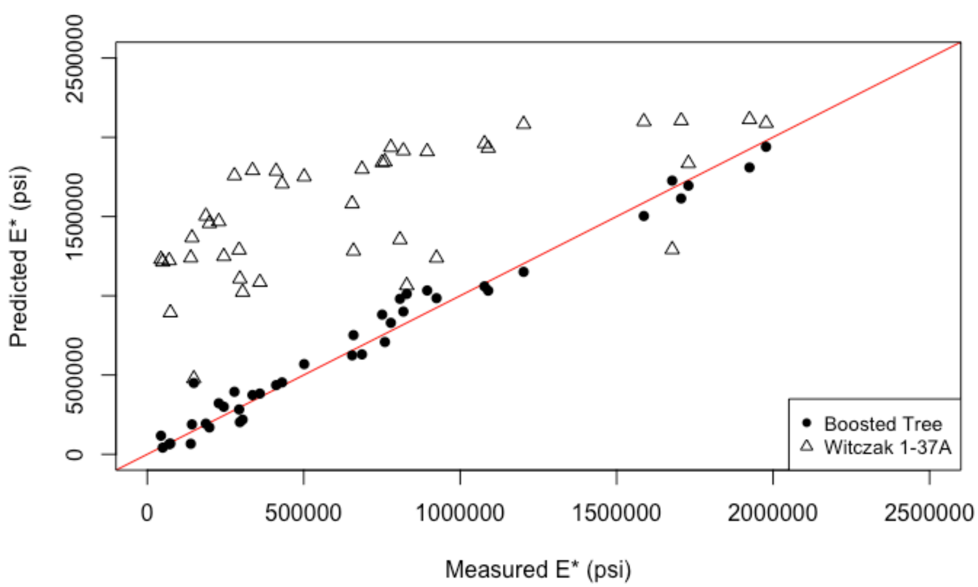

Figure 5.7. Boosted Tree Comparison to Witczak Equation

6.0 INTERCONVERSION OF DYNAMIC MODULUS TO CREEP COMPLIANCE

6.1 Application to Prony Series

Based on the results of previous literature, a Prony series representation of the LVE properties was selected as the basis for interconversion. The relaxation modulus of an LVE material can be derived from the generalized Maxwell (Wiechert) model, consisting of a spring and m Maxwell elements connected in parallel. Therefore, the relaxation modulus is represented using the Prony series as the following.

$$E(t) = E_\infty + \sum_{i=1}^{m} E_i e^{-\frac{t}{\rho_i}} \tag{6.1}$$

where:

E_∞	=	equilibrium modulus (Prony coefficient)
E_i	=	relaxation strengths (Prony coefficient)
ρ_i	=	relaxation times

Similarly, using the generalized Voigt (Kelvin) model, a spring and n Voigt element connected in series can be used to express the creep compliance of LVE materials. The Prony series representation for creep compliance is shown below.

$$D(t) = D_0 + \sum_{i=1}^{n} D_i (1 - e^{-\frac{t}{\tau_i}}) \tag{6.2}$$

where:

D_0	=	equilibrium (glassy) compliance (Prony coefficient)
D_i	=	retardation strengths (Prony coefficient)

τ_i = relaxation times

Applying the interrelationship defined by Park and Kim (1999) from Equation 3.33 to Equation 6.2, the Prony series parameters for relaxation modulus are derived as follows.

$$E_\infty = \frac{1}{D(t \to \infty)} \tag{6.3a}$$

$$E_i(\rho_i) = \frac{1}{D\left(\frac{\tau_i}{\alpha}\right)} \tag{6.3b}$$

$$\rho_i = \frac{\tau_i}{\alpha} \tag{6.3c}$$

Correspondingly, the Prony series parameters for creep compliance as expressed by the following.

$$D_0 = \frac{1}{E(t=0)} \tag{6.4a}$$

$$D_i(\tau_i) = \frac{1}{E(\alpha\rho_i)} \tag{6.4b}$$

$$\tau_i = \alpha\rho_i \tag{6.4c}$$

6.2 Time-Temperature Superposition Shift

With known Prony series coefficients, it is possible to characterize the master curve for LVE unit response functions. The master curve is used to express asphalt moduli as a function of temperature and loading rate. Asphalt's thermorheological behavior suggests that changes in its material properties due to variations in temperature and rate of loading are equivalent (Kim, 2009). Therefore, the principles of time-Temperature super position (t-Ts) can be applied. This principle permits the shift of modulus values relative to the time of loading or frequency, to an equivalent value along a single master curve (Figure 6.1).

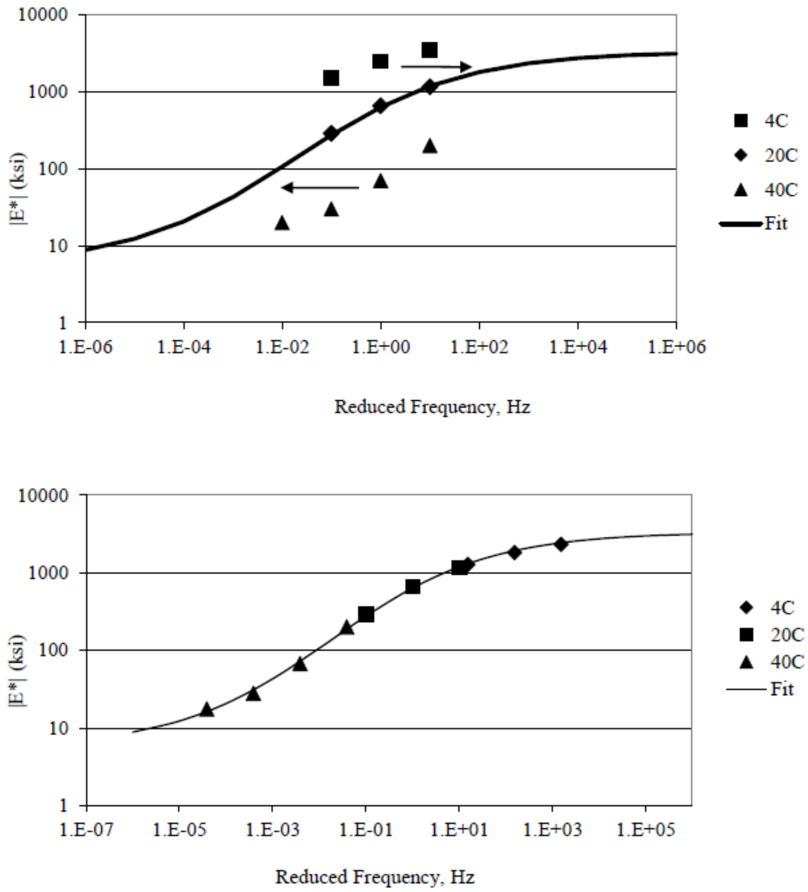

Figure 6.1. Sample Master Curve Development (Kim, et al., 2019)

The shift factor, *a*(*T*), defines the required shift for a given temperature and is a constant by which the reduced loading time, t_r, can be acquired.

$$t_r = \frac{t}{a(T)} \tag{6.5}$$

where:

t_r	=	reduced time of loading
t	=	actual time of loading
a(T)	=	shift factor as function of temperature, T

A common method for determining the shift factor is to use the following quadratic fit.

$$\log_{10}\left(a(T)\right) = aT^2 + bT + c \quad (6.5)$$

where:

T	=	desired temperature
a, b, c	=	regression coefficients

6.3 Interconversion Procedure

Using the principles outlined in the previous sections, the dynamic modulus library established for GDOT through the efforts of Kim, et al. (2019) was utilized to perform relaxation modulus to creep compliance interconversion. The following sections outline the steps required to achieve conversion and produce the results necessary for the PMED sensitivity analysis.

6.3.1 Model Inputs

In addition to the available dynamic modulus test results, the Prony coefficients, E_∞ and E_i, and relaxation times, ρ_i, for each of the 17 asphalt mixtures were generated prior to this investigation. These asphalt mixture characterizations are summarized for the first six mixtures in Table 6.1 and represent the inputs required for the conversion model. The coefficients and relaxation times for the remaining mixtures are located in Appendix B.

Table 6.1. Asphalt Mixture Prony Coefficients

A_12.5_64_M1		A_12.5_64_M2		A_12.5_67_N	
E∞	11,571.97	E∞	832.27	E∞	17,393.04
ρ*i*(s)	**E*i***	**ρ*i*(s)**	**E*i***	**ρ*i*(s)**	**E*i***
2.00E+08	5,323.92	2.00E+08	2,217.82	2.00E+08	11,772.59
2.00E+07	2,495.92	2.00E+07	1,462.60	2.00E+07	4,825.86
2.00E+06	6,710.90	2.00E+06	4,391.64	2.00E+06	13,256.04
2.00E+05	13,317.46	2.00E+05	11,358.37	2.00E+05	25,095.61
2.00E+04	30,287.13	2.00E+04	32,944.28	2.00E+04	53,679.75
2.00E+03	75,254.30	2.00E+03	98,773.77	2.00E+03	121,211.84
2.00E+02	198,804.11	2.00E+02	282,271.63	2.00E+02	280,528.92
2.00E+01	516,708.24	2.00E+01	702,517.22	2.00E+01	624,516.38
2.00E+00	1,189,381.06	2.00E+00	1,424,581.16	2.00E+00	1,242,534.43
2.00E-01	2,214,042.21	2.00E-01	2,292,146.06	2.00E-01	2,082,133.54
2.00E-02	3,199,098.01	2.00E-02	2,958,297.49	2.00E-02	2,861,620.54
2.00E-03	3,632,703.62	2.00E-03	3,168,805.07	2.00E-03	3,250,004.09
2.00E-04	3,392,167.02	2.00E-04	2,937,233.67	2.00E-04	3,142,419.52
2.00E-05	2,747,167.40	2.00E-05	2,448,991.43	2.00E-05	2,684,865.25
2.00E-06	2,019,458.53	2.00E-06	1,894,947.42	2.00E-06	2,097,940.84
2.00E-07	1,392,055.31	2.00E-07	1,391,153.19	2.00E-07	1,539,115.61
2.00E-08	953,374.33	2.00E-08	1,023,034.58	2.00E-08	1,122,623.96
A_12.5_76_N		**A_19_64_N**		**A_19_64_N2**	
E∞	23,717.09	E∞	16,794.19	E∞	36,886.99
ρ*i*(s)	**E*i***	**ρ*i*(s)**	**E*i***	**ρ*i*(s)**	**E*i***
2.00E+08	11,522.40	2.00E+08	13,493.79	2.00E+08	20,101.30
2.00E+07	4,704.30	2.00E+07	5,995.55	2.00E+07	9,920.00
2.00E+06	12,718.37	2.00E+06	16,499.57	2.00E+06	26,614.17
2.00E+05	23,530.23	2.00E+05	32,604.90	2.00E+05	53,479.79
2.00E+04	49,205.28	2.00E+04	72,499.49	2.00E+04	120,439.22
2.00E+03	109,329.75	2.00E+03	168,857.88	2.00E+03	283,598.58
2.00E+02	252,766.12	2.00E+02	394,311.82	2.00E+02	659,272.38
2.00E+01	572,880.63	2.00E+01	857,331.56	2.00E+01	1,378,983.00
2.00E+00	1,177,160.53	2.00E+00	1,611,499.33	2.00E+00	2,382,344.04
2.00E-01	2,043,812.26	2.00E-01	2,494,210.61	2.00E-01	3,255,499.90
2.00E-02	2,888,365.35	2.00E-02	3,144,208.62	2.00E-02	3,545,591.39
2.00E-03	3,329,276.96	2.00E-03	3,295,816.17	2.00E-03	3,206,859.04
2.00E-04	3,225,211.05	2.00E-04	2,980,377.89	2.00E-04	2,533,034.01
2.00E-05	2,734,416.93	2.00E-05	2,416,421.46	2.00E-05	1,825,071.64
2.00E-06	2,107,591.33	2.00E-06	1,814,681.17	2.00E-06	1,238,619.05
2.00E-07	1,520,329.26	2.00E-07	1,292,272.61	2.00E-07	808,540.02
2.00E-08	1,088,007.54	2.00E-08	920,991.42	2.00E-08	532,708.73

*Mixture IDs signify: Binder Plant ID_NMAS_PG ##-22_Region

Though not required for E(t) to D(t) interconversion, the loading temperature and shift factor coefficients are also considered inputs for the conversion model. The associated variables for each asphalt mixture are found in Table 6.2. These variables are necessary for determining creep compliance values at any combination of loading temperature and frequency as defined by the master curve. This is a crucial function of the model when considering the required Level 2 creep compliance inputs in PMED are specific to loading times of 1, 2, 5, 10, 20, 50, and 100 seconds at a mid-range temperature of 14°F (AASHTO, 2015a).

Table 6.2. Asphalt Mixture Shift Factors

Mixture ID	T_{ref}	a_1	a_2	a_3
A_12.5_64_M1	21.1	0.0010	-0.1637	3.0061
A_12.5_64_M2	21.1	0.0016	-0.1906	3.3311
A_12.5_67_N	21.1	0.0010	-0.1675	3.1055
A_12.5_76_N	21.1	0.0012	-0.1814	3.3000
A_19_64_N	21.1	0.0013	-0.1878	3.3923
A_19_64_N2	21.1	0.0018	-0.2138	3.7192
A_25_64_N2	21.1	0.0012	-0.1920	3.5038
B_9.5_64_M1	21.1	0.0013	-0.1791	3.2211
B_9.5_64_M2	21.1	0.0011	-0.1671	3.0454
B_9.5_67_S	21.1	0.0014	-0.1872	3.3239
B_12.5_64_M	21.1	0.0009	-0.1572	2.9034
B_12.5_67_S	21.1	0.0015	-0.1843	3.2201
B_19_64_M	21.1	0.0005	-0.1711	3.3876
B_25_64_M	21.1	0.0010	-0.1649	3.0177
C_9.5_67_M	21.1	0.0011	-0.1820	3.3618
C_12.5_67_M	21.1	0.0012	-0.1755	3.1886
C_12.5_76_M	21.1	0.0007	-0.1488	2.8172

*Mixture IDs signify: Binder Plant ID_NMAS_PG ##-22_Region

6.3.2 Model Conversion

Using the inputs from Table 6.1, Equation 6.1 was evaluated to model the relaxation modulus for all times $1.0\times10^{-6} \leq t \leq 1.0\times10^{7}$. Next, the creep compliance was estimated by applying the relationship in Equation 3.26 utilizing the principle of equivalent time, where t is adjusted by a factor of α, defined below.

$$\propto = \left(\frac{\sin n\pi}{n\pi}\right)^{\frac{1}{n}} \tag{6.6}$$

At this point, the relaxation curve and estimated creep compliance curve may be generated for comparison. The output for each of the 17 mixtures are highlighted in Figure 6.2. It is seen that each mixture follows the conventional decrease in relaxation modulus and increase in creep compliance as loading time increases, highlighting their nearly reciprocal relationship in the time domain.

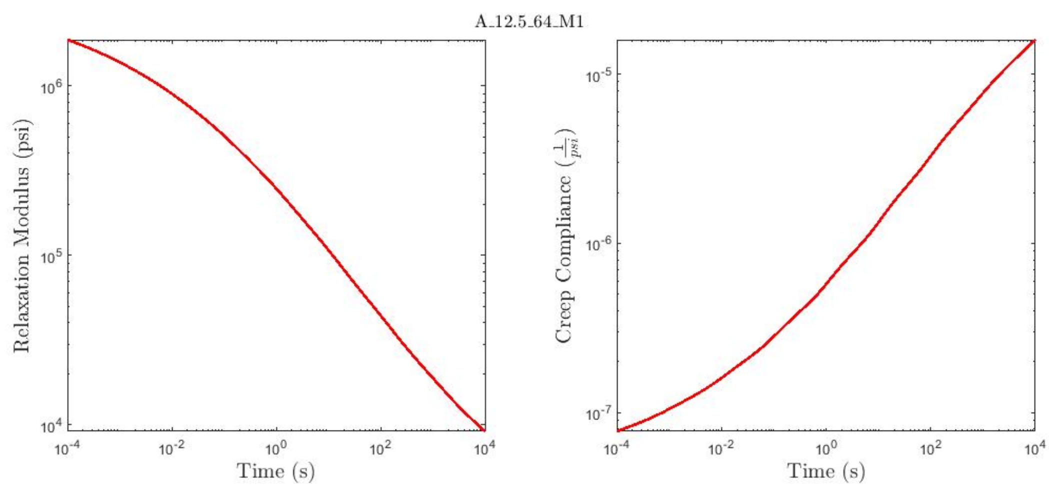

Figure 6.2.a. Relaxation Modulus and Creep Compliance Curves

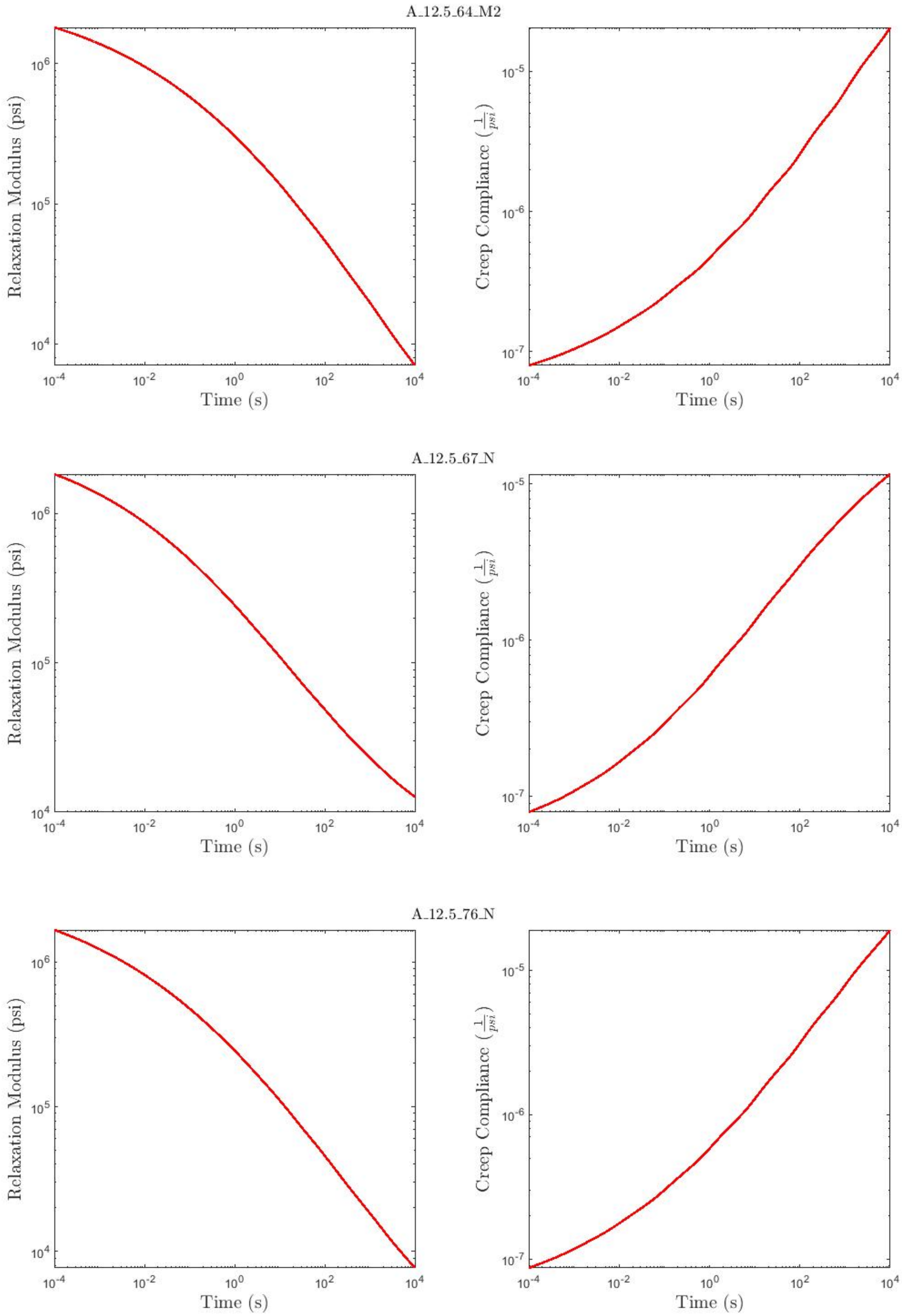

Figure 6.2.b. Relaxation Modulus and Creep Compliance Curves

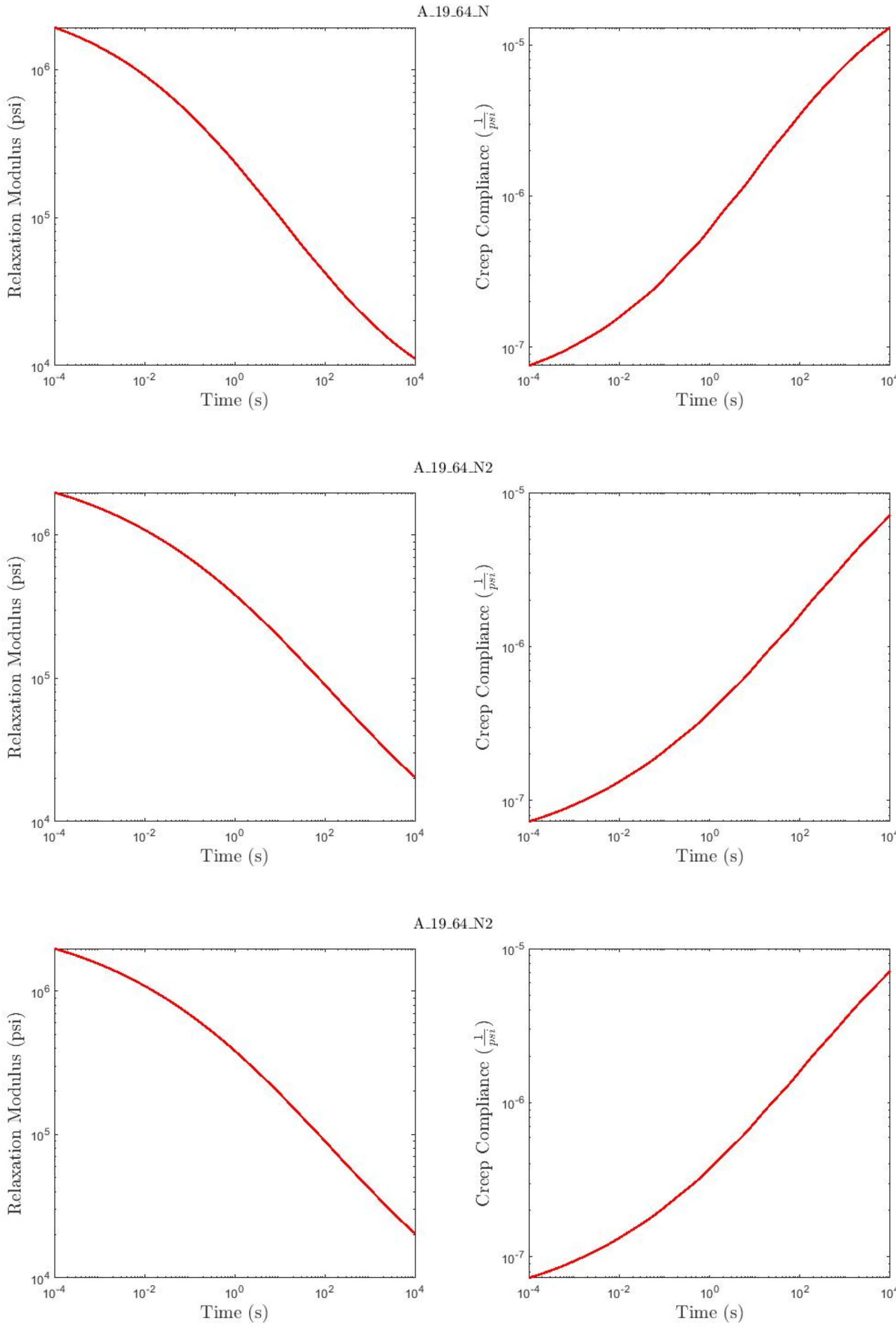

Figure 6.2.c. Relaxation Modulus and Creep Compliance Curves

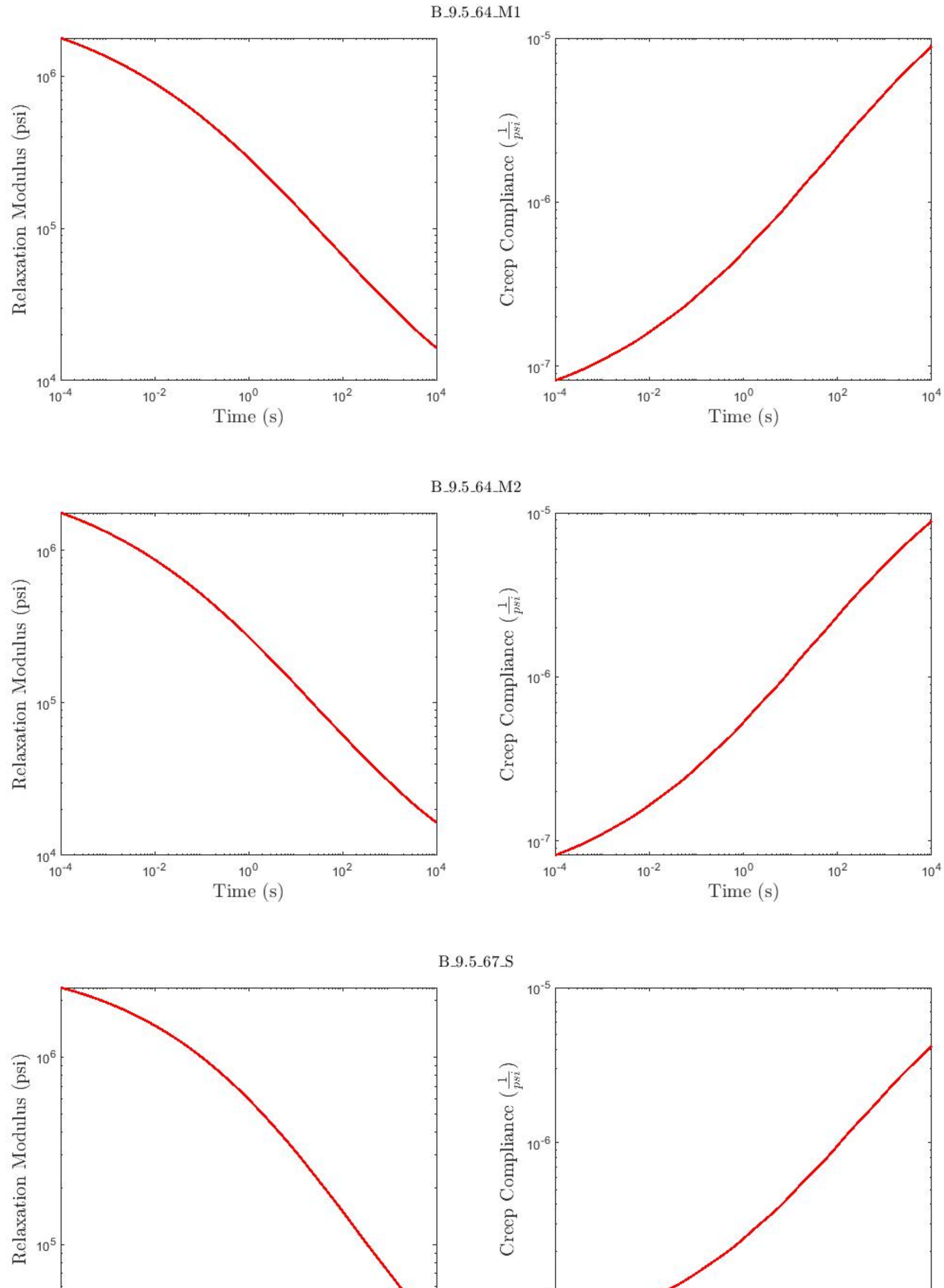

Figure 6.2.d. Relaxation Modulus and Creep Compliance Curves

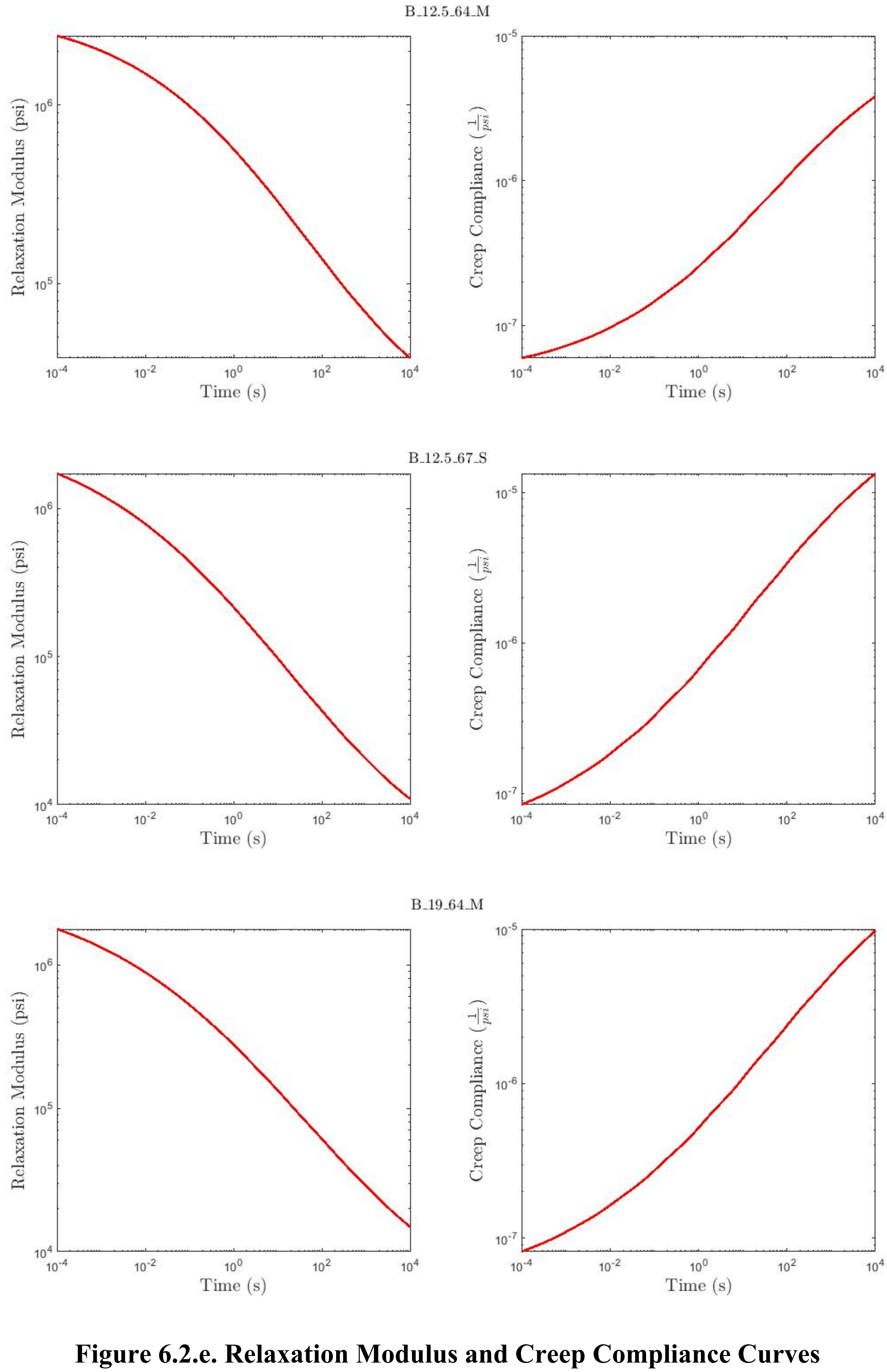

Figure 6.2.e. Relaxation Modulus and Creep Compliance Curves

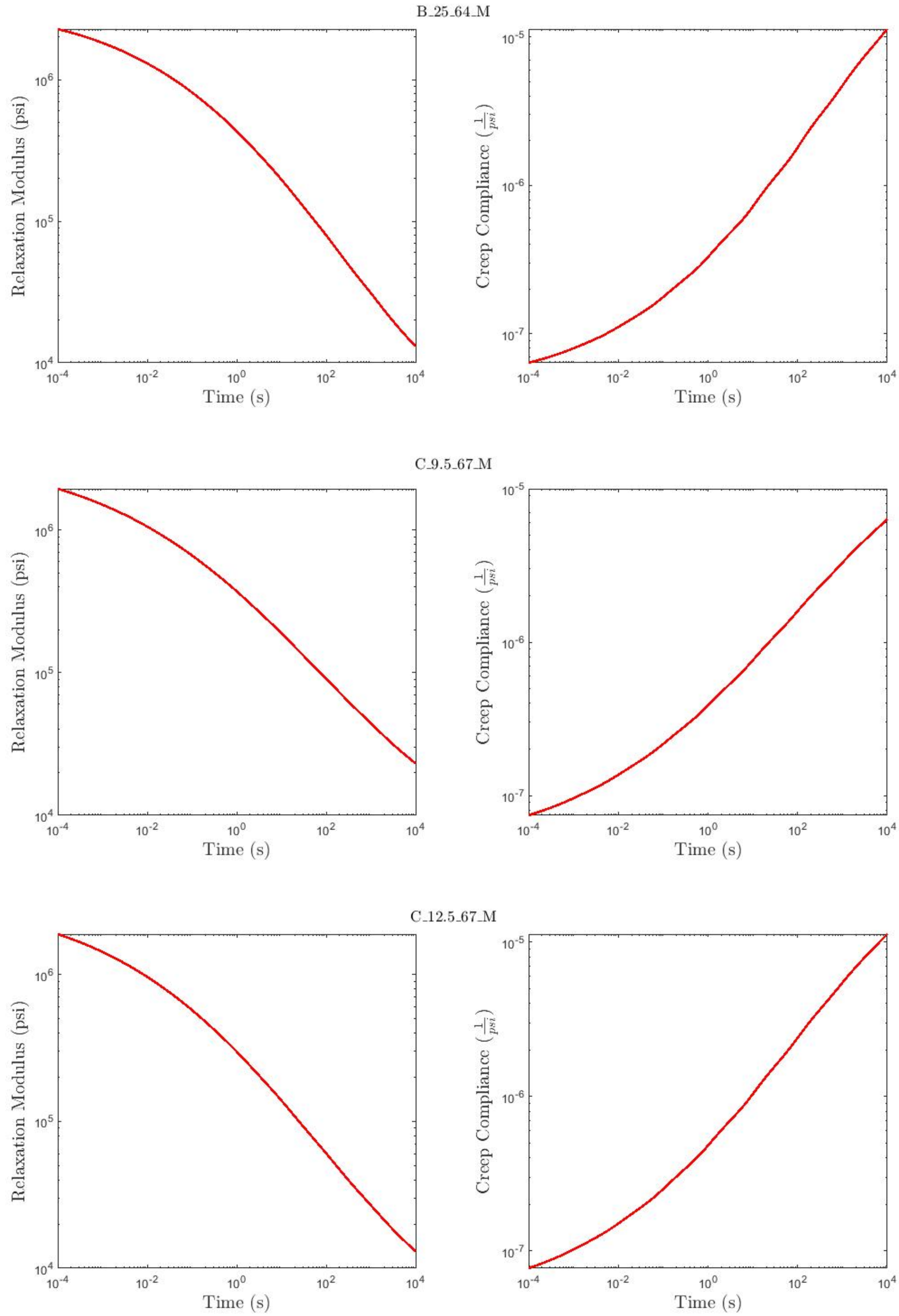

Figure 6.2.f. Relaxation Modulus and Creep Compliance Curves

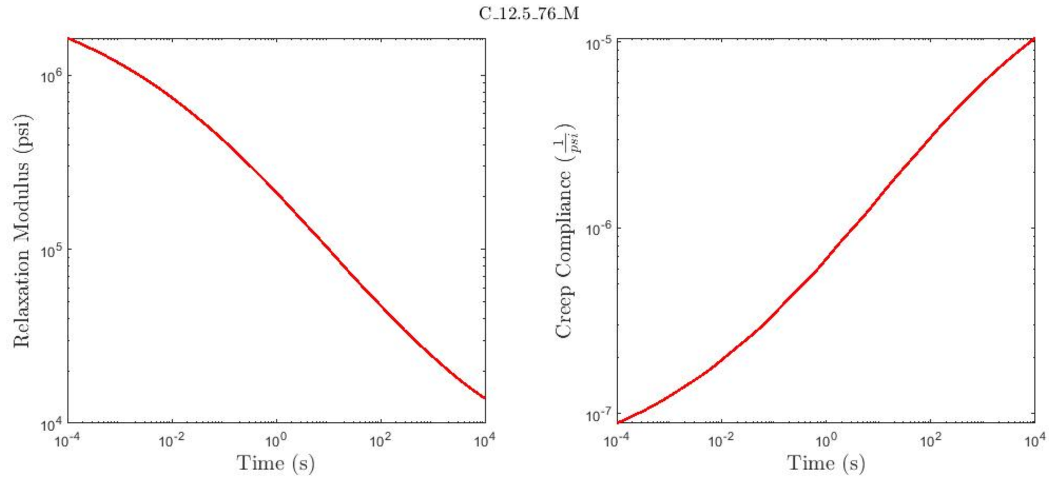

Figure 6.2.g. Relaxation Modulus and Creep Compliance Curves

6.4 Results and Discussion

As the primary utilization of the interconversion model is to analyze the effects of creep compliance in PMED, the most important output is the D(t) values at discrete loading times and temperatures. As previously stated, the model relies on the usage of three shift factors and a reference loading temperature to develop the creep compliance master curve for each mixture. Once generated, D(t) values may be extracted within a quantifiable range of temperatures and frequencies. As a result, the preferred output for this investigation is consistent with the inputs required for Level 2 creep compliance in PMED. These inputs are defined as 1/psi D(t) values at a temperature of 14°F and loading times of 1, 2, 5, 10, 20, 50, and 100 seconds. Using the model to extract the appropriate values, the results are summarized in Table 6.3. Supported by their representation in Figure 6.2, the values tend to increase as loading time increases. It can also be seen that mixtures with the largest NMAS contain the lowest creep compliance values.

Table 6.3. Creep Compliance Interconversion Model Outputs

	Mixture ID	Loading Time (s)						
		1	2	5	10	20	50	100
D(t) (1/psi) Mid Temperature (14F)	A_12.5_64_M1	1.67E-04	1.97E-04	2.27E-04	2.62E-04	2.92E-04	3.24E-04	3.56E-04
	A_12.5_64_M2	4.68E-04	6.07E-04	9.12E-04	1.06E-03	1.33E-03	1.69E-03	1.69E-03
	A_12.5_67_N	9.99E-05	1.13E-04	1.33E-04	1.54E-04	1.69E-04	1.91E-04	2.11E-04
	A_12.5_76_N	1.08E-04	1.20E-04	1.40E-04	1.50E-04	1.63E-04	1.80E-04	1.82E-04
	A_19_64_N	1.06E-04	1.25E-04	1.49E-04	1.64E-04	1.86E-04	2.04E-04	2.04E-04
	A_19_64_N2	8.19E-05	8.92E-05	1.03E-04	1.10E-04	1.10E-04	1.10E-04	1.10E-04
	A_25_64_N2	4.77E-05	5.24E-05	5.66E-05	6.01E-05	6.34E-05	6.46E-05	6.46E-05
	B_9.5_64_M1	1.56E-04	1.72E-04	2.00E-04	2.16E-04	2.31E-04	2.55E-04	2.62E-04
	B_9.5_64_M2	1.17E-04	1.30E-04	1.47E-04	1.64E-04	1.75E-04	1.91E-04	2.04E-04
	B_9.5_67_S	3.31E-04	4.01E-04	5.35E-04	6.04E-04	7.07E-04	8.51E-04	8.51E-04
	B_12.5_64_M	1.14E-04	1.31E-04	1.45E-04	1.58E-04	1.71E-04	1.83E-04	1.93E-04
	B_12.5_67_S	1.24E-04	1.39E-04	1.67E-04	1.81E-04	1.98E-04	2.23E-04	2.27E-04
	B_19_64_M	1.70E-04	1.94E-04	2.49E-04	2.81E-04	3.11E-04	3.66E-04	3.81E-04
	B_25_64_M	4.87E-05	5.51E-05	6.22E-05	6.96E-05	7.53E-05	8.20E-05	8.80E-05
	C_9.5_67_M	8.26E-05	9.40E-05	1.12E-04	1.21E-04	1.33E-04	1.49E-04	1.49E-04
	C_12.5_67_M	1.43E-04	1.60E-04	1.95E-04	2.18E-04	2.38E-04	2.73E-04	2.89E-04
	C_12.5_76_M	8.37E-05	9.68E-05	1.13E-04	1.23E-04	1.36E-04	1.51E-04	1.61E-04

*Mixture IDs signify: Binder Plant ID_NMAS_PG ##-22_Region

7.0 PMED EVALUATION

7.1 Introduction

Developing a comprehensive library of material inputs for the MEPDG is a time-consuming and costly process that requires material acquisition, specimen fabrication, laboratory testing, result validation, and more. Therefore, the objective of this section is to evaluate the necessity of laboratory-quantified creep compliance values for typical Georgia asphalt mixtures. Without a D(t) library, GDOT currently relies on the creep compliance prediction model within the PMED software associated with Level 3 inputs. As of version 2.5 of the software, this model relies only on the binder properties of the asphalt mixture to determine a creep compliance estimate. By using the interconversion model presented in Section 6, more accurate estimates of D(t) may be used to evaluate the impact of creep compliance on the PMED performance indicators.

To effectively evaluate the impact of higher-level D(t) inputs in PMED, a testing matrix was developed for 7 asphalt surface mixtures gathered from experiments conducted by Kim et al. (2019). The matrix accounts for four scenarios of differing input levels for both dynamic modulus and creep compliance, as these are the primary mechanical properties for asphalt materials. A summary of this approach is found in Table 7.1.

In this scenario, Level 3 inputs represent the recommended global default values for each property provided by the GDOT Pavement ME Design User Guide and developed by National Cooperative Highway Research Program (NCHRP) projects 1-37A and 1-40D (ARA, 2015). Level 1 inputs are the dynamic modulus values determined by uniaxial compression testing under standard procedure AASHTO TP 79 performed by Kim et al. (2019). These values take the form of discrete |E*| measurements at differing temperatures and frequencies. Level 2 D(t) inputs are considered the converted creep compliance values produced from the dynamic modulus library using the interconversion method discussed in Section 6. Inputs at this level require D(t) values at 14°F for loading times of 1, 2, 5, 10, 20, 50, and 100 seconds. A comprehensive summary of the remaining design inputs is provided in the next section.

Table 7.1. PMED Sensitivity Analysis Matrix

Scenario No.	Input Types	Mixture No.	Mixture ID
1 (Control)	Level 3 |E*| Level 3 D(t)	1	A_12.5_64_M1
		2	A_12.5_67_N
		3	A_12.5_76_N
		4	B_9.5_64_M1
		5	B_12.5_64_M
		6	B_12.5_67_S
		7	C_9.5_67_M
2	Level 1 |E*| Level 3 D(t)	1	A_12.5_64_M1
		2	A_12.5_67_N
		3	A_12.5_76_N
		4	B_9.5_64_M1
		5	B_12.5_64_M
		6	B_12.5_67_S
		7	C_9.5_67_M
3	Level 1 |E*| Level 2 D(t)	1	A_12.5_64_M1
		2	A_12.5_67_N
		3	A_12.5_76_N
		4	B_9.5_64_M1
		5	B_12.5_64_M
		6	B_12.5_67_S
		7	C_9.5_67_M
4	Level 3 |E*| Level 2 D(t)	1	A_12.5_64_M1
		2	A_12.5_67_N
		3	A_12.5_76_N
		4	B_9.5_64_M1
		5	B_12.5_64_M
		6	B_12.5_67_S
		7	C_9.5_67_M

*Mixture IDs signify: Binder Plant ID_NMAS_PG ##-22_Region

7.2 PMED Pavement Design

To reduce the impact of extraneous variables, the pavement structure as well as the traffic and climate inputs remained constant across each trial for all four scenarios. Consequently, a representative flexible pavement design was developed for the PMED evaluation. Using GDOT's Traffic Analysis and Data Application (TADA) tool, a roadway section of I-85 was selected in the north-eastern region of Georgia (Figure 7.1). The section is a 6-lane divided highway that is considered both an interstate route and freight route with a posted speed limit of 65 mph. For the purpose of this analysis, all design inputs are selected using recommended values for new flexible pavements derived from *The GDOT Pavement ME Design User Input Guide* (ARA, 2015).

Figure 7.1. PMED Analysis Roadway Section Location

7.2.1 Pavement Structure

The pavement structure used in this design was selected based on typical GDOT flexible pavement profiles and the thickness recommendations found in the aforementioned user guide. The layers and associated thicknesses are displayed in Figure 7.2. An adjusted thickness of 2.75 inches for the surface HMA mixture was used to satisfy the PMED restriction of three asphalt layers. The adjusted thickness is a combined value representative of the surface HMA layer and an open-grade friction coarse (OGFC) layer.

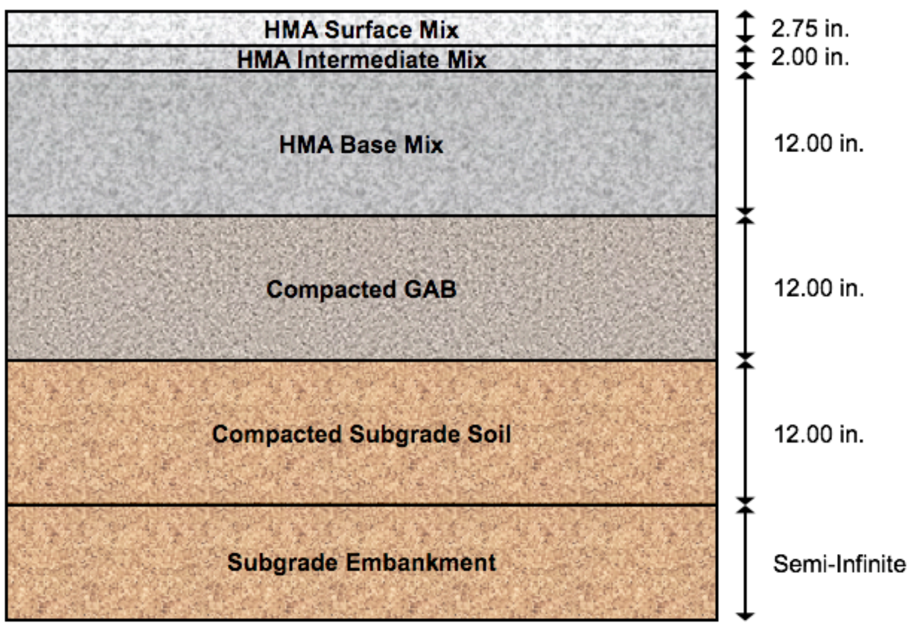

Figure 7.2. PMED Analysis Pavement Profile

While only 7 surface asphalt mixtures are included in the analysis, HMA base and binder mixtures from the GDOT library were selected to model the base and intermediate layers of the pavement. The mixtures used for the base and binder layers were A_19_64_N and B_25_64_M, respectively. This selection remained constant throughout each trial; however, the material inputs were adjusted appropriately for each scenario based on the design level.

7.2.2 Design Inputs

This section serves to identify all primary inputs required to run the flexible pavement analysis in PMED to achieve the performance output. These inputs may be categorized by calibration factors, traffic, climate, and pavement layer inputs. Each category is discussed in the order in which they were defined in the software.

The use of Georgia-specific calibration factors is necessary to achieve an accurate and indicative performance prediction in PMED. These factors have a direct effect on the empirical part of the distress prediction model that relate the critical pavement response to the pavement distress, known as the transfer function (AASHTO, 2015a). The most updated Georgia calibration factors and transfer functions in PMED version 2.5 were used for the analysis conducted herein and are referenced in Table 7.2. The pavement performance predicted using these factors is noticeably different than that generated using global calibration coefficients in that the localized factors predict greater bottom-up fatigue cracking and lesser IRI, rutting, and thermal cracking.

Table 7.2. PMED Calibration Factors for New Flexible Pavements

Performance Indicator	Transfer Function Coefficient	GDOT Value
AC Cracking- Bottom Up	C1	2.2
	C2	2.2
	C3	6000
	Standard Deviation	1.0+10/(1+exp(7.57-6.5*LOG10(BOTTOM+0.0001)))
AC Cracking- Top Down	C1	7.0
	C2	3.5
	C3	0.0
	C4	1000
	Standard Deviation	200+2300/(1+exp(1.072-2.1654*LOG10(TOP+0.001)))

Performance Indicator		Transfer Function Coefficient	GDOT Value
AC Fatigue		BF1	1.0
		BF2	1.0
		BF3	1.0
		K1	0.00151
		K2	3.9492
		K3	1.281
AC Rutting		BR1	1.0
		BR2	1.0
		BR3	1.0
		K1	-2.45
		K2	1.5606
		K3	0.30
		Standard Deviation	0.2*Pow(RUT,0.500)+0.001
IRI		C1	40
		C2	0.40
		C3	0.008
		C4	0.015
Thermal Fraction	All Levels	K	0.35
	Level 1	Standard Deviation	0.1468*THERMAL+65.027
	Level 2	Standard Deviation	0.2841*THERMAL+55.462
	Level 3	Standard Deviation	0.3972*THERMAL+20.422
Subgrade Rutting	Subgrade	BS1	0.50
		K1	1.35
		Standard Deviation	0.1235*Pow(BASERUT,0.6711)+0.001
	Granular Base	BS2	0.50
		K1	2.03
		Standard Deviation	0.2841*Pow(BASERUT,0.6711)+0.001

Basic traffic inputs, such as AADTT, were selected using the information provided via GDOT's TADA tool from the I-85 roadway section. The truck volume distribution factors and axle load distribution factors were provided through GDOT's traffic library. Monthly seasonal independent distributions are recommended for freight routes and the GDOT Heavy 2 distributions are preferred for roadway ADTs greater than 2,000. The remaining inputs are default values provided by the software and recommended by GDOT's user guide. The complete list of traffic input parameters is shown in Table 7.3.

Table 7.3. PMED Traffic Inputs

Type	Name	Value
Truck Volume Distribution Factors	Truck Volume Distribution Factors	GA Monthly Seasonal Independent
AADTT	Two-way AADTT	14000
	Number of lanes	3
	Percent trucks in design direction	50
	Percent trucks in design lane	80
	Operational speed (mph)	65
Traffic Capacity	Traffic Capacity	Not Enforced
Axle Configuration	Average axle width (ft)	8.5
	Tandem axle spacing (in)	51.6
	Dual tire spacing (in)	12
	Quad axle spacing (in)	49.2
	Tire pressure (psi)	120
	Tridem axle spacing (in)	49.2
Lateral Wander	Design lane width (ft)	12
	Mean wheel location (in)	18
	Traffic wander standard deviation (in)	10
Wheelbase	Average spacing of long axle (ft)	18
	Average spacing of medium axle (ft)	15
	Percent trucks with long axle (%)	61
	Percent trucks with medium axle (%)	22
	Percent trucks with short axle (%)	17
	Average spacing of short axles (ft)	12
Axle Load Configuration	Load Default Distribution	TTC-2
	Growth Rate	1.5
	Growth Function	Linear
	Axle Load Distribution Factors	GDOT H2

The climate inputs in version 2.5 of PMED are defined by selecting a MERRA-2 climate station in close proximity to the roadway section. Custom Georgia climate stations were generated for GDOT as part of an ongoing climate study conducted by the University of Georgia and Michigan State University. A singular custom station, US GA 137243, was integrated into PMED at the time of this study and was selected for all analysis.

The subgrade and GAB layer inputs remained constant throughout the analysis to reduce their impact on the performance predictions. The inputs selected for these layers are presented in Table 7.4 and were defined by following the steps outline in the GDOT user guide for unbound materials in the northeast regions of Georgia.

The HMA layer properties varied for each mixture at each design level. Seven surface mixtures were investigated along with one base mixture and one binder mixture that remained constant for each trial under the four scenarios outlined in Table 7.1. Table 7.5 depicts the input properties associated with the three layers of HMA. Due to the variation in input parameters across design levels for asphalt binder, dynamic modulus, and creep compliance inputs, Appendix C is referenced for specific values. To illustrate the difference between Level 1, 2, and 3 asphalt mechanical property inputs, the input values at each level for mixture A_12.5_64_M1 are found in Table 7.6.

Table 7.4. PMED Unbound Material Inputs

Pavement Material	Input Type	Input Name	Input Value
Subgrade Embankment	Identifiers	Display Identifier	A-6
	Unbound	Coefficient of lateral earth pressure (k0)	0.5
		Thickness (in)	Semi-Infinite
		Poisson's ratio	0.45
	Modulus	Resilient Modulus	8000
	Sieve	Gradation	A-6
		Liquid Limit	39
		Plasticity Index	13
		Maximum dry unit weight (pcf)	100
		Water content (%)	19.1
		Is Layer Compacted?	FALSE
Compacted Subgrade	Identifiers	Display Identifier	A-6
	Unbound	Coefficient of lateral earth pressure (k0)	0.5
		Thickness (in)	12
		Poisson's ratio	0.45
	Modulus	Resilient Modulus	8000
	Sieve	Gradation	A-6
		Liquid Limit	39
		Plasticity Index	13
		Maximum dry unit weight (pcf)	100
		Water content (%)	19.1
		Is Layer Compacted?	TRUE
Compacted GAB	Identifiers	Display Identifier	A-1-a
	Unbound	Coefficient of lateral earth pressure (k0)	0.5
		Thickness (in)	12
		Poisson's ratio	0.3
	Modulus	Resilient Modulus	23000
	Sieve	Gradation	A-1-a
		Liquid Limit	6.0
		Plasticity Index	1.0
		Maximum dry unit weight (pcf)	136.5
		Water content (%)	6.0
		Is Layer Compacted?	TRUE

Table 7.5. PMED AC Pavement Material Inputs

Pavement Material	Input Type	Input Name	Input Value
HMA Base Layer	Identifiers	Display Identifier	Default_Asphalt Concrete
	Asphalt Layer	Thickness (in)	12
	Mixture Volumetrics	Air voids (%)	5.9
		Effective binder content (%)	9.4
		Poisson's ratio	*Calculated*
		Unit weight (pcf)	145
	Mechanical Properties	Asphalt binder	SEE APPENDIX C
		Creep compliance (1/psi)	SEE APPENDIX C
		Dynamic modulus	SEE APPENDIX C
		Select HMA Estar predictive model	Viscosity Based Model
		Reference temperature (deg F)	70
	Thermal	Heat capacity (BTU/lb-deg F)	0.23
		Thermal conductivity (BTU/hr-ft-deg F)	0.67
		Thermal contraction	*Calculated*
HMA Binder Layer	Identifiers	Display Identifier	Default_Asphalt Concrete
	Asphalt Layer	Thickness (in)	2
	Mixture Volumetrics	Air voids (%)	5.5
		Effective binder content (%)	11.6
		Poisson's ratio	*Calculated*
		Unit weight (pcf)	145
	Mechanical Properties	Asphalt binder	SEE APPENDIX C
		Creep compliance (1/psi)	SEE APPENDIX C
		Dynamic modulus	SEE APPENDIX C
		Select HMA Estar predictive model	Viscosity Based Model
		Reference temperature (deg F)	70
	Thermal	Heat capacity (BTU/lb-deg F)	0.23
		Thermal conductivity (BTU/hr-ft-deg F)	0.67
		Thermal contraction	*Calculated*
HMA Surface Layer	Identifiers	Display Identifier	Default_Asphalt Concrete
	Asphalt Layer	Thickness (in)	2.75
	Mixture Volumetrics	Air voids (%)	SEE APPENDIX C
		Effective binder content (%)	SEE APPENDIX C
		Poisson's ratio	*Calculated*
		Unit weight (pcf)	SEE APPENDIX C
	Mechanical Properties	Asphalt binder	SEE APPENDIX C
		Creep compliance (1/psi)	SEE APPENDIX C
		Dynamic modulus	SEE APPENDIX C
		Select HMA Estar predictive model	Viscosity Based Model
		Reference temperature (deg F)	70
		Indirect Tensile Strength at 14 deg F (psi)	*Calculated*
	Thermal	Heat capacity (BTU/lb-deg F)	0.23
		Thermal conductivity (BTU/hr-ft-deg F)	0.67
		Thermal contraction	*Calculated*

Table 7.6.a. Mechanical Property Inputs for Mixture A_12.5_64_M1

<table>
<tr><th>Input Name</th><th>Design Level</th><th colspan="7">Input Value</th></tr>
<tr><td rowspan="16">Dynamic Modulus</td><td rowspan="5">3</td><td colspan="3">Gradation</td><td colspan="4">Percent Passing</td></tr>
<tr><td colspan="3">3/4-inch-sieve</td><td colspan="4">100</td></tr>
<tr><td colspan="3">3/8-inch-sieve</td><td colspan="4">86</td></tr>
<tr><td colspan="3">No. 4 sieve</td><td colspan="4">74</td></tr>
<tr><td colspan="3">No. 200 sieve</td><td colspan="4">5.8</td></tr>
<tr><td rowspan="5">2</td><td colspan="3">Gradation</td><td colspan="4">Percent Passing</td></tr>
<tr><td colspan="3">3/4-inch-sieve</td><td colspan="4">100</td></tr>
<tr><td colspan="3">3/8-inch-sieve</td><td colspan="4">86</td></tr>
<tr><td colspan="3">No. 4 sieve</td><td colspan="4">74</td></tr>
<tr><td colspan="3">No. 200 sieve</td><td colspan="4">5.8</td></tr>
<tr><td rowspan="6">1</td><td></td><td colspan="6">Frequency (Hz)</td></tr>
<tr><td>Temperature (deg F)</td><td>0.1</td><td>0.5</td><td>1.0</td><td>5.0</td><td>10</td><td>25</td></tr>
<tr><td>39.2</td><td>740802</td><td>1082794</td><td>1202705</td><td>1586888</td><td>1706096</td><td>1924615</td></tr>
<tr><td>68</td><td>150334</td><td>278518</td><td>336268</td><td>564559</td><td>658669</td><td>818440</td></tr>
<tr><td>104</td><td>24296</td><td>46335</td><td>58625</td><td>113719</td><td>142644</td><td>198566</td></tr>
<tr><td>130</td><td>11119</td><td>19491</td><td>24290</td><td>46322</td><td>58611</td><td>83996</td></tr>
</table>

Table 7.6.b. Mechanical Property Inputs for Mixture A_12.5_64_M1

<table>
<tr><th>Input Name</th><th>Design Level</th><th colspan="3">Input Value</th></tr>
<tr><td rowspan="9">Asphalt Binder</td><td>3</td><td colspan="3">SuperPave: 64-22</td></tr>
<tr><td rowspan="4">2</td><td>Temperature (deg F)</td><td>Binder Gstar (Pa)</td><td>Phase angle (deg)</td></tr>
<tr><td>147.2</td><td>8850</td><td>79.1</td></tr>
<tr><td>158</td><td>4220</td><td>82</td></tr>
<tr><td>168.8</td><td>2070</td><td>84.1</td></tr>
<tr><td rowspan="4">1</td><td>Temperature (deg F)</td><td>Binder Gstar (Pa)</td><td>Phase angle (deg)</td></tr>
<tr><td>147.2</td><td>8850</td><td>79.1</td></tr>
<tr><td>158</td><td>4220</td><td>82</td></tr>
<tr><td>168.8</td><td>2070</td><td>84.1</td></tr>
</table>

Table 7.6.c. Mechanical Property Inputs for Mixture A_12.5_64_M1

<table>
<tr><th>Input Name</th><th>Design Level</th><th colspan="4">Input Value</th></tr>
<tr><td rowspan="19">Creep Compliance</td><td>3</td><td colspan="4">Calculated</td></tr>
<tr><td rowspan="8">2</td><td>Loading Time (sec)</td><td colspan="3">Mid Temp (14 deg F)</td></tr>
<tr><td>1</td><td colspan="3">0.000167</td></tr>
<tr><td>2</td><td colspan="3">0.000197</td></tr>
<tr><td>5</td><td colspan="3">0.000227</td></tr>
<tr><td>10</td><td colspan="3">0.000262</td></tr>
<tr><td>20</td><td colspan="3">0.000292</td></tr>
<tr><td>50</td><td colspan="3">0.000324</td></tr>
<tr><td>100</td><td colspan="3">0.000356</td></tr>
<tr><td rowspan="8">1</td><td>Loading Time (sec)</td><td>Low Temp (-4 deg F)</td><td>Mid Temp (14 deg F)</td><td>High Temp (32 deg F)</td></tr>
<tr><td>1</td><td>NA</td><td>NA</td><td>NA</td></tr>
<tr><td>2</td><td>NA</td><td>NA</td><td>NA</td></tr>
<tr><td>5</td><td>NA</td><td>NA</td><td>NA</td></tr>
<tr><td>10</td><td>NA</td><td>NA</td><td>NA</td></tr>
<tr><td>20</td><td>NA</td><td>NA</td><td>NA</td></tr>
<tr><td>50</td><td>NA</td><td>NA</td><td>NA</td></tr>
<tr><td>100</td><td>NA</td><td>NA</td><td>NA</td></tr>
</table>

7.2.3 Performance Output

The output report published by PMED includes the prediction values for terminal IRI, permanent deformation of the total pavement, bottom-up fatigue cracking, thermal cracking, top-down fatigue cracking, and permanent deformation of the asphalt layers for a 20-year design life. Currently, the output generated for the top-down fatigue cracking and permanent deformation of the asphalt layers is considered inconsequential and should be ignored as of version 2.5 of the software. As a result, all subsequent analysis will only consider the four remaining distress types. A summary of the PMED performance output is shown in Table 7.7.

Table 7.7. PMED Pavement Performance Predictions

Scenario No.	Input Types	Mixture ID	Terminal IRI (in/mile)	Perm. Def.- Total Pavement (in.)	AC Bot-Up Fatigue Crack. (%)	AC Thermal Cracking (ft/mile)	AC Top-Down Fat. Crack. (ft/mile)	Perm. Def.- AC only (in)
1	Level 3 |E*| Level 3 D(t)	A_12.5_64_M1	177.58	0.44	1.70	1330.56	1599.04	0.48
		A_12.5_67_N	185.68	0.45	1.70	1235.52	14710.80	0.48
		A_12.5_76_N	172.64	0.38	1.70	1193.28	1330.78	0.40
		B_9.5_64_M1	183.69	0.48	1.71	1267.20	9910.72	0.52
		B_12.5_64_M	177.46	0.44	1.70	1330.56	1537.06	0.47
		B_12.5_67_S	184.51	0.45	1.70	1267.20	12695.65	0.48
		C_9.5_67_M	185.71	0.46	1.71	1393.92	11551.11	0.50
2	Level 1 |E*| Level 3 D(t)	A_12.5_64_M1	184.41	0.58	1.70	1288.32	2045.84	0.65
		A_12.5_67_N	183.35	0.56	1.71	1288.32	3683.32	0.62
		A_12.5_76_N	168.13	0.50	1.68	1.00	6753.98	0.55
		B_9.5_64_M1	176.89	0.58	1.70	629.38	2749.27	0.64
		B_12.5_64_M	171.54	0.59	1.69	3.63	4159.44	0.67
		B_12.5_67_S	190.34	0.49	1.70	1457.28	14712.08	0.53
		C_9.5_67_M	183.22	0.51	1.70	1499.52	1310.40	0.57
3	Level 1 |E*| Level 2 D(t)	A_12.5_64_M1	192.09	0.58	1.70	2006.40	2045.84	0.65
		A_12.5_67_N	192.20	0.56	1.71	2112.00	3683.32	0.62
		A_12.5_76_N	168.13	0.50	1.68	1.00	6753.98	0.55
		B_9.5_64_M1	193.04	0.58	1.70	2112.00	2749.28	0.64
		B_12.5_64_M	194.47	0.59	1.69	2112.00	4159.44	0.67
		B_12.5_67_S	197.25	0.49	1.70	2112.00	14712.08	0.53
		C_9.5_67_M	189.73	0.51	1.70	2112.00	1310.40	0.57
4	Level 3 |E*| Level 2 D(t)	A_12.5_64_M1	184.86	0.44	1.70	2006.40	1599.04	0.48
		A_12.5_67_N	195.09	0.45	1.70	2112.00	14710.80	0.48
		A_12.5_76_N	159.32	0.38	1.70	1.00	1330.78	0.40
		B_9.5_64_M1	192.77	0.48	1.71	2112.00	9910.72	0.52
		B_12.5_64_M	185.92	0.44	1.70	2112.00	1537.06	0.47
		B_12.5_67_S	193.58	0.45	1.70	2112.00	12695.65	0.48
		C_9.5_67_M	193.36	0.46	1.71	2112.00	11551.11	0.50

7.3 Analysis of Pavement Performance

To determine if these responses show any significant variance across differing input levels, the results of Table 7.7 were analyzed both graphically and statistically. Figure 7.3 depicts the distress predictions one at a time for each asphalt mixture across the four different scenarios. The conglomerate output of each scenario was then utilized to generate a set of summary statistics located in Table 7.8.

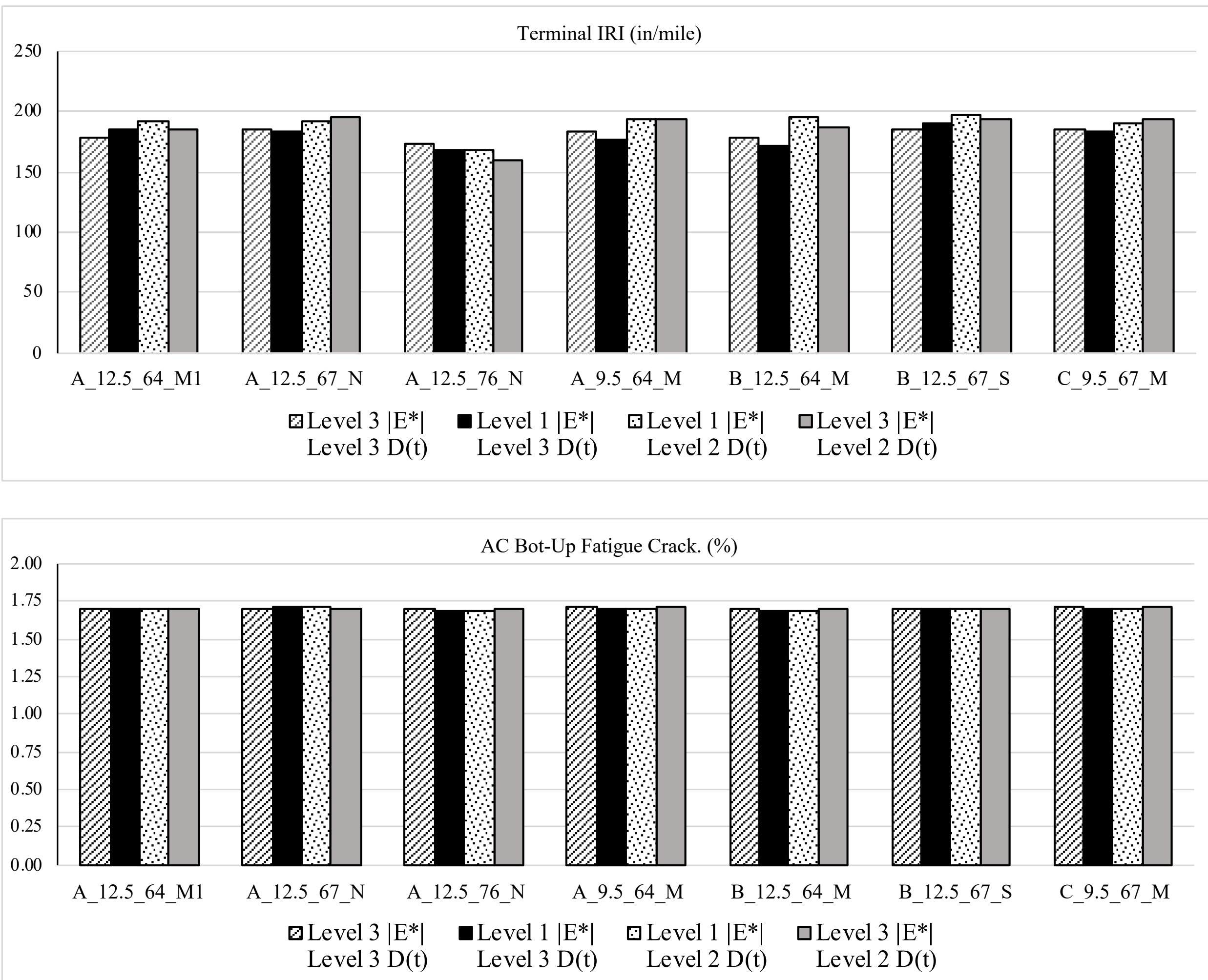

Figure 7.3.a. PMED Pavement Performance Predictions

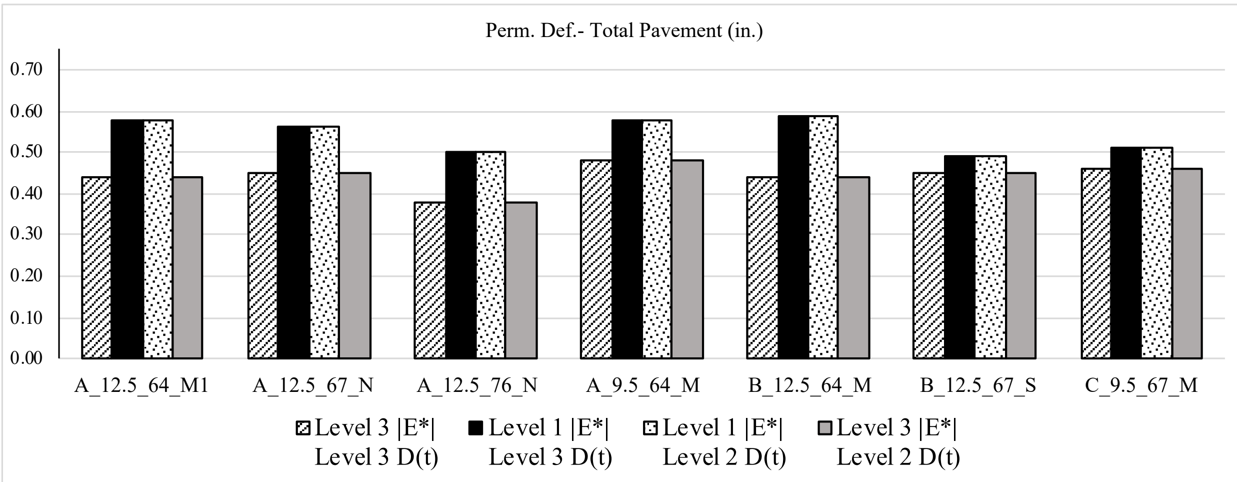

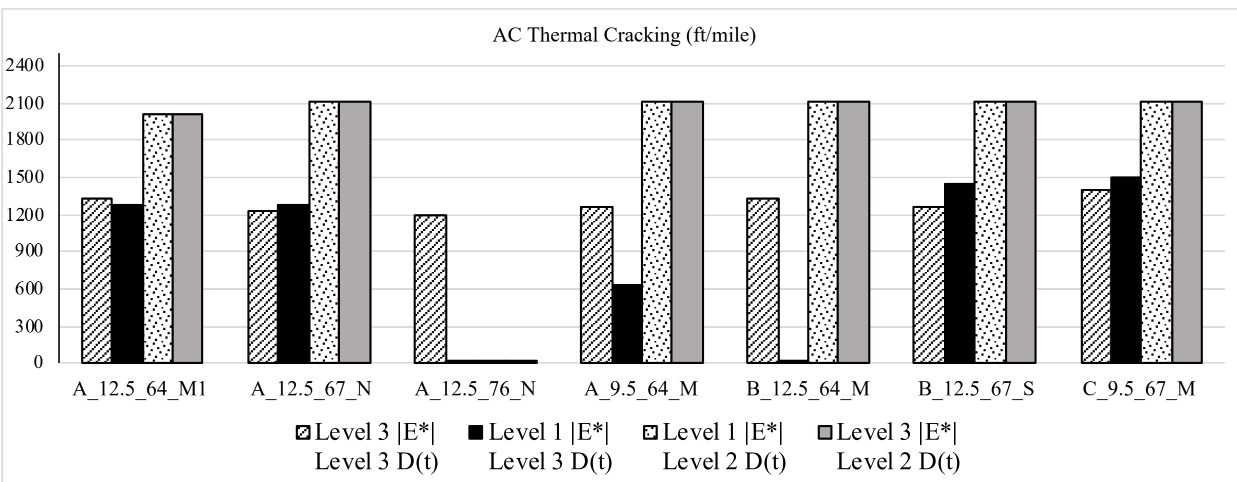

Figure 7.3.b. PMED Pavement Performance Predictions

Table 7.8. Summary Statistics and ANOVA Results

PMED Pavement Distress Prediction	Summary Statistic	Scenario No.			
		1	2	3	4
Terminal IRI (in/mile)	Minimum	172.6	168.1	168.1	159.3
	Median	183.7	183.2	192.2	192.8
	Mean	181.0	179.7	189.6	186.4
	Maximum	185.7	190.3	197.2	195.1
	Stand. Dev.	5.13	7.85	9.73	12.60
Permanent Deformation-Total Pavement (in.)	Minimum	0.3800	0.4900	0.4900	0.3800
	Median	0.4500	0.5600	0.5600	0.4500
	Mean	0.4429	0.5443	0.5443	0.4429
	Maximum	0.4800	0.5900	0.5900	0.4800
	Stand. Dev.	0.0309	0.0428	0.0428	0.0309
AC Bottom-Up Fatigue Cracking (%)	Minimum	1.700	0.168	0.168	1.700
	Median	1.700	0.700	0.700	1.700
	Mean	1.703	1.697	1.697	1.703
	Maximum	1.710	1.710	1.710	1.710
	Stand. Dev.	0.0049	0.0095	0.0095	0.0049
AC Thermal Cracking (ft/mile)	Minimum	1193.0	1.0	1.0	1.0
	Median	1267.0	1288.3	2112.0	2112.0
	Mean	1288.0	881.1	1795.0	1795.0
	Maximum	1394.0	1499.5	2112.0	2112.0
	Stand. Dev.	67.62	665.08	792.21	792.21

The performance predictions in Figure 7.3 and the mean values in Table 7.8 show that input scenarios 3 and 4 tend to predict greater distress quantities for Terminal IRI and AC Thermal Cracking as a result of the greater creep compliance values associated with the LVE interconversion inputs. These results are consistent with the findings of Yin et al. (2010) and Esfandiapour and Shalaby (2017) in which the Level 3 D(t) inputs underpredicted the same distresses. The singular exception to this trend is mixture A_12.5_76_N, which is the only PMA mixture in the tested group. Referencing the AC Thermal Cracking performance model of Equation 3.11, fracture parameters *A* and *n* are obtained from the indirect tensile, creep compliance, and strength of the HMA mixture (AASHTO, 2015a). Because the accompanying properties remained constant across these scenarios, it may be inferred that D(t) inputs influence these parameters significantly enough alter the model predictions.

The above results also suggest the Level 1 dynamic modulus values used in scenarios 2 and 3 tend to show an increase in permanent deformation (rutting) and a decrease in fatigue cracking predictions. Once again, the sensitivity of |E*| inputs to these distress outputs are precedented by the sensitivity studies conducted by previous researchers (Li et al., 2009; El-Badawy et al., 2011; El-Badawy et al., 2012). However, only a marginal variance is documented across fatigue cracking predictions compared to the significant variance documented across rutting performance. These results contradict the global sensitivity results of Schwartz et al. (2013) in which alligator and longitudinal cracking deformations are considered equally as sensitive as permanent deformation. Such a discrepancy is likely attributed to other influencing factors such as the local calibration coefficients and transfer functions.

8.0 CONCLUSIONS

8.1 Summary of Results

Within the scope of this study, an existing library of 17 GDOT approved asphalt mixtures were utilized to develop a dynamic modulus prediction model using tree analysis and a dynamic modulus to creep compliance interconversion model using the principles of viscoelastic theory. The results of these efforts were then evaluated for use in the PMED software and as resources for MEPDG implementation.

The primary findings of this investigation suggest it is not only possible, but advantageous to use the prediction and interconversion models for determining asphalt mechanical properties when laboratory tested data is unavailable. Further, it was found that dynamic modulus and creep compliance properties have significant influence on the pavement performance predictions generated by PMED. A thorough list of conclusions regarding the processes included herein are best summarized in the following sections.

8.2 Tree Analysis Conclusions

- The nationally calibrated dynamic modulus prediction model in PMED (Witczak 1-37A) is not a highly accurate predictor for the HMA materials library established for GDOT
- Advanced tree regression algorithms (bagging, random forest, boosting) are effective ways to generate more accurate |E*| estimates using the same inputs as Witczak 1-37A

- The boosted tree approach produced the most accurate |E*| predictions for both the model generated using only the original Witczak equation inputs and the model generated using all readily available GDOT material properties
- Loading temperature, loading frequency, and asphalt binder properties are the most influential variables for |E*| prediction using tree regression

8.3 PMED Analysis Conclusions

- A notable difference was seen across varying design levels of dynamic modulus and creep compliance inputs when considering terminal IRI, permanent deformation, and AC thermal cracking performance indicators.
- Significant increase in the Permanent Deformation of the Total Pavement output is documented for scenarios using Level 1 dynamic modulus inputs as compared to Level 3.
- Marginal increase in the AC Fatigue Cracking output is documented for scenarios using Level 1 dynamic modulus inputs as compared to Level 3.
- Notable increases in the Terminal IRI and AC Thermal Cracking outputs are documented for scenarios with Level 2 (LVE interconverted) creep compliance inputs.
- The polymer-modified asphalt mixture saw a decrease in Terminal IRI and AC Thermal Cracking outputs under the same scenarios.
- Terminal IRI and AC thermal cracking predictions achieved the greatest distress quantities when using the “highest-available” inputs (Level 1 dynamic modulus and Level 2 creep compliance).

9.0 RECOMMENDATIONS

9.1 Recommendations Based on This Study

Based on the results of this study, a few recommendations are brought forward for the considerations of future research endeavors. First, the successful development of a dynamic modulus prediction model using tree regression suggests that alternative methods for determining these values are available for GDOT engineers. Future pavement design endeavors should practice caution when utilizing the nationally calibration PMED prediction models due to the low correlation accuracy between the measured and predicted values. Instead, machine-learning methods using the locally-source materials database are recommended for use externally to the PMED software.

Second, the results of the included analysis conclude that creep compliance inputs significantly impact the results of the PMED pavement performance output. Although the LVE interconversion is believed to be an accurate indicator of D(t), this method is only applicable for Level 2 design inputs. To achieve Level 1 creep compliance inputs in PMED, discrete creep compliance measurements at the seven loading times for two additional temperatures are required. A preliminary analysis found that extrapolating these additional temperatures from the interconverted creep compliance master curve produced the same results as the Level 2 analysis. Therefore, it is recommended that creep compliance laboratory testing be conducted on standardized asphalt mixtures to expand the asphalt materials library and validate the LVE interconversion model.

9.2 Resource Integration in GDOT MEPDG

The overall objective of this research document was to expand the existing library of tools and resources available for MEPDG in Georgia. To accomplish this, the results of this report must be integrated into the flexible pavement design approach and MEPDG training documents. This phase of the study contained herein was conducted as part of a separate, ongoing GDOT report entitled "Research Project 17-18: Development of Innovative & Effective Training Modules and Methods for Pavement Designers for Rapid Deployment and Continuous Operation of MEPDG." All subsequent interest in the incorporation of these material in the MEPDG is referred to the final RP 17-18 GDOT report on this topic and the revised *GDOT Pavement ME Design User Input Guide*. For convenience, a summary of the relevant tasks found within the scope of the referenced report is provided below. Additional details may be found in Appendix D.

- In cooperation with Applied Research Associates, Inc. (ARA), the research team developed training materials to aid the GDOT Steering Technical and Educational Committees in managing the MEPDG implementation effort. This project provided detailed recommendations as to what data is needed and how best to grow the library with a strategic plan and consideration on the topics of: the importance of specific material properties and their effect on pavement designs, the current MEPDG materials library and its limitations, and strategic approaches for growing the materials library.
- Incorporated the latest GDOT materials input library and resources into the proposed training documents for PMED implementation. Existing data that was collected but not yet integrated was included in GDOT's user manuals and input sheets. Additionally, training workshop materials were developed to update GDOT engineers on the

principles and application of the most recent design approach. This involved a full depth flexible pavement design example at all three design input levels.

- Developed an innovative training program and delivery methods for new or inexperienced pavement engineers. To successfully deliver the training modules and hands-on training workshop, important MEPDG topics were divided into a series of modules. Each module was organized into an informative, consumable video outlining the step-by-step procedure for pavement design in PMED. The final module topics are listed below and referenced in the Appendix.
    - Module 0- MEPDG Basics and Level Hierarchy
    - Module 1A- MEPDG Traffic and Climate Inputs
    - Module 2A- MEPDG Inputs and Implementation for Subgrade and Base Materials
    - Module 3A- MEPDG Inputs and Implementation for AC Pavement
    - Module 4A- MEPDG Inputs and Implementation for JPCP
    - Module 5A- MEPDG Inputs and Implementation for CRCP
    - Module 1B- MEPDG Calibration Factors & Baseline Files
    - Module 2B- MEPDG Traffic Inputs
    - Module 3B- MEPDG Inputs and Implementation for Subgrade and Base Materials
    - Module 4B- MEPDG Inputs and Implementation for AC Pavement
    - Module 5B- MEPDG Inputs and Implementation for PCC Pavement

9.3 Future Works

The collective work developed within this study was not completed without consideration for future research that may expand upon the findings. The successful development of asphalt mechanical property resources for MEPDG also highlighted some issues that should be addressed in future pavement design practices. A set of recommendations for future works are found below:

- Investigate the implications of external dynamic modulus prediction models by evaluating PMED designs using both the default and machine learning methods to acquire unknown |E*| inputs
- Compare the results of the boosted tree regression model to those of more advanced machine learning techniques such as ANN or SVR using the GDOT materials library
- Validate the LVE interconversion model by comparing the estimated creep compliance values with laboratory tested values for a set of standardized Georgia asphalt mixtures. The verification process for this model was conducted with asphalt mixtures that are not found in the GDOT materials library. Although it is still considered highly accurate, an official validation is recommended before application.
- Investigate the results of using both the dynamic modulus prediction model and creep compliance interconversion method to determine both mechanical properties for a single asphalt mixture. Examining the viability of this approach will provide valuable information toward the application of these methods as GDOT expands its material library.
- Perform a global sensitivity analysis for all flexible pavement design inputs in PMED. A foundational piece for MEPDG implementation, global sensitivity analysis will provide pavement designers will critical information regarding the enhancement of modern pavement design practices.

- Development of a Level 1 creep compliance library for Georgia MEPDG. As discussed in a previous section, the accumulation of creep compliance data and expansion of the asphalt material database will improve the MEPDG implementation efforts and enhance the capabilities of the model included in this study.
- Investigate the transverse (thermal) cracking prediction model with consideration of the mean annual air temperature (MAAT)-dependent calibration coefficients and creep compliance of asphalt mixtures.

REFERENCES

American Association of State and Highway Transportation Officials (AASHTO). (2015a). Mechanistic-Empirical Pavement Design Guide: A Manual of Practice. American Association of State and Highway Transportation Officials, Washington D.C.

American Association of State and Highway Transportation Officials (AASHTO). (2015b). Pavement Design, Construction, and Management. American Association of State and Highway Transportation Officials, Washington D.C.

Andrei, D., Witczak, M. W., & Mirza, M. W. (1999). Development of a Revised Predictive Model for the Dynamic (Complex) Modulus of Asphalt Mixtures. NCHRP 1-37, an Interim Rep., Univ. of Maryland, College Park, Md.

Applied Research Associates (ARA). (2015). Implementation of the Mechanistic-Empirical Pavement Design Guide in Georgia. (FHWA-GA-14-11-17).

Bari, J., & Witczak, M. W. (2006). Development of a New Revised Version of the Witczak E* Predictive Model for Hot Mix Asphalt Mixtures. Electron. J. Assoc. Asph. Paving Technol., 75, 381–423.

Brown, R. (2000). Density of Asphalt Concrete- How Much is Needed? Publication NCAT Report No. 90-3. Auburn University. National Center for Asphalt Technology.

Carvalho, R., Ayres, M., Shirazi, H., Selezneva, O., & Darter, M. (2011). Impact of Design Features on Pavement Responses and Performance in Rehabilitated Flexible and Rigid Pavements. Federal Highway Administration.

Ceylan, H., Kim, S., & Gopalakrishnan, K. (2007). Hot Mix Asphalt Dynamic Modulus Prediction Models using Neural Network Approach. Proc., ANNIE 2007, ASME, New York.

Ceylan, H., Schwartz, C.W., Kim, S., & Gopalakrishnan, K. (2009). Accuracy of Predictive Models for Dynamic Modulus of Hot Mix Asphalt. ASCE Journal of Materials in Civil Engineering, Vol. 21, No. 6, pp. 286-293.

Christensen, R. M. (1982). Theory of Viscoelasticity. Academic, 2nd Edn. New York.

Deepa, C., SathiyaKumari, K., & Pream Sudha, V. (2010). Prediction of the Compressive Strength of High Performance Concrete Mix using Tree Based Modeling. International Journal of Computer Applications (0975-8887), Vol. 6, No. 5, pp. 18-24.

del Pilar Vivar, E. & Haddock, J.E. (2006). HMA Pavement Performance and Durability. Joint Transportation Research Program, Indiana Department of Transportation and Purdue University. https://docs.lib.purdue.edu/jtrp/268/

Denby, E. F. (1975). A Note on the Interconversion of Creep, Relaxation, and Recovery. Rheologica Acta, 14 (591-593).

Deshpande, N., Londhe, S., & Kulkarni, S. (2014). Modeling Compressive Strength of Recycle Aggregate Concrete by Artificial Neural Network, Model Tree and Non-linear Regression. International Journal for Sustainable Built Environment, Vol. 3, Iss. 2, pp. 187-198.

El-Badawy, S., Awed, A., & Bayomy, F. (2011). Evaluation of the MEPDG Dynamic Modulus Prediction Models for Asphalt Concrete Mixtures. Proc., 1st Integrated Transportation and Development Institute Congress, I. Al-Qadi and S. Murrell, eds., ASCE, Reston, VA, 576–585.

El-Badawy, S., Bayomy, F., & Awed, A. (2012) Performance of MEPDG Dynamic Modulus Predictive Models for Asphalt Concrete Mixtures: Local Calibration for Idaho. Journal of Materials in Civil Engineering, 24(11): 1412-1421.

Esfandiarpour, S. & Shalaby, A. (2017). Local Calibration of Creep Compliance Models of Asphalt Concrete. Construction & Building Materials 132: 313. Web.

Ferry, J.D. (1980). Viscoelastic Properties of Polymers, 3rd Edn. New York, NY: John Wiley and Sons.

Georgia Department of Transportation (GDOT). (2019). Pavement Design Manual. The Office of Materials and Research.

Gholampour, A., Mansouri, I., Kisi, O., & Ozbakkaloglu, Togay. (2018). Evaluation of Mechanical Properties of Concretes Containing Coarse Recycled Concrete Aggregates using Multivariate Adaptive Regression Splines (MARS), M5 Model Tree (M5Tree), and Least Squares Support Vector Regression (LSSVR) models. Neural Computing and Applications (32), pp. 295-308. https://doi.org/10.1007/s00521-018-3630-y

Gogula, A., Hossain, M., Boyer, J., & Romanoschi, S. (2003). Effect of PG Binder Grade and Source on Performance of Superpave Mixtures under Hamburg Wheel Tester. Mid-Continent Transportation Research Symposium.

Gopalakrishnan, K., Kim, S., & Ceylan, H. (2009). Hot Mix Asphalt Dynamic Modulus Prediction Using Kernel Machines. ANNIE 2009, ANNs in Engineering, St. Louis, Missouri, November 2-4, pp. 131-138.

Highway Research Board (HRB). (1961). Special Report 61A: The AASHTO Road Test, History and Description of Project. Highway Research Board, National Research Council, Washington DC.

Jeong, Myunggoo (2005). Comparison of Creep Compliacen Master Curve Models for Hot Mix Asphalt. MS Thesis. Virginia Polytechnic Institute and State University, Blacksburg, Virginia.

Kim, S.-H. (2013). Measurements of Dynamic and Resilient Moduli of Roadway Test Sites, Final Report. Research Project Number 12-07, Georgia Department of Transportation. Office of Materials and Research, Research and Development Branch, Forest Park, GA.

Kim, S.-H., Kim, Y.R., Yang, J., Norouzi, A., & Kim, D. (2016). Effects of Reclaimed Asphalt Pavement (RAP) Contents and Sources on Dynamic Modulus (|E*|) and Fatigue Performance of Asphalt Mixtures in Georgia. Research Project Number 14-12, Georgia Department of Transportation. Office of Materials and Research, Research and Development Branch, Forest Park, GA.

Kim, S.-H., Etheridge, A., Chorzepa, M.G., & Kim, Y.R. (2019). Effects of Asphalt Mixture Characteristics of Dynamic Modulus and Fatigue Performance. Research Project Number 16-19, Georgia Department of Transportation. Office of Materials and Research, Research and Development Branch, Forest Park, GA.

Kim, Y. R. (2009). Modeling of Asphalt Concrete. ASCE Press. New York, NY: McGraw-Hill.

Li, J., Pierce, L. M., & Uhlmeyer, J. S. (2009). Calibration of Flexible Pavement in Mechanistic-Empirical Pavement Design Guide for Washington State. Transportation Research Record 2095, Transportation Research Board, Washington, D.C., 73–83.

Li, Q., Xiao, Danny X., Wang, Kelvin C.P., Hall, Kevin D., & Qui, Y. (2011). Mechanistic-Empirical Pavement Design Guide (MEPDG): A Bird's-eye View. Journal of Modern Transportation, 19 (114-133). jmt.swjtu.edu.cn

Maher, A., & Bennert, T. (2008). Evaluation of Poisson’s Ratio for use in the Mechanistic Empirical Pavement Design Guide (MEPDG). Transportation Research Board.

Masad, S., & Little, D. N. (2004). Sensitivity Analysis of Flexible Pavement Response and AASHTO 2002 Design Guide for Properties of Unbound Layers. ICAR 504-1. International Center for Aggregates Research, Austin, Tex.

Mohammad, L.N., Raghavandra, A., & Huang, B. (2000). Laboratory Performance Evaluation of Cement-Stabilized Soil Base Mixtures. Transportation Research Record, 1721 (19-28). https://journals.sagepub.com/doi/abs/10.3141/1721-03

National Cooperative Highway Research Program (NCHRP). (2004). Guide for Mechanistic-Empirical Design of New and Rehabilitated Pavement Structures. NCHRP 1-37A, Final Report. Transportation Research Board, Washington, D.C. http://onlinepubs.trb.org/onlinepubs/archive/mepdg/guide.htm

National Cooperative Highway Research Program (NCHRP). (2006). Independent Review of the Mechanistic-Empirical Pavement Design Guide and Software. NCHRP 1-40, A Research Results Digest 307, Transportation Research Board, Washington, D.C.

Park, S.W., & Kim, Y.R. (1999). Interconversion Between Relaxation Modulus and Creep Compliance for Viscoelastic Solids. Journal of Materials in Civil Engineering, 11(1): 76-82.

Park, S.W., & Schapery, R.A. (1999). Methods of Interconversion between Linear Viscoelastic Material Functions. Part I: A Numerical Method based on Prony Series. International Journal of Solids and Structures. 36. 1677-1699.

Pavement Interactive (PI). (n.d.). Poisson's Ratio. Retrieved from https://www.pavementinteractive.org/reference-desk/design/structural-design/poissons-ratio/

Schapery, R.A., & Park, S.W. (1999). Methods of Interconversion between Linear Viscoelastic Material Functions. Part II: An Approximate Analytical Method. International Journal of Solids and Structures. 36. 1677-1699.

Sreedhar, S., & Coleri, E. (2018). Effects of Binder Content, Density, Gradation, and Polymer Modification on Cracking and Rutting Resistance of Asphalt Mixtures Used in Oregon. Journal of Materials in Civil Engineering, 30-11.

Schwartz, C. W. (2005). Evaluation of the Witczak dynamic modulus prediction model. Proc., 84th Annual Meeting of the Transportation Research Board (CD-ROM), Transportation Research Board, Washington, D.C.

Schwartz, C. W., Li, R., Ceylan, H., Kim, S., & Gopalakrishnan, K. (2013). Global Sensitivity Analysis of Mechanistic–Empirical Performance Predictions for Flexible Pavements. Transportation Research Record, 2368 (1), 12–23. https://doi.org/10.3141/2368-02

Tarefder, R. A. (2016). Interconversion of Dynamic Modulus to Creep Compliance and Relaxation Modulus: Numerical Modeling and Laboratory Validation

Transportation Research Board (TRB). (2007). Pavement Lessons Learned from the AASHO Road Test and Performance of the Interstate Highway System. Transportation Research Board, Washington, DC.: http://onlinepubs.trb.org/onlinepubs/circulars/ec118.pdf.

American Society for Testing and Materials (ASTM). (1998). Viscosity-Temperature Chart for Asphalts. 1998 Annual Book of ASTM Standards. Vol. 4.03, pp. 230-234.

Von Quintus, H. L., Darter, M. I., Bhattacharya, B. B., & Titus-Glover, L. (2016). Implementation and Calibration of the MEPDG in Georgia Task Order 3 Final Report (FHWA/GA-014-11-17).

Yildirim, Yetkin. (2007). Polymer Modified Asphalt Binders. Construction and Building Materials, 21 (66-72).

Yin, H., Chehab, G.R., Stoffels, S.M., Kumar, T., & Premkumar, L. (2010). Use of Creep Compliance Interconverted from Complex Modulus for Thermal Cracking Prediction using the M-E Pavement Design Guide. Int. J. Pavement Eng. 11 95–105.

APPENDICES

Appendix A

Table A.1.A

mix_id	A 12.5_64_M1																
north	0	0	0	0	0	0	0	0	0	0	0	0	0	0	0	0	0	0
middle	1	1	1	1	1	1	1	1	1	1	1	1	1	1	1	1	1	1
south	0	0	0	0	0	0	0	0	0	0	0	0	0	0	0	0	0	0
pg64	1	1	1	1	1	1	1	1	1	1	1	1	1	1	1	1	1	1
pg67	0	0	0	0	0	0	0	0	0	0	0	0	0	0	0	0	0	0
pg76	0	0	0	0	0	0	0	0	0	0	0	0	0	0	0	0	0	0
nmas	12.5	12.5	12.5	12.5	12.5	12.5	12.5	12.5	12.5	12.5	12.5	12.5	12.5	12.5	12.5	12.5	12.5	12.5
rap	30	30	30	30	30	30	30	30	30	30	30	30	30	30	30	30	30	30
binder	5.46	5.46	5.46	5.46	5.46	5.46	5.46	5.46	5.46	5.46	5.46	5.46	5.46	5.46	5.46	5.46	5.46	5.46
gmm	2.459	2.459	2.459	2.459	2.459	2.459	2.459	2.459	2.459	2.459	2.459	2.459	2.459	2.459	2.459	2.459	2.459	2.459
av	5.5	5.5	5.5	5.5	5.5	5.5	5.5	5.5	5.5	5.5	5.5	5.5	5.5	5.5	5.5	5.5	5.5	5.5
vma	17.69	17.69	17.69	17.69	17.69	17.69	17.69	17.69	17.69	17.69	17.69	17.69	17.69	17.69	17.69	17.69	17.69	17.69
vfa	70.68	70.68	70.68	70.68	70.68	70.68	70.68	70.68	70.68	70.68	70.68	70.68	70.68	70.68	70.68	70.68	70.68	70.68
eff_binder	12.5	12.5	12.5	12.5	12.5	12.5	12.5	12.5	12.5	12.5	12.5	12.5	12.5	12.5	12.5	12.5	12.5	12.5
dr	0.48	0.48	0.48	0.48	0.48	0.48	0.48	0.48	0.48	0.48	0.48	0.48	0.48	0.48	0.48	0.48	0.48	0.48
sapp	9.37	9.37	9.37	9.37	9.37	9.37	9.37	9.37	9.37	9.37	9.37	9.37	9.37	9.37	9.37	9.37	9.37	9.37
pp200	5.80	5.80	5.80	5.80	5.80	5.80	5.80	5.80	5.80	5.80	5.80	5.80	5.80	5.80	5.80	5.80	5.80	5.80
pp4	74.00	74.00	74.00	74.00	74.00	74.00	74.00	74.00	74.00	74.00	74.00	74.00	74.00	74.00	74.00	74.00	74.00	74.00
pr38	14.00	14.00	14.00	14.00	14.00	14.00	14.00	14.00	14.00	14.00	14.00	14.00	14.00	14.00	14.00	14.00	14.00	14.00
pr34	0.00	0.00	0.00	0.00	0.00	0.00	0.00	0.00	0.00	0.00	0.00	0.00	0.00	0.00	0.00	0.00	0.00	0.00
A	20.29	20.29	20.29	20.29	20.29	20.29	20.29	20.29	20.29	20.29	20.29	20.29	20.29	20.29	20.29	20.29	20.29	20.29
VTS	-7.12	-7.12	-7.12	-7.12	-7.12	-7.12	-7.12	-7.12	-7.12	-7.12	-7.12	-7.12	-7.12	-7.12	-7.12	-7.12	-7.12	-7.12
eta	1.210E+12	1.210E+12	1.210E+12	1.210E+12	1.210E+12	1.210E+12	1.265E+08	1.265E+08	1.265E+08	1.265E+08	1.265E+08	1.265E+08	1.159E+05	1.159E+05	1.159E+05	1.159E+05	1.159E+05	1.159E+05
temp_f	39.2	39.2	39.2	39.2	39.2	39.2	68	68	68	68	68	68	104	104	104	104	104	104
freq	0.1	0.50	1.00	5.00	10.00	25.00	0.1	0.50	1.00	5.00	10.00	25.00	0.1	0.50	1.00	5.00	10.00	25.00
estar	740801.8	1082794.3	1202705.2	1586888.5	1706095.6	1924615.0	150334.3	278518.0	336267.5	564559.2	658668.9	818439.5	24295.7	46335.0	58625.2	113718.8	142644.5	198566.5
mix_id	A 12.5_64_M2																	
north	0	0	0	0	0	0	0	0	0	0	0	0	0	0	0	0	0	0
middle	1	1	1	1	1	1	1	1	1	1	1	1	1	1	1	1	1	1
south	0	0	0	0	0	0	0	0	0	0	0	0	0	0	0	0	0	0
pg64	1	1	1	1	1	1	1	1	1	1	1	1	1	1	1	1	1	1
pg67	0	0	0	0	0	0	0	0	0	0	0	0	0	0	0	0	0	0
pg76	0	0	0	0	0	0	0	0	0	0	0	0	0	0	0	0	0	0
nmas	12.5	12.5	12.5	12.5	12.5	12.5	12.5	12.5	12.5	12.5	12.5	12.5	12.5	12.5	12.5	12.5	12.5	12.5
rap	30	30	30	30	30	30	30	30	30	30	30	30	30	30	30	30	30	30
binder	5.42	5.42	5.42	5.42	5.42	5.42	5.42	5.42	5.42	5.42	5.42	5.42	5.42	5.42	5.42	5.42	5.42	5.42
gmm	2.468	2.468	2.468	2.468	2.468	2.468	2.468	2.468	2.468	2.468	2.468	2.468	2.468	2.468	2.468	2.468	2.468	2.468
av	5.5	5.5	5.5	5.5	5.5	5.5	5.5	5.5	5.5	5.5	5.5	5.5	5.5	5.5	5.5	5.5	5.5	5.5
vma	17.69	17.69	17.69	17.69	17.69	17.69	17.69	17.69	17.69	17.69	17.69	17.69	17.69	17.69	17.69	17.69	17.69	17.69
vfa	68.73	68.73	68.73	68.73	68.73	68.73	68.73	68.73	68.73	68.73	68.73	68.73	68.73	68.73	68.73	68.73	68.73	68.73
eff_binder	12.2	12.2	12.2	12.2	12.2	12.2	12.2	12.2	12.2	12.2	12.2	12.2	12.2	12.2	12.2	12.2	12.2	12.2
dr	0.49	0.49	0.49	0.49	0.49	0.49	0.49	0.49	0.49	0.49	0.49	0.49	0.49	0.49	0.49	0.49	0.49	0.49
sapp	8.90	8.90	8.90	8.90	8.90	8.90	8.90	8.90	8.90	8.90	8.90	8.90	8.90	8.90	8.90	8.90	8.90	8.90
pp200	5.90	5.90	5.90	5.90	5.90	5.90	5.90	5.90	5.90	5.90	5.90	5.90	5.90	5.90	5.90	5.90	5.90	5.90
pp4	73.00	73.00	73.00	73.00	73.00	73.00	73.00	73.00	73.00	73.00	73.00	73.00	73.00	73.00	73.00	73.00	73.00	73.00
pr38	12.00	12.00	12.00	12.00	12.00	12.00	12.00	12.00	12.00	12.00	12.00	12.00	12.00	12.00	12.00	12.00	12.00	12.00
pr34	0.00	0.00	0.00	0.00	0.00	0.00	0.00	0.00	0.00	0.00	0.00	0.00	0.00	0.00	0.00	0.00	0.00	0.00
A	17.29	17.29	17.29	17.29	17.29	17.29	17.29	17.29	17.29	17.29	17.29	17.29	17.29	17.29	17.29	17.29	17.29	17.29
VTS	-6.02	-6.02	-6.02	-6.02	-6.02	-6.02	-6.02	-6.02	-6.02	-6.02	-6.02	-6.02	-6.02	-6.02	-6.02	-6.02	-6.02	-6.02
eta	2.268E+11	2.268E+11	2.268E+11	2.268E+11	2.268E+11	2.268E+11	1.262E+08	1.262E+08	1.262E+08	1.262E+08	1.262E+08	1.262E+08	2.793E+05	2.793E+05	2.793E+05	2.793E+05	2.793E+05	2.793E+05
temp_f	39.2	39.2	39.2	39.2	39.2	39.2	68	68	68	68	68	68	104	104	104	104	104	104
freq	0.1	0.50	1.00	5.00	10.00	25.00	0.1	0.50	1.00	5.00	10.00	25.00	0.1	0.50	1.00	5.00	10.00	25.00
estar	913266.0	1203332.0	1342315.0	1646168.0	1775603.0	1961809.0	196746.1	348622.4	411795.8	649273.9	741029.7	894447.9	33990.5	70120.2	89932.3	173205.4	212727.3	301364.0

Table A.1.B

mix_id	A 12.5_67_N																	
north	1	1	1	1	1	1	1	1	1	1	1	1	1	1	1	1	1	1
middle	0	0	0	0	0	0	0	0	0	0	0	0	0	0	0	0	0	0
south	0	0	0	0	0	0	0	0	0	0	0	0	0	0	0	0	0	0
pg64	0	0	0	0	0	0	0	0	0	0	0	0	0	0	0	0	0	0
pg67	1	1	1	1	1	1	1	1	1	1	1	1	1	1	1	1	1	1
pg76	0	0	0	0	0	0	0	0	0	0	0	0	0	0	0	0	0	0
nmas	12.5	12.5	12.5	12.5	12.5	12.5	12.5	12.5	12.5	12.5	12.5	12.5	12.5	12.5	12.5	12.5	12.5	12.5
rap	30	30	30	30	30	30	30	30	30	30	30	30	30	30	30	30	30	30
binder	5.52	5.52	5.52	5.52	5.52	5.52	5.52	5.52	5.52	5.52	5.52	5.52	5.52	5.52	5.52	5.52	5.52	5.52
gmm	2.466	2.466	2.466	2.466	2.466	2.466	2.466	2.466	2.466	2.466	2.466	2.466	2.466	2.466	2.466	2.466	2.466	2.466
av	6.3	6.3	6.3	6.3	6.3	6.3	6.3	6.3	6.3	6.3	6.3	6.3	6.3	6.3	6.3	6.3	6.3	6.3
vma	18.04	18.04	18.04	18.04	18.04	18.04	18.04	18.04	18.04	18.04	18.04	18.04	18.04	18.04	18.04	18.04	18.04	18.04
vfa	65.35	65.35	65.35	65.35	65.35	65.35	65.35	65.35	65.35	65.35	65.35	65.35	65.35	65.35	65.35	65.35	65.35	65.35
eff_binder	11.8	11.8	11.8	11.8	11.8	11.8	11.8	11.8	11.8	11.8	11.8	11.8	11.8	11.8	11.8	11.8	11.8	11.8
dr	0.54	0.54	0.54	0.54	0.54	0.54	0.54	0.54	0.54	0.54	0.54	0.54	0.54	0.54	0.54	0.54	0.54	0.54
sapp	13.34	13.34	13.34	13.34	13.34	13.34	13.34	13.34	13.34	13.34	13.34	13.34	13.34	13.34	13.34	13.34	13.34	13.34
pp200	6.30	6.30	6.30	6.30	6.30	6.30	6.30	6.30	6.30	6.30	6.30	6.30	6.30	6.30	6.30	6.30	6.30	6.30
pp4	75.00	75.00	75.00	75.00	75.00	75.00	75.00	75.00	75.00	75.00	75.00	75.00	75.00	75.00	75.00	75.00	75.00	75.00
pr38	13.00	13.00	13.00	13.00	13.00	13.00	13.00	13.00	13.00	13.00	13.00	13.00	13.00	13.00	13.00	13.00	13.00	13.00
pr34	0.00	0.00	0.00	0.00	0.00	0.00	0.00	0.00	0.00	0.00	0.00	0.00	0.00	0.00	0.00	0.00	0.00	0.00
A	18.84	18.84	18.84	18.84	18.84	18.84	18.84	18.84	18.84	18.84	18.84	18.84	18.84	18.84	18.84	18.84	18.84	18.84
VTS	-6.57	-6.57	-6.57	-6.57	-6.57	-6.57	-6.57	-6.57	-6.57	-6.57	-6.57	-6.57	-6.57	-6.57	-6.57	-6.57	-6.57	-6.57
eta	6.580E+12	6.580E+12	6.580E+12	6.580E+12	6.580E+12	6.580E+12	7.313E+08	7.313E+08	7.313E+08	7.313E+08	7.313E+08	7.313E+08	5.555E+05	5.555E+05	5.555E+05	5.555E+05	5.555E+05	5.555E+05
temp_f	39.2	39.2	39.2	39.2	39.2	39.2	68	68	68	68	68	68	104	104	104	104	104	104
freq	0.1	0.50	1.00	5.00	10.00	25.00	0.1	0.50	1.00	5.00	10.00	25.00	0.1	0.50	1.00	5.00	10.00	25.00
estar	787225.4	1089504.8	1207066.6	1545324.6	1661797.7	1870709.2	192088.2	325597.5	382568.4	599750.1	686072.6	833911.8	38301.2	66256.1	82045.6	142791.1	175826.7	228559.3
mix_id	A 12.5_76_N																	
north	1	1	1	1	1	1	1	1	1	1	1	1	1	1	1	1	1	1
middle	0	0	0	0	0	0	0	0	0	0	0	0	0	0	0	0	0	0
south	0	0	0	0	0	0	0	0	0	0	0	0	0	0	0	0	0	0
pg64	0	0	0	0	0	0	0	0	0	0	0	0	0	0	0	0	0	0
pg67	0	0	0	0	0	0	0	0	0	0	0	0	0	0	0	0	0	0
pg76	1	1	1	1	1	1	1	1	1	1	1	1	1	1	1	1	1	1
nmas	12.5	12.5	12.5	12.5	12.5	12.5	12.5	12.5	12.5	12.5	12.5	12.5	12.5	12.5	12.5	12.5	12.5	12.5
rap	30	30	30	30	30	30	30	30	30	30	30	30	30	30	30	30	30	30
binder	5.41	5.41	5.41	5.41	5.41	5.41	5.41	5.41	5.41	5.41	5.41	5.41	5.41	5.41	5.41	5.41	5.41	5.41
gmm	2.549	2.549	2.549	2.549	2.549	2.549	2.549	2.549	2.549	2.549	2.549	2.549	2.549	2.549	2.549	2.549	2.549	2.549
av	5.7	5.7	5.7	5.7	5.7	5.7	5.7	5.7	5.7	5.7	5.7	5.7	5.7	5.7	5.7	5.7	5.7	5.7
vma	18.36	18.36	18.36	18.36	18.36	18.36	18.36	18.36	18.36	18.36	18.36	18.36	18.36	18.36	18.36	18.36	18.36	18.36
vfa	68.71	68.71	68.71	68.71	68.71	68.71	68.71	68.71	68.71	68.71	68.71	68.71	68.71	68.71	68.71	68.71	68.71	68.71
eff_binder	12.6	12.6	12.6	12.6	12.6	12.6	12.6	12.6	12.6	12.6	12.6	12.6	12.6	12.6	12.6	12.6	12.6	12.6
dr	0.52	0.52	0.52	0.52	0.52	0.52	0.52	0.52	0.52	0.52	0.52	0.52	0.52	0.52	0.52	0.52	0.52	0.52
sapp	11.81	11.81	11.81	11.81	11.81	11.81	11.81	11.81	11.81	11.81	11.81	11.81	11.81	11.81	11.81	11.81	11.81	11.81
pp200	6.30	6.30	6.30	6.30	6.30	6.30	6.30	6.30	6.30	6.30	6.30	6.30	6.30	6.30	6.30	6.30	6.30	6.30
pp4	73.00	73.00	73.00	73.00	73.00	73.00	73.00	73.00	73.00	73.00	73.00	73.00	73.00	73.00	73.00	73.00	73.00	73.00
pr38	10.00	10.00	10.00	10.00	10.00	10.00	10.00	10.00	10.00	10.00	10.00	10.00	10.00	10.00	10.00	10.00	10.00	10.00
pr34	0.00	0.00	0.00	0.00	0.00	0.00	0.00	0.00	0.00	0.00	0.00	0.00	0.00	0.00	0.00	0.00	0.00	0.00
A	7.39	7.39	7.39	7.39	7.39	7.39	7.39	7.39	7.39	7.39	7.39	7.39	7.39	7.39	7.39	7.39	7.39	7.39
VTS	-2.46	-2.46	-2.46	-2.46	-2.46	-2.46	-2.46	-2.46	-2.46	-2.46	-2.46	-2.46	-2.46	-2.46	-2.46	-2.46	-2.46	-2.46
eta	3.434E+05	3.434E+05	3.434E+05	3.434E+05	3.434E+05	3.434E+05	6.625E+04	6.625E+04	6.625E+04	6.625E+04	6.625E+04	6.625E+04	1.253E+04	1.253E+04	1.253E+04	1.253E+04	1.253E+04	1.253E+04
temp_f	39.2	39.2	39.2	39.2	39.2	39.2	68	68	68	68	68	68	104	104	104	104	104	104
freq	0.1	0.50	1.00	5.00	10.00	25.00	0.1	0.50	1.00	5.00	10.00	25.00	0.1	0.50	1.00	5.00	10.00	25.00
estar	829118.7	1118110.8	1264046.4	1585167.4	1726851.3	1930604.8	177586.6	304657.1	359764.1	573195.2	658991.2	807522.4	35227.3	59261.2	73823.6	127259.9	158583.4	205713.5

Table A.1.C

mix_id	A 19_64_N																	
north	1	1	1	1	1	1	1	1	1	1	1	1	1	1	1	1	1	1
middle	0	0	0	0	0	0	0	0	0	0	0	0	0	0	0	0	0	0
south	0	0	0	0	0	0	0	0	0	0	0	0	0	0	0	0	0	0
pg64	1	1	1	1	1	1	1	1	1	1	1	1	1	1	1	1	1	1
pg67	0	0	0	0	0	0	0	0	0	0	0	0	0	0	0	0	0	0
pg76	0	0	0	0	0	0	0	0	0	0	0	0	0	0	0	0	0	0
nmas	19	19	19	19	19	19	19	19	19	19	19	19	19	19	19	19	19	19
rap	30	30	30	30	30	30	30	30	30	30	30	30	30	30	30	30	30	30
binder	5.25	5.25	5.25	5.25	5.25	5.25	5.25	5.25	5.25	5.25	5.25	5.25	5.25	5.25	5.25	5.25	5.25	5.25
gmm	2.501	2.501	2.501	2.501	2.501	2.501	2.501	2.501	2.501	2.501	2.501	2.501	2.501	2.501	2.501	2.501	2.501	2.501
av	5.5	5.5	5.5	5.5	5.5	5.5	5.5	5.5	5.5	5.5	5.5	5.5	5.5	5.5	5.5	5.5	5.5	5.5
vma	17.06	17.06	17.06	17.06	17.06	17.06	17.06	17.06	17.06	17.06	17.06	17.06	17.06	17.06	17.06	17.06	17.06	17.06
vfa	67.96	67.96	67.96	67.96	67.96	67.96	67.96	67.96	67.96	67.96	67.96	67.96	67.96	67.96	67.96	67.96	67.96	67.96
eff_binder	11.6	11.6	11.6	11.6	11.6	11.6	11.6	11.6	11.6	11.6	11.6	11.6	11.6	11.6	11.6	11.6	11.6	11.6
dr	0.41	0.41	0.41	0.41	0.41	0.41	0.41	0.41	0.41	0.41	0.41	0.41	0.41	0.41	0.41	0.41	0.41	0.41
sapp	8.72	8.72	8.72	8.72	8.72	8.72	8.72	8.72	8.72	8.72	8.72	8.72	8.72	8.72	8.72	8.72	8.72	8.72
pp200	5.80	5.80	5.80	5.80	5.80	5.80	5.80	5.80	5.80	5.80	5.80	5.80	5.80	5.80	5.80	5.80	5.80	5.80
pp4	73.00	73.00	73.00	73.00	73.00	73.00	73.00	73.00	73.00	73.00	73.00	73.00	73.00	73.00	73.00	73.00	73.00	73.00
pr38	11.00	11.00	11.00	11.00	11.00	11.00	11.00	11.00	11.00	11.00	11.00	11.00	11.00	11.00	11.00	11.00	11.00	11.00
pr34	5.00	5.00	5.00	5.00	5.00	5.00	5.00	5.00	5.00	5.00	5.00	5.00	5.00	5.00	5.00	5.00	5.00	5.00
A	12.24	12.24	12.24	12.24	12.24	12.24	12.24	12.24	12.24	12.24	12.24	12.24	12.24	12.24	12.24	12.24	12.24	12.24
VTS	-4.18	-4.18	-4.18	-4.18	-4.18	-4.18	-4.18	-4.18	-4.18	-4.18	-4.18	-4.18	-4.18	-4.18	-4.18	-4.18	-4.18	-4.18
eta	1.253E+09	1.253E+09	1.253E+09	1.253E+09	1.253E+09	1.253E+09	1.564E+07	1.564E+07	1.564E+07	1.564E+07	1.564E+07	1.564E+07	2.877E+05	2.877E+05	2.877E+05	2.877E+05	2.877E+05	2.877E+05
temp_f	39.2	39.2	39.2	39.2	39.2	39.2	68	68	68	68	68	68	104	104	104	104	104	104
freq	0.1	0.50	1.00	5.00	10.00	25.00	0.1	0.50	1.00	5.00	10.00	25.00	0.1	0.50	1.00	5.00	10.00	25.00
estar	1080201.5	1378093.3	1534187.9	1835809.5	1977396.4	2154776.1	259963.5	430810.6	501396.3	759377.8	859191.5	1021609.0	49659.7	86728.1	108869.6	187265.7	232492.1	296429.7
mix_id	B 9.5_64_M1																	
north	0	0	0	0	0	0	0	0	0	0	0	0	0	0	0	0	0	0
middle	1	1	1	1	1	1	1	1	1	1	1	1	1	1	1	1	1	1
south	0	0	0	0	0	0	0	0	0	0	0	0	0	0	0	0	0	0
pg64	1	1	1	1	1	1	1	1	1	1	1	1	1	1	1	1	1	1
pg67	0	0	0	0	0	0	0	0	0	0	0	0	0	0	0	0	0	0
pg76	0	0	0	0	0	0	0	0	0	0	0	0	0	0	0	0	0	0
nmas	9.5	9.5	9.5	9.5	9.5	9.5	9.5	9.5	9.5	9.5	9.5	9.5	9.5	9.5	9.5	9.5	9.5	9.5
rap	30	30	30	30	30	30	30	30	30	30	30	30	30	30	30	30	30	30
binder	5.90	5.90	5.90	5.90	5.90	5.90	5.90	5.90	5.90	5.90	5.90	5.90	5.90	5.90	5.90	5.90	5.90	5.90
gmm	2.447	2.447	2.447	2.447	2.447	2.447	2.447	2.447	2.447	2.447	2.447	2.447	2.447	2.447	2.447	2.447	2.447	2.447
av	6.5	6.5	6.5	6.5	6.5	6.5	6.5	6.5	6.5	6.5	6.5	6.5	6.5	6.5	6.5	6.5	6.5	6.5
vma	19.32	19.32	19.32	19.32	19.32	19.32	19.32	19.32	19.32	19.32	19.32	19.32	19.32	19.32	19.32	19.32	19.32	19.32
vfa	65.20	65.20	65.20	65.20	65.20	65.20	65.20	65.20	65.20	65.20	65.20	65.20	65.20	65.20	65.20	65.20	65.20	65.20
eff_binder	12.6	12.6	12.6	12.6	12.6	12.6	12.6	12.6	12.6	12.6	12.6	12.6	12.6	12.6	12.6	12.6	12.6	12.6
dr	0.49	0.49	0.49	0.49	0.49	0.49	0.49	0.49	0.49	0.49	0.49	0.49	0.49	0.49	0.49	0.49	0.49	0.49
sapp	9.21	9.21	9.21	9.21	9.21	9.21	9.21	9.21	9.21	9.21	9.21	9.21	9.21	9.21	9.21	9.21	9.21	9.21
pp200	6.00	6.00	6.00	6.00	6.00	6.00	6.00	6.00	6.00	6.00	6.00	6.00	6.00	6.00	6.00	6.00	6.00	6.00
pp4	72.00	72.00	72.00	72.00	72.00	72.00	72.00	72.00	72.00	72.00	72.00	72.00	72.00	72.00	72.00	72.00	72.00	72.00
pr38	1.00	1.00	1.00	1.00	1.00	1.00	1.00	1.00	1.00	1.00	1.00	1.00	1.00	1.00	1.00	1.00	1.00	1.00
pr34	0.00	0.00	0.00	0.00	0.00	0.00	0.00	0.00	0.00	0.00	0.00	0.00	0.00	0.00	0.00	0.00	0.00	0.00
A	15.84	15.84	15.84	15.84	15.84	15.84	15.84	15.84	15.84	15.84	15.84	15.84	15.84	15.84	15.84	15.84	15.84	15.84
VTS	-5.52	-5.52	-5.52	-5.52	-5.52	-5.52	-5.52	-5.52	-5.52	-5.52	-5.52	-5.52	-5.52	-5.52	-5.52	-5.52	-5.52	-5.52
eta	9.582E+08	9.582E+08	9.582E+08	9.582E+08	9.582E+08	9.582E+08	3.882E+06	3.882E+06	3.882E+06	3.882E+06	3.882E+06	3.882E+06	3.781E+04	3.781E+04	3.781E+04	3.781E+04	3.781E+04	3.781E+04
temp_f	39.2	39.2	39.2	39.2	39.2	39.2	68	68	68	68	68	68	104	104	104	104	104	104
freq	0.1	0.50	1.00	5.00	10.00	25.00	0.1	0.50	1.00	5.00	10.00	25.00	0.1	0.50	1.00	5.00	10.00	25.00
estar	707903.0	1004841.9	1143468.6	1491895.8	1631092.8	1857805.3	135248.6	244566.9	293578.9	492605.7	573873.5	723054.2	26469.7	47500.6	58461.9	108497.1	133204.8	186317.6

Table A.1.D

mix_id	B 9.5_64_M2																
north	0	0	0	0	0	0	0	0	0	0	0	0	0	0	0	0	0	0
middle	1	1	1	1	1	1	1	1	1	1	1	1	1	1	1	1	1	1
south	0	0	0	0	0	0	0	0	0	0	0	0	0	0	0	0	0	0
pg64	1	1	1	1	1	1	1	1	1	1	1	1	1	1	1	1	1	1
pg67	0	0	0	0	0	0	0	0	0	0	0	0	0	0	0	0	0	0
pg76	0	0	0	0	0	0	0	0	0	0	0	0	0	0	0	0	0	0
nmas	9.5	9.5	9.5	9.5	9.5	9.5	9.5	9.5	9.5	9.5	9.5	9.5	9.5	9.5	9.5	9.5	9.5	9.5
rap	30	30	30	30	30	30	30	30	30	30	30	30	30	30	30	30	30	30
binder	5.60	5.60	5.60	5.60	5.60	5.60	5.60	5.60	5.60	5.60	5.60	5.60	5.60	5.60	5.60	5.60	5.60	5.60
gmm	2.498	2.498	2.498	2.498	2.498	2.498	2.498	2.498	2.498	2.498	2.498	2.498	2.498	2.498	2.498	2.498	2.498	2.498
av	6.5	6.5	6.5	6.5	6.5	6.5	6.5	6.5	6.5	6.5	6.5	6.5	6.5	6.5	6.5	6.5	6.5	6.5
vma	18.09	18.09	18.09	18.09	18.09	18.09	18.09	18.09	18.09	18.09	18.09	18.09	18.09	18.09	18.09	18.09	18.09	18.09
vfa	64.30	64.30	64.30	64.30	64.30	64.30	64.30	64.30	64.30	64.30	64.30	64.30	64.30	64.30	64.30	64.30	64.30	64.30
eff_binder	11.6	11.6	11.6	11.6	11.6	11.6	11.6	11.6	11.6	11.6	11.6	11.6	11.6	11.6	11.6	11.6	11.6	11.6
dr	0.48	0.48	0.48	0.48	0.48	0.48	0.48	0.48	0.48	0.48	0.48	0.48	0.48	0.48	0.48	0.48	0.48	0.48
sapp	10.36	10.36	10.36	10.36	10.36	10.36	10.36	10.36	10.36	10.36	10.36	10.36	10.36	10.36	10.36	10.36	10.36	10.36
pp200	6.50	6.50	6.50	6.50	6.50	6.50	6.50	6.50	6.50	6.50	6.50	6.50	6.50	6.50	6.50	6.50	6.50	6.50
pp4	73.00	73.00	73.00	73.00	73.00	73.00	73.00	73.00	73.00	73.00	73.00	73.00	73.00	73.00	73.00	73.00	73.00	73.00
pr38	6.00	6.00	6.00	6.00	6.00	6.00	6.00	6.00	6.00	6.00	6.00	6.00	6.00	6.00	6.00	6.00	6.00	6.00
pr34	0.00	0.00	0.00	0.00	0.00	0.00	0.00	0.00	0.00	0.00	0.00	0.00	0.00	0.00	0.00	0.00	0.00	0.00
A	-14.41	-14.41	-14.41	-14.41	-14.41	-14.41	-14.41	-14.41	-14.41	-14.41	-14.41	-14.41	-14.41	-14.41	-14.41	-14.41	-14.41	-14.41
VTS	5.34	5.34	5.34	5.34	5.34	5.34	5.34	5.34	5.34	5.34	5.34	5.34	5.34	5.34	5.34	5.34	5.34	5.34
eta	9.581E+00	9.581E+00	9.581E+00	9.581E+00	9.581E+00	9.581E+00	2.110E+01	2.110E+01	2.110E+01	2.110E+01	2.110E+01	2.110E+01	7.648E+01	7.648E+01	7.648E+01	7.648E+01	7.648E+01	7.648E+01
temp_f	39.2	39.2	39.2	39.2	39.2	39.2	68	68	68	68	68	68	104	104	104	104	104	104
freq	0.1	0.50	1.00	5.00	10.00	25.00	0.1	0.50	1.00	5.00	10.00	25.00	0.1	0.50	1.00	5.00	10.00	25.00
estar	726462.8	1059151.3	1180868.2	1560876.4	1682118.0	1905370.7	151093.0	273424.5	328404.9	548293.3	638449.9	796579.6	29618.9	52882.3	65149.4	121002.6	148834.2	207462.1
mix_id	B 9.5_67_S																	
north	0	0	0	0	0	0	0	0	0	0	0	0	0	0	0	0	0	0
middle	0	0	0	0	0	0	0	0	0	0	0	0	0	0	0	0	0	0
south	1	1	1	1	1	1	1	1	1	1	1	1	1	1	1	1	1	1
pg64	0	0	0	0	0	0	0	0	0	0	0	0	0	0	0	0	0	0
pg67	1	1	1	1	1	1	1	1	1	1	1	1	1	1	1	1	1	1
pg76	0	0	0	0	0	0	0	0	0	0	0	0	0	0	0	0	0	0
nmas	9.5	9.5	9.5	9.5	9.5	9.5	9.5	9.5	9.5	9.5	9.5	9.5	9.5	9.5	9.5	9.5	9.5	9.5
rap	25	25	25	25	25	25	25	25	25	25	25	25	25	25	25	25	25	25
binder	5.84	5.84	5.84	5.84	5.84	5.84	5.84	5.84	5.84	5.84	5.84	5.84	5.84	5.84	5.84	5.84	5.84	5.84
gmm	2.454	2.454	2.454	2.454	2.454	2.454	2.454	2.454	2.454	2.454	2.454	2.454	2.454	2.454	2.454	2.454	2.454	2.454
av	5.5	5.5	5.5	5.5	5.5	5.5	5.5	5.5	5.5	5.5	5.5	5.5	5.5	5.5	5.5	5.5	5.5	5.5
vma	18.21	18.21	18.21	18.21	18.21	18.21	18.21	18.21	18.21	18.21	18.21	18.21	18.21	18.21	18.21	18.21	18.21	18.21
vfa	70.28	70.28	70.28	70.28	70.28	70.28	70.28	70.28	70.28	70.28	70.28	70.28	70.28	70.28	70.28	70.28	70.28	70.28
eff_binder	12.8	12.8	12.8	12.8	12.8	12.8	12.8	12.8	12.8	12.8	12.8	12.8	12.8	12.8	12.8	12.8	12.8	12.8
dr	0.50	0.50	0.50	0.50	0.50	0.50	0.50	0.50	0.50	0.50	0.50	0.50	0.50	0.50	0.50	0.50	0.50	0.50
sapp	9.80	9.80	9.80	9.80	9.80	9.80	9.80	9.80	9.80	9.80	9.80	9.80	9.80	9.80	9.80	9.80	9.80	9.80
pp200	5.30	5.30	5.30	5.30	5.30	5.30	5.30	5.30	5.30	5.30	5.30	5.30	5.30	5.30	5.30	5.30	5.30	5.30
pp4	72.00	72.00	72.00	72.00	72.00	72.00	72.00	72.00	72.00	72.00	72.00	72.00	72.00	72.00	72.00	72.00	72.00	72.00
pr38	3.00	3.00	3.00	3.00	3.00	3.00	3.00	3.00	3.00	3.00	3.00	3.00	3.00	3.00	3.00	3.00	3.00	3.00
pr34	0.00	0.00	0.00	0.00	0.00	0.00	0.00	0.00	0.00	0.00	0.00	0.00	0.00	0.00	0.00	0.00	0.00	0.00
A	19.68	19.68	19.68	19.68	19.68	19.68	19.68	19.68	19.68	19.68	19.68	19.68	19.68	19.68	19.68	19.68	19.68	19.68
VTS	-6.88	-6.88	-6.88	-6.88	-6.88	-6.88	-6.88	-6.88	-6.88	-6.88	-6.88	-6.88	-6.88	-6.88	-6.88	-6.88	-6.88	-6.88
eta	2.455E+13	2.455E+13	2.455E+13	2.455E+13	2.455E+13	2.455E+13	1.265E+09	1.265E+09	1.265E+09	1.265E+09	1.265E+09	1.265E+09	6.039E+05	6.039E+05	6.039E+05	6.039E+05	6.039E+05	6.039E+05
temp_f	39.2	39.2	39.2	39.2	39.2	39.2	68	68	68	68	68	68	104	104	104	104	104	104
freq	0.1	0.50	1.00	5.00	10.00	25.00	0.1	0.50	1.00	5.00	10.00	25.00	0.1	0.50	1.00	5.00	10.00	25.00
estar	778385.7	1050892.3	1189408.6	1493083.7	1629393.3	1824385.8	154454.7	275616.6	328314.9	530523.2	612483.9	750601.3	24939.2	49369.8	62358.9	119532.0	148018.5	202299.2

Table A.1.E

mix_id	B 12.5_64_M																
north	0	0	0	0	0	0	0	0	0	0	0	0	0	0	0	0	0	0
middle	1	1	1	1	1	1	1	1	1	1	1	1	1	1	1	1	1	1
south	0	0	0	0	0	0	0	0	0	0	0	0	0	0	0	0	0	0
pg64	1	1	1	1	1	1	1	1	1	1	1	1	1	1	1	1	1	1
pg67	0	0	0	0	0	0	0	0	0	0	0	0	0	0	0	0	0	0
pg76	0	0	0	0	0	0	0	0	0	0	0	0	0	0	0	0	0	0
nmas	12.5	12.5	12.5	12.5	12.5	12.5	12.5	12.5	12.5	12.5	12.5	12.5	12.5	12.5	12.5	12.5	12.5	12.5
rap	30	30	30	30	30	30	30	30	30	30	30	30	30	30	30	30	30	30
binder	5.50	5.50	5.50	5.50	5.50	5.50	5.50	5.50	5.50	5.50	5.50	5.50	5.50	5.50	5.50	5.50	5.50	5.50
gmm	2.463	2.463	2.463	2.463	2.463	2.463	2.463	2.463	2.463	2.463	2.463	2.463	2.463	2.463	2.463	2.463	2.463	2.463
av	5.6	5.6	5.6	5.6	5.6	5.6	5.6	5.6	5.6	5.6	5.6	5.6	5.6	5.6	5.6	5.6	5.6	5.6
vma	18.01	18.01	18.01	18.01	18.01	18.01	18.01	18.01	18.01	18.01	18.01	18.01	18.01	18.01	18.01	18.01	18.01	18.01
vfa	69.16	69.16	69.16	69.16	69.16	69.16	69.16	69.16	69.16	69.16	69.16	69.16	69.16	69.16	69.16	69.16	69.16	69.16
eff_binder	12.5	12.5	12.5	12.5	12.5	12.5	12.5	12.5	12.5	12.5	12.5	12.5	12.5	12.5	12.5	12.5	12.5	12.5
dr	0.49	0.49	0.49	0.49	0.49	0.49	0.49	0.49	0.49	0.49	0.49	0.49	0.49	0.49	0.49	0.49	0.49	0.49
sapp	8.30	8.30	8.30	8.30	8.30	8.30	8.30	8.30	8.30	8.30	8.30	8.30	8.30	8.30	8.30	8.30	8.30	8.30
pp192	6.00	6.00	6.00	6.00	6.00	6.00	6.00	6.00	6.00	6.00	6.00	6.00	6.00	6.00	6.00	6.00	6.00	6.00
pp388	75.00	75.00	75.00	75.00	75.00	75.00	75.00	75.00	75.00	75.00	75.00	75.00	75.00	75.00	75.00	75.00	75.00	75.00
pr30	13.00	13.00	13.00	13.00	13.00	13.00	13.00	13.00	13.00	13.00	13.00	13.00	13.00	13.00	13.00	13.00	13.00	13.00
pr26	0.00	0.00	0.00	0.00	0.00	0.00	0.00	0.00	0.00	0.00	0.00	0.00	0.00	0.00	0.00	0.00	0.00	0.00
A	13.32	13.32	13.32	13.32	13.32	13.32	13.32	13.32	13.32	13.32	13.32	13.32	13.32	13.32	13.32	13.32	13.32	13.32
VTS	-4.60	-4.60	-4.60	-4.60	-4.60	-4.60	-4.60	-4.60	-4.60	-4.60	-4.60	-4.60	-4.60	-4.60	-4.60	-4.60	-4.60	-4.60
eta	9.125E+07	9.125E+07	9.125E+07	9.125E+07	9.125E+07	9.125E+07	1.404E+06	1.404E+06	1.404E+06	1.404E+06	1.404E+06	1.404E+06	3.440E+04	3.440E+04	3.440E+04	3.440E+04	3.440E+04	3.440E+04
temp_f	39.2	39.2	39.2	39.2	39.2	39.2	68	68	68	68	68	68	104	104	104	104	104	104
freq	0.1	0.50	1.00	5.00	10.00	25.00	0.1	0.50	1.00	5.00	10.00	25.00	0.1	0.50	1.00	5.00	10.00	25.00
estar	713383.3	1077654.1	1200054.4	1606245.4	1729371.3	1937672.3	139056.0	263347.9	321364.5	555823.0	654698.4	822028.1	24366.0	43769.0	54863.6	105352.5	132700.9	187019.7
mix_id	B 12.5_67_S																	
north	0	0	0	0	0	0	0	0	0	0	0	0	0	0	0	0	0	0
middle	0	0	0	0	0	0	0	0	0	0	0	0	0	0	0	0	0	0
south	1	1	1	1	1	1	1	1	1	1	1	1	1	1	1	1	1	1
pg64	0	0	0	0	0	0	0	0	0	0	0	0	0	0	0	0	0	0
pg67	1	1	1	1	1	1	1	1	1	1	1	1	1	1	1	1	1	1
pg76	0	0	0	0	0	0	0	0	0	0	0	0	0	0	0	0	0	0
nmas	12.5	12.5	12.5	12.5	12.5	12.5	12.5	12.5	12.5	12.5	12.5	12.5	12.5	12.5	12.5	12.5	12.5	12.5
rap	25	25	25	25	25	25	25	25	25	25	25	25	25	25	25	25	25	25
binder	5.41	5.41	5.41	5.41	5.41	5.41	5.41	5.41	5.41	5.41	5.41	5.41	5.41	5.41	5.41	5.41	5.41	5.41
gmm	2.468	2.468	2.468	2.468	2.468	2.468	2.468	2.468	2.468	2.468	2.468	2.468	2.468	2.468	2.468	2.468	2.468	2.468
av	6.0	6.0	6.0	6.0	6.0	6.0	6.0	6.0	6.0	6.0	6.0	6.0	6.0	6.0	6.0	6.0	6.0	6.0
vma	18.06	18.06	18.06	18.06	18.06	18.06	18.06	18.06	18.06	18.06	18.06	18.06	18.06	18.06	18.06	18.06	18.06	18.06
vfa	66.76	66.76	66.76	66.76	66.76	66.76	66.76	66.76	66.76	66.76	66.76	66.76	66.76	66.76	66.76	66.76	66.76	66.76
eff_binder	12.1	12.1	12.1	12.1	12.1	12.1	12.1	12.1	12.1	12.1	12.1	12.1	12.1	12.1	12.1	12.1	12.1	12.1
dr	0.47	0.47	0.47	0.47	0.47	0.47	0.47	0.47	0.47	0.47	0.47	0.47	0.47	0.47	0.47	0.47	0.47	0.47
sapp	9.02	9.02	9.02	9.02	9.02	9.02	9.02	9.02	9.02	9.02	9.02	9.02	9.02	9.02	9.02	9.02	9.02	9.02
pp584	5.00	5.00	5.00	5.00	5.00	5.00	5.00	5.00	5.00	5.00	5.00	5.00	5.00	5.00	5.00	5.00	5.00	5.00
pp780	75.00	75.00	75.00	75.00	75.00	75.00	75.00	75.00	75.00	75.00	75.00	75.00	75.00	75.00	75.00	75.00	75.00	75.00
pr22	14.00	14.00	14.00	14.00	14.00	14.00	14.00	14.00	14.00	14.00	14.00	14.00	14.00	14.00	14.00	14.00	14.00	14.00
pr18	0.00	0.00	0.00	0.00	0.00	0.00	0.00	0.00	0.00	0.00	0.00	0.00	0.00	0.00	0.00	0.00	0.00	0.00
A	19.99	19.99	19.99	19.99	19.99	19.99	19.99	19.99	19.99	19.99	19.99	19.99	19.99	19.99	19.99	19.99	19.99	19.99
VTS	-6.99	-6.99	-6.99	-6.99	-6.99	-6.99	-6.99	-6.99	-6.99	-6.99	-6.99	-6.99	-6.99	-6.99	-6.99	-6.99	-6.99	-6.99
eta	5.809E+13	5.809E+13	5.809E+13	5.809E+13	5.809E+13	5.809E+13	1.995E+09	1.995E+09	1.995E+09	1.995E+09	1.995E+09	1.995E+09	7.328E+05	7.328E+05	7.328E+05	7.328E+05	7.328E+05	7.328E+05
temp_f	39.2	39.2	39.2	39.2	39.2	39.2	68	68	68	68	68	68	104	104	104	104	104	104
freq	0.1	0.50	1.00	5.00	10.00	25.00	0.1	0.50	1.00	5.00	10.00	25.00	0.1	0.50	1.00	5.00	10.00	25.00
estar	713383.3	1077654.1	1200054.4	1606245.4	1729371.3	1937672.3	139056.0	263347.9	321364.5	555823.0	654698.4	822028.1	24366.0	43769.0	54863.6	105352.5	132700.9	187019.7

Table A.1.F

mix_id	B 25_64_M																
north	0	0	0	0	0	0	0	0	0	0	0	0	0	0	0	0	0	0
middle	1	1	1	1	1	1	1	1	1	1	1	1	1	1	1	1	1	1
south	0	0	0	0	0	0	0	0	0	0	0	0	0	0	0	0	0	0
pg64	1	1	1	1	1	1	1	1	1	1	1	1	1	1	1	1	1	1
pg67	0	0	0	0	0	0	0	0	0	0	0	0	0	0	0	0	0	0
pg76	0	0	0	0	0	0	0	0	0	0	0	0	0	0	0	0	0	0
nmas	25	25	25	25	25	25	25	25	25	25	25	25	25	25	25	25	25	25
rap	30	30	30	30	30	30	30	30	30	30	30	30	30	30	30	30	30	30
binder	4.40	4.40	4.40	4.40	4.40	4.40	4.40	4.40	4.40	4.40	4.40	4.40	4.40	4.40	4.40	4.40	4.40	4.40
gmm	2.554	2.554	2.554	2.554	2.554	2.554	2.554	2.554	2.554	2.554	2.554	2.554	2.554	2.554	2.554	2.554	2.554	2.554
av	5.9	5.9	5.9	5.9	5.9	5.9	5.9	5.9	5.9	5.9	5.9	5.9	5.9	5.9	5.9	5.9	5.9	5.9
vma	15.33	15.33	15.33	15.33	15.33	15.33	15.33	15.33	15.33	15.33	15.33	15.33	15.33	15.33	15.33	15.33	15.33	15.33
vfa	61.42	61.42	61.42	61.42	61.42	61.42	61.42	61.42	61.42	61.42	61.42	61.42	61.42	61.42	61.42	61.42	61.42	61.42
eff_binder	9.4	9.4	9.4	9.4	9.4	9.4	9.4	9.4	9.4	9.4	9.4	9.4	9.4	9.4	9.4	9.4	9.4	9.4
dr	0.42	0.42	0.42	0.42	0.42	0.42	0.42	0.42	0.42	0.42	0.42	0.42	0.42	0.42	0.42	0.42	0.42	0.42
sapp	8.57	8.57	8.57	8.57	8.57	8.57	8.57	8.57	8.57	8.57	8.57	8.57	8.57	8.57	8.57	8.57	8.57	8.57
pp976	5.00	5.00	5.00	5.00	5.00	5.00	5.00	5.00	5.00	5.00	5.00	5.00	5.00	5.00	5.00	5.00	5.00	5.00
pp1172	83.00	83.00	83.00	83.00	83.00	83.00	83.00	83.00	83.00	83.00	83.00	83.00	83.00	83.00	83.00	83.00	83.00	83.00
pr14	10.00	10.00	10.00	10.00	10.00	10.00	10.00	10.00	10.00	10.00	10.00	10.00	10.00	10.00	10.00	10.00	10.00	10.00
pr10	8.00	8.00	8.00	8.00	8.00	8.00	8.00	8.00	8.00	8.00	8.00	8.00	8.00	8.00	8.00	8.00	8.00	8.00
A	7.77	7.77	7.77	7.77	7.77	7.77	7.77	7.77	7.77	7.77	7.77	7.77	7.77	7.77	7.77	7.77	7.77	7.77
VTS	-2.59	-2.59	-2.59	-2.59	-2.59	-2.59	-2.59	-2.59	-2.59	-2.59	-2.59	-2.59	-2.59	-2.59	-2.59	-2.59	-2.59	-2.59
eta	8.515E+05	8.515E+05	8.515E+05	8.515E+05	8.515E+05	8.515E+05	1.340E+05	1.340E+05	1.340E+05	1.340E+05	1.340E+05	1.340E+05	2.093E+04	2.093E+04	2.093E+04	2.093E+04	2.093E+04	2.093E+04
temp_f	39.2	39.2	39.2	39.2	39.2	39.2	68	68	68	68	68	68	104	104	104	104	104	104
freq	0.1	0.50	1.00	5.00	10.00	25.00	0.1	0.50	1.00	5.00	10.00	25.00	0.1	0.50	1.00	5.00	10.00	25.00
estar	1155864.7	1551696.6	1677457.0	2059317.7	2169614.9	2361790.6	312971.6	521710.4	611118.8	924418.2	1050408.2	1234732.3	65956.8	113106.7	139265.9	241926.6	295963.7	383008.7

FIGURE A.1.A

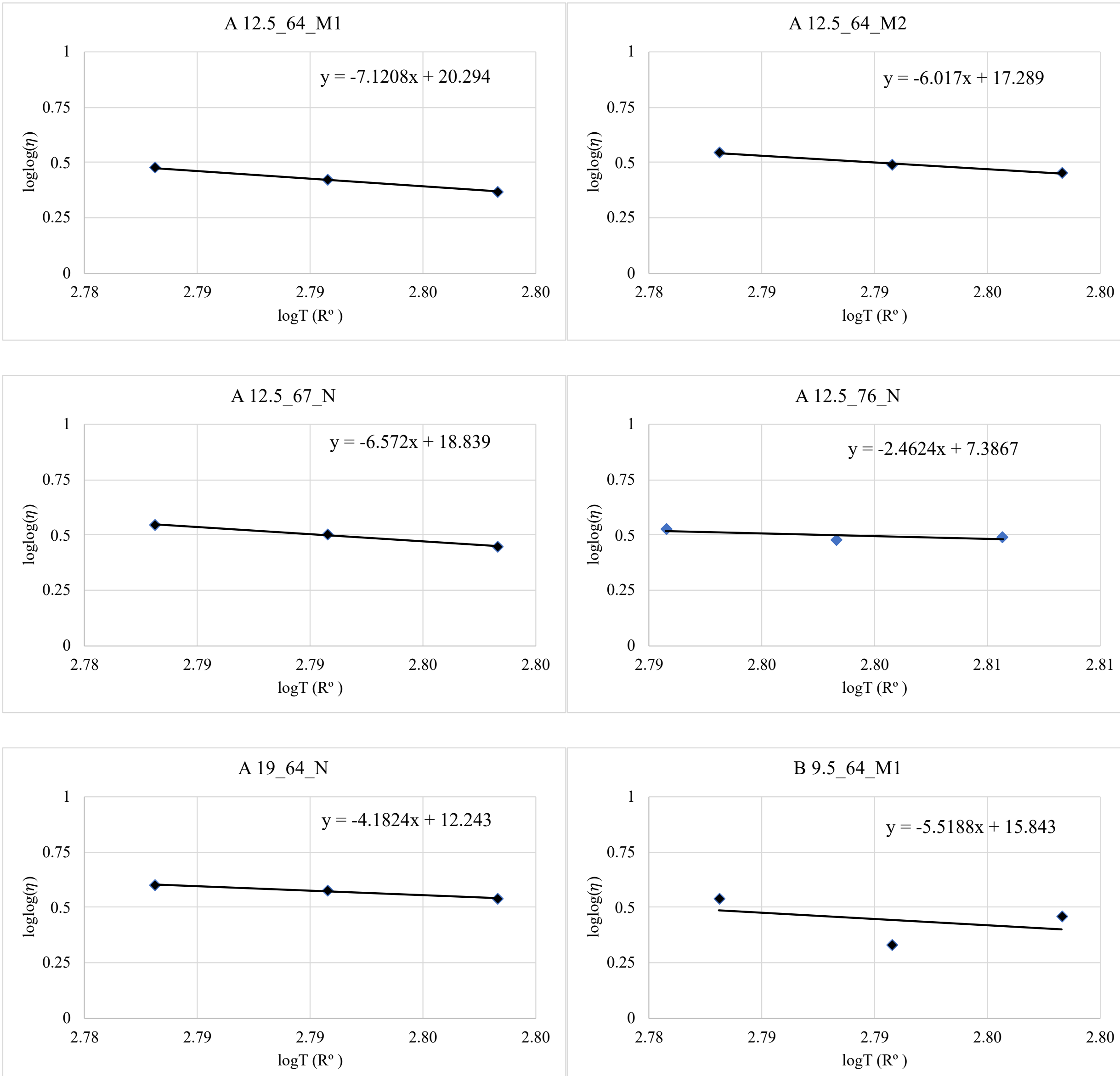
A 12.5_64_M1
y = -7.1208x + 20.294
A 12.5_64_M2
y = -6.017x + 17.289
A 12.5_67_N
y = -6.572x + 18.839
A 12.5_76_N
y = -2.4624x + 7.3867
A 19_64_N
y = -4.1824x + 12.243
B 9.5_64_M1
y = -5.5188x + 15.843
loglog(η)
logT (Rº)

FIGURE A.1.B

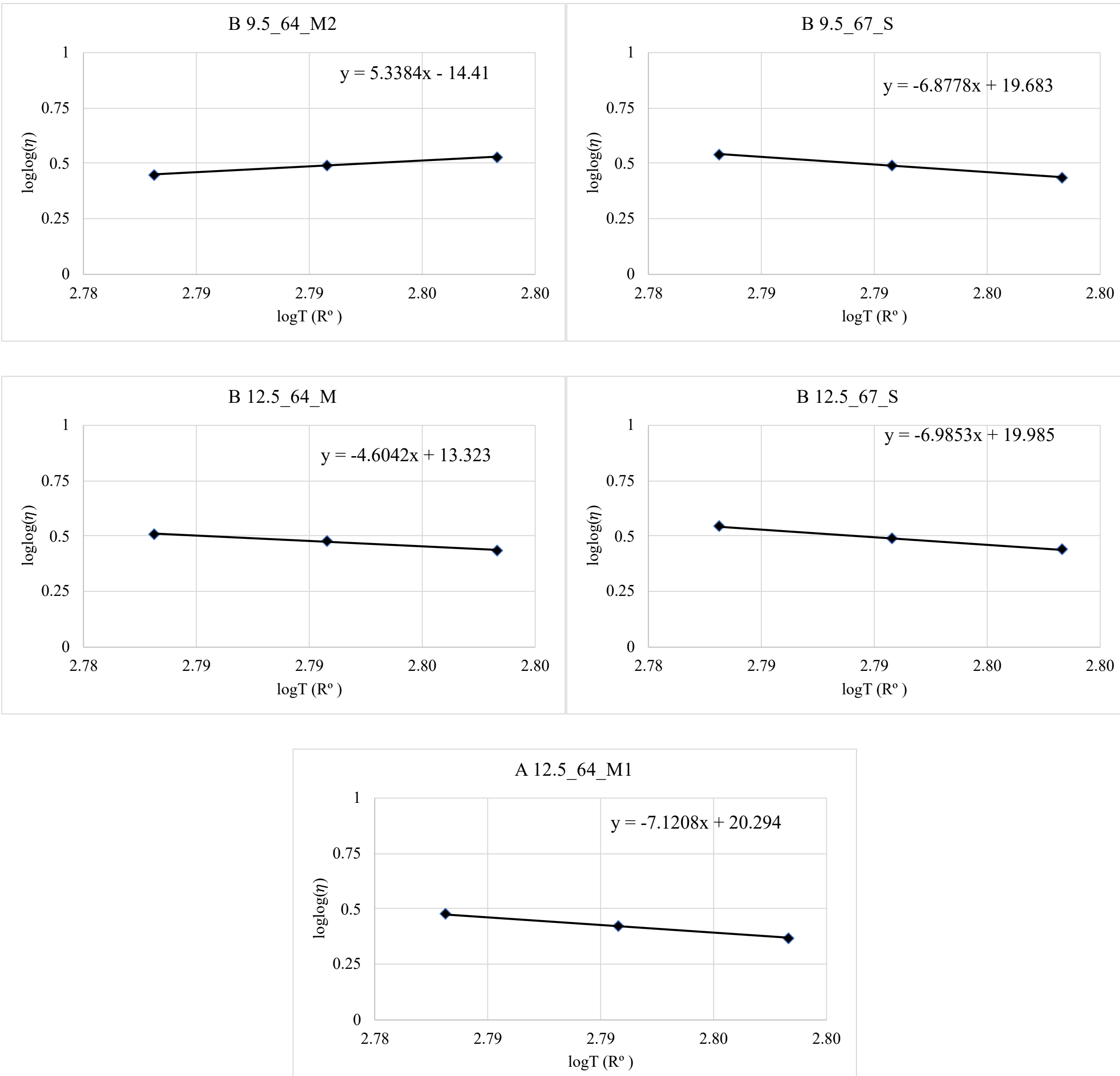

B 9.5_64_M2
y = 5.3384x - 14.41
B 9.5_67_S
y = -6.8778x + 19.683
B 12.5_64_M
y = -4.6042x + 13.323
B 12.5_67_S
y = -6.9853x + 19.985
A 12.5_64_M1
y = -7.1208x + 20.294
loglog(η)
logT (Rº)
0
0.25
0.5
0.75
1
2.78
2.79
2.79
2.80
2.80

Appendix B

Table B.1.A

A_12.5_64_M1		A_12.5_64_M2		A_12.5_67_N	
E∞	11,571.97	**E∞**	832.27	**E∞**	17,393.04
ρ*i*(s)	**E*i***	**ρ*i*(s)**	**E*i***	**ρ*i*(s)**	**E*i***
2.00E+08	5,323.92	2.00E+08	2,217.82	2.00E+08	11,772.59
2.00E+07	2,495.92	2.00E+07	1,462.60	2.00E+07	4,825.86
2.00E+06	6,710.90	2.00E+06	4,391.64	2.00E+06	13,256.04
2.00E+05	13,317.46	2.00E+05	11,358.37	2.00E+05	25,095.61
2.00E+04	30,287.13	2.00E+04	32,944.28	2.00E+04	53,679.75
2.00E+03	75,254.30	2.00E+03	98,773.77	2.00E+03	121,211.84
2.00E+02	198,804.11	2.00E+02	282,271.63	2.00E+02	280,528.92
2.00E+01	516,708.24	2.00E+01	702,517.22	2.00E+01	624,516.38
2.00E+00	1,189,381.06	2.00E+00	1,424,581.16	2.00E+00	1,242,534.43
2.00E-01	2,214,042.21	2.00E-01	2,292,146.06	2.00E-01	2,082,133.54
2.00E-02	3,199,098.01	2.00E-02	2,958,297.49	2.00E-02	2,861,620.54
2.00E-03	3,632,703.62	2.00E-03	3,168,805.07	2.00E-03	3,250,004.09
2.00E-04	3,392,167.02	2.00E-04	2,937,233.67	2.00E-04	3,142,419.52
2.00E-05	2,747,167.40	2.00E-05	2,448,991.43	2.00E-05	2,684,865.25
2.00E-06	2,019,458.53	2.00E-06	1,894,947.42	2.00E-06	2,097,940.84
2.00E-07	1,392,055.31	2.00E-07	1,391,153.19	2.00E-07	1,539,115.61
2.00E-08	953,374.33	2.00E-08	1,023,034.58	2.00E-08	1,122,623.96
A_12.5_76_N		**A_19_64_N**		**A_19_64_N2**	
E∞	23,717.09	**E∞**	16,794.19	**E∞**	36,886.99
ρ*i*(s)	**E*i***	**ρ*i*(s)**	**E*i***	**ρ*i*(s)**	**E*i***
2.00E+08	11,522.40	2.00E+08	13,493.79	2.00E+08	20,101.30
2.00E+07	4,704.30	2.00E+07	5,995.55	2.00E+07	9,920.00
2.00E+06	12,718.37	2.00E+06	16,499.57	2.00E+06	26,614.17
2.00E+05	23,530.23	2.00E+05	32,604.90	2.00E+05	53,479.79
2.00E+04	49,205.28	2.00E+04	72,499.49	2.00E+04	120,439.22
2.00E+03	109,329.75	2.00E+03	168,857.88	2.00E+03	283,598.58
2.00E+02	252,766.12	2.00E+02	394,311.82	2.00E+02	659,272.38
2.00E+01	572,880.63	2.00E+01	857,331.56	2.00E+01	1,378,983.00
2.00E+00	1,177,160.53	2.00E+00	1,611,499.33	2.00E+00	2,382,344.04
2.00E-01	2,043,812.26	2.00E-01	2,494,210.61	2.00E-01	3,255,499.90
2.00E-02	2,888,365.35	2.00E-02	3,144,208.62	2.00E-02	3,545,591.39
2.00E-03	3,329,276.96	2.00E-03	3,295,816.17	2.00E-03	3,206,859.04
2.00E-04	3,225,211.05	2.00E-04	2,980,377.89	2.00E-04	2,533,034.01
2.00E-05	2,734,416.93	2.00E-05	2,416,421.46	2.00E-05	1,825,071.64
2.00E-06	2,107,591.33	2.00E-06	1,814,681.17	2.00E-06	1,238,619.05
2.00E-07	1,520,329.26	2.00E-07	1,292,272.61	2.00E-07	808,540.02
2.00E-08	1,088,007.54	2.00E-08	920,991.42	2.00E-08	532,708.73

Table B.1.B

A 25_64_N2		B 9.5_64_M1		B 9.5_64_M2	
E∞	82,349.34	E∞	17,501.43	E∞	23,596.74
ρ*i*(s)	**E*i***	**ρ*i*(s)**	**E*i***	**ρ*i*(s)**	**E*i***
2.00E+08	18,783.00	2.00E+08	7,121.30	2.00E+08	7,547.00
2.00E+07	9,782.64	2.00E+07	3,021.45	2.00E+07	3,384.88
2.00E+06	25,089.97	2.00E+06	8,094.32	2.00E+06	8,916.81
2.00E+05	48,363.15	2.00E+05	15,134.59	2.00E+05	16,741.68
2.00E+04	103,846.03	2.00E+04	32,155.64	2.00E+04	35,591.36
2.00E+03	237,595.77	2.00E+03	73,688.70	2.00E+03	81,833.28
2.00E+02	561,417.67	2.00E+02	179,580.34	2.00E+02	201,010.79
2.00E+01	1,254,610.64	2.00E+01	439,287.77	2.00E+01	496,676.67
2.00E+00	2,366,928.29	2.00E+00	989,187.83	2.00E+00	1,122,516.71
2.00E-01	3,470,158.43	2.00E-01	1,880,367.54	2.00E-01	2,108,329.26
2.00E-02	3,892,448.55	2.00E-02	2,863,335.16	2.00E-02	3,113,453.31
2.00E-03	3,482,377.10	2.00E-03	3,473,978.09	2.00E-03	3,611,951.08
2.00E-04	2,647,991.00	2.00E-04	3,462,793.73	2.00E-04	3,421,674.83
2.00E-05	1,811,058.87	2.00E-05	2,968,497.06	2.00E-05	2,789,426.21
2.00E-06	1,160,011.26	2.00E-06	2,286,836.93	2.00E-06	2,051,820.04
2.00E-07	713,674.72	2.00E-07	1,637,351.54	2.00E-07	1,409,760.54
2.00E-08	442,481.12	2.00E-08	1,157,873.29	2.00E-08	959,877.84

B 9.5_67_S		B 12.5_64_M		B 12.5_67_S	
E∞	2,759.60	E∞	26,794.63	E∞	17,656.61
ρ*i*(s)	**E*i***	**ρ*i*(s)**	**E*i***	**ρ*i*(s)**	**E*i***
2.00E+08	4,050.99	2.00E+08	5,299.72	2.00E+08	10,305.02
2.00E+07	2,029.26	2.00E+07	2,696.16	2.00E+07	4,315.65
2.00E+06	5,790.13	2.00E+06	6,917.05	2.00E+06	11,759.71
2.00E+05	12,713.89	2.00E+05	13,249.32	2.00E+05	22,312.38
2.00E+04	31,669.46	2.00E+04	28,590.15	2.00E+04	47,951.23
2.00E+03	83,435.31	2.00E+03	67,571.05	2.00E+03	109,555.95
2.00E+02	220,373.47	2.00E+02	174,721.30	2.00E+02	258,854.15
2.00E+01	539,376.38	2.00E+01	466,488.93	2.00E+01	592,550.99
2.00E+00	1,134,873.24	2.00E+00	1,146,898.21	2.00E+00	1,213,588.86
2.00E-01	1,956,260.97	2.00E-01	2,284,732.03	2.00E-01	2,080,640.74
2.00E-02	2,730,521.04	2.00E-02	3,418,405.50	2.00E-02	2,894,944.40
2.00E-03	3,143,387.89	2.00E-03	3,844,706.46	2.00E-03	3,292,482.94
2.00E-04	3,089,745.19	2.00E-04	3,433,229.65	2.00E-04	3,161,425.81
2.00E-05	2,693,002.90	2.00E-05	2,608,760.03	2.00E-05	2,668,744.66
2.00E-06	2,151,712.74	2.00E-06	1,786,824.16	2.00E-06	2,055,252.47
2.00E-07	1,615,765.63	2.00E-07	1,147,105.07	2.00E-07	1,484,831.37
2.00E-08	1,207,560.06	2.00E-08	731,491.72	2.00E-08	1,065,947.99

Table B.1.C

B 19_64_M		B 25_64_M		C 9.5_67_M	
E∞	10,000.00	E∞	54,153.37	E∞	26,059.06
ρ*i*(s)	**E*i***	**ρ*i*(s)**	**E*i***	**ρ*i*(s)**	**E*i***
2.00E+08	6,069.75	2.00E+08	16,816.07	2.00E+08	16,184.32
2.00E+07	3,314.49	2.00E+07	8,090.87	2.00E+07	6,814.04
2.00E+06	9,091.97	2.00E+06	21,110.07	2.00E+06	18,546.05
2.00E+05	19,924.23	2.00E+05	40,334.75	2.00E+05	35,122.13
2.00E+04	50,347.33	2.00E+04	86,425.53	2.00E+04	74,793.60
2.00E+03	138,475.39	2.00E+03	197,252.50	2.00E+03	167,128.94
2.00E+02	388,071.39	2.00E+02	464,991.14	2.00E+02	378,755.76
2.00E+01	986,992.06	2.00E+01	1,044,574.04	2.00E+01	813,379.01
2.00E+00	2,031,268.18	2.00E+00	2,020,413.75	2.00E+00	1,536,022.88
2.00E-01	3,177,224.84	2.00E-01	3,114,552.55	2.00E-01	2,413,571.01
2.00E-02	3,789,161.25	2.00E-02	3,744,121.00	2.00E-02	3,096,404.48
2.00E-03	3,614,865.12	2.00E-03	3,613,520.54	2.00E-03	3,292,940.89
2.00E-04	2,933,386.30	2.00E-04	2,953,043.69	2.00E-04	3,005,558.01
2.00E-05	2,135,710.00	2.00E-05	2,153,155.58	2.00E-05	2,447,644.01
2.00E-06	1,450,383.08	2.00E-06	1,458,146.16	2.00E-06	1,839,496.39
2.00E-07	942,106.01	2.00E-07	941,943.65	2.00E-07	1,307,669.11
2.00E-08	615,499.83	2.00E-08	610,869.33	2.00E-08	928,737.55

C 12.5_67_M		C 12.5_76_M	
E∞	13,621.50	E∞	26,322.15
ρ*i*(s)	**E*i***	**ρ*i*(s)**	**E*i***
2.00E+08	8,076.26	2.00E+08	9,480.07
2.00E+07	3,668.22	2.00E+07	3,796.37
2.00E+06	9,979.73	2.00E+06	10,145.51
2.00E+05	19,753.63	2.00E+05	18,268.85
2.00E+04	44,512.99	2.00E+04	37,144.33
2.00E+03	107,608.96	2.00E+03	80,613.60
2.00E+02	269,193.35	2.00E+02	185,243.87
2.00E+01	644,811.71	2.00E+01	429,593.01
2.00E+00	1,350,084.11	2.00E+00	932,298.18
2.00E-01	2,303,656.95	2.00E-01	1,746,152.47
2.00E-02	3,122,259.68	2.00E-02	2,671,653.40
2.00E-03	3,418,437.47	2.00E-03	3,296,534.31
2.00E-04	3,150,221.56	2.00E-04	3,356,688.65
2.00E-05	2,557,995.13	2.00E-05	2,937,948.93
2.00E-06	1,903,114.91	2.00E-06	2,304,773.28
2.00E-07	1,334,303.60	2.00E-07	1,675,436.39
2.00E-08	932,393.15	2.00E-08	1,200,334.43

Appendix C

Table C.1

Mixture Type: A 12.5_64_M1
XML File: L1_PG64_12.5_A_R3-LG

Level 1

Asphalt Mix: Dynamic Modulus Table

Temperature	Mixture |E*|, psi					
(°F)	**0.1 Hz**	**0.5 Hz**	**1 Hz**	**5 Hz**	**10 Hz**	**25 Hz**
39.2	740,802	1,082,794	1,202,705	1,586,888	1,706,096	1,924,615
68	150,334	278,518	336,268	564,559	658,669	818,440
104	24,296	46,335	58,625	113,719	142,644	198,566
130	11,119	19,491	24,290	46,322	58,611	83,996

Asphalt Binder: Superpave Binder Test Data

Temperature	Angular Freq. = 10 rad/sec	
(°F)	G* (Pa)	Delta (degree)
147.2	8850	79.1
158	4220	82
168.8	2070	84.1

Asphalt General: Volumetric Properties as Built

Effective Binder Content (%)	12.5
Air Voids (%)	5.5
Total Unit Weight (pcf)	145

Level 2

Asphalt Mix: Aggregate Gradation

	Cumulative Percent Retained	Percent Passing
3/4 Inch Sieve	0	100
3/8 Inch Sieve	14	86
#4 Sieve	26	74
#200 Sieve	94.2	5.8

Asphalt Mix: LVE Converted Creep Compliance

Loading Time (s)	D(t) (1/psi)
	Mid Temp (14 F)
1	1.67E-04
2	1.97E-04
5	2.27E-04
10	2.62E-04
20	2.92E-04
50	3.24E-04
100	3.56E-04

Asphalt Binder: Superpave Binder Test Data

Temperature	Angular Freq. = 10 rad/sec	
(°F)	G* (Pa)	Delta (degree)
147.2	8850	79.1
158	4220	82
168.8	2070	84.1

Asphalt General: Volumetric Properties as Built

Effective Binder Content (%)	12.5
Air Voids (%)	5.5
Total Unit Weight (pcf)	145

Level 3

Asphalt Mix: Aggregate Gradation

Cumulative % Retained on 3/4 Inch Sieve	0
Cumulative % Retained on 3/8 Inch Sieve	14
Cumulative % Retained on #4 Sieve	26
% Passing #200 Sieve	5.8

Asphalt General: Volumetric Properties as Built

Effective Binder Content (%)	12.5
Air Voids (%)	5.5
Total Unit Weight (pcf)	145

Asphalt Binder: Superpave Binder Grading:	PG 64-22

Table C.2

Mixture Type: A 12.5_64_M2	
XML File:	L1_PG64_12.5_A_R3-FP

Level 1

Asphalt Mix: Dynamic Modulus Table

Temperature	Mixture |E*|, psi					
(°F)	**0.1 Hz**	**0.5 Hz**	**1 Hz**	**5 Hz**	**10 Hz**	**25 Hz**
39.2	913,266	1,203,332	1,342,315	1,646,168	1,775,603	1,961,809
68	196,746	348,622	411,796	649,274	741,030	894,448
104	33,991	70,120	89,932	173,205	212,727	301,364
130	19,970	39,240	55,296	102,271	139,928	188,459

Asphalt Binder: Superpave Binder Test Data

Temperature	Angular Freq. = 10 rad/sec	
(°F)	G* (Pa)	Delta (degree)
147.2	27500	73.7
158	10800	76.8
168.8	6600	79.2

Asphalt General: Volumetric Properties as Built

Effective Binder Content (%)	12.2
Air Voids (%)	5.5
Total Unit Weight (pcf)	145

Level 2

Asphalt Mix: Aggregate Gradation

	Cumulative Percent Retained	Percent Passing
3/4 Inch Sieve	0	100
3/8 Inch Sieve	12	88
#4 Sieve	27	73
#200 Sieve	94.1	5.9

Asphalt Mix: LVE Converted Creep Compliance

Loading Time (s)	D(t) (1/psi)
	Mid Temp (14 F)
1	4.68E-04
2	6.07E-04
5	9.12E-04
10	1.06E-03
20	1.33E-03
50	1.69E-03
100	1.69E-03

Asphalt Binder: Superpave Binder Test Data

Temperature	Angular Freq. = 10 rad/sec	
(°F)	G* (Pa)	Delta (degree)
147.2	27500	73.7
158	10800	76.8
168.8	6600	79.2

Asphalt General: Volumetric Properties as Built

Effective Binder Content (%)	12.2
Air Voids (%)	5.5
Total Unit Weight (pcf)	145

Level 3

Asphalt Mix: Aggregate Gradation

Cumulative % Retained on 3/4 Inch Sieve	0
Cumulative % Retained on 3/8 Inch Sieve	12
Cumulative % Retained on #4 Sieve	27
% Passing #200 Sieve	5.9

Asphalt General: Volumetric Properties as Built

Effective Binder Content (%)	12.2
Air Voids (%)	5.5
Total Unit Weight (pcf)	145

Asphalt Binder: Superpave Binder Grading:	PG 64-22

Table C.3

Mixture Type: A 12.5_67_N
XML File: L1_PG67_12.5_A_R2

Level 1

Asphalt Mix: Dynamic Modulus Table

Temperature	Mixture |E*|, psi					
(°F)	**0.1 Hz**	**0.5 Hz**	**1 Hz**	**5 Hz**	**10 Hz**	**25 Hz**
39.2	787,225	1,089,505	1,207,067	1,545,325	1,661,798	1,870,709
68	192,088	325,597	382,568	599,750	686,073	833,912
104	38,301	66,256	82,046	142,791	175,827	228,559
130	18,543	29,902	37,036	63,196	79,242	104,091

Asphalt Binder: Superpave Binder Test Data

Temperature	Angular Freq. = 10 rad/sec	
(°F)	G* (Pa)	Delta (degree)
147.2	26600	72.1
158	12400	75.3
168.8	5780	78.5

Asphalt General: Volumetric Properties as Built

Effective Binder Content (%)	11.8
Air Voids (%)	6.3
Total Unit Weight (pcf)	145

Level 2

Asphalt Mix: Aggregate Gradation

	Cumulative Percent Retained	Percent Passing
3/4 Inch Sieve	0	100
3/8 Inch Sieve	13	87
#4 Sieve	25	75
#200 Sieve	93.7	6.3

Asphalt Mix: LVE Converted Creep Compliance

Loading Time (s)	D(t) (1/psi)
	Mid Temp (14 F)
1	9.99E-05
2	1.13E-04
5	1.33E-04
10	1.54E-04
20	1.69E-04
50	1.91E-04
100	2.11E-04

Asphalt Binder: Superpave Binder Test Data

Temperature	Angular Freq. = 10 rad/sec	
(°F)	G* (Pa)	Delta (degree)
147	26600	72.1
158	12400	75.3
169	5780	78.5

Asphalt General: Volumetric Properties as Built

Effective Binder Content (%)	11.8
Air Voids (%)	6.3
Total Unit Weight (pcf)	145

Level 3

Asphalt Mix: Aggregate Gradation

Cumulative % Retained on 3/4 Inch Sieve	0
Cumulative % Retained on 3/8 Inch Sieve	13
Cumulative % Retained on #4 Sieve	25
% Passing #200 Sieve	6.3

Asphalt General: Volumetric Properties as Built

Effective Binder Content (%)	11.8
Air Voids (%)	6.3
Total Unit Weight (pcf)	145

Asphalt Binder: Superpave Binder Grading: PG 67-22

Table C.4

Mixture Type: A 12.5_76_N

XML File: L1_PG76_12.5_A_R2

Level 1

Asphalt Mix: Dynamic Modulus Table

Temperature	Mixture |E*|, psi					
(°F)	**0.1 Hz**	**0.5 Hz**	**1 Hz**	**5 Hz**	**10 Hz**	**25 Hz**
39.2	829,119	1,118,111	1,264,046	1,585,167	1,726,851	1,930,605
68	177,587	304,657	359,764	573,195	658,991	807,522
104	35,227	59,261	73,824	127,260	158,583	205,713
130	18,567	29,167	35,573	60,107	74,603	98,547

Asphalt Binder: Superpave Binder Test Data

Temperature	Angular Freq. = 10 rad/sec	
(°F)	G* (Pa)	Delta (degree)
158	14100	65.8
168.8	6770	67.2
179.6	8140	67.8

Asphalt General: Volumetric Properties as Built

Effective Binder Content (%)	12.6
Air Voids (%)	5.7
Total Unit Weight (pcf)	145

Level 2

Asphalt Mix: Aggregate Gradation

	Cumulative Percent Retained	Percent Passing
3/4 Inch Sieve	0	100
3/8 Inch Sieve	10	90
#4 Sieve	27	73
#200 Sieve	93.7	6.3

Asphalt Mix: LVE Converted Creep Compliance

Loading Time (s)	D(t) (1/psi)
	Mid Temp (14 F)
1	1.08E-04
2	1.20E-04
5	1.40E-04
10	1.50E-04
20	1.63E-04
50	1.80E-04
100	1.82E-04

Asphalt Binder: Superpave Binder Test Data

Temperature	Angular Freq. = 10 rad/sec	
(°F)	G* (Pa)	Delta (degree)
158	14100	65.8
168.8	6770	67.2
179.6	8140	67.8

Asphalt General: Volumetric Properties as Built

Effective Binder Content (%)	12.6
Air Voids (%)	5.7
Total Unit Weight (pcf)	145

Level 3

Asphalt Mix: Aggregate Gradation

Cumulative % Retained on 3/4 Inch Sieve	0
Cumulative % Retained on 3/8 Inch Sieve	10
Cumulative % Retained on #4 Sieve	27
% Passing #200 Sieve	6.3

Asphalt General: Volumetric Properties as Built

Effective Binder Content (%)	12.6
Air Voids (%)	5.7
Total Unit Weight (pcf)	145

Asphalt Binder: Superpave Binder Grading: PG 76-22

Table C.5

Mixture Type: A 19_64_N
XML File: L1_PG64_19_A_R2

Level 1

Asphalt Mix: Dynamic Modulus Table

Temperature	Mixture |E*|, psi					
(°F)	**0.1 Hz**	**0.5 Hz**	**1 Hz**	**5 Hz**	**10 Hz**	**25 Hz**
39.2	1,080,201	1,378,093	1,534,188	1,835,810	1,977,396	2,154,776
68	259,963	430,811	501,396	759,378	859,191	1,021,609
104	49,660	86,728	108,870	187,266	232,492	296,430
130	24,494	41,822	51,610	91,408	113,125	150,931

Asphalt Binder: Superpave Binder Test Data

Temperature	Angular Freq. = 10 rad/sec	
(°F)	G* (Pa)	Delta (degree)
147.2	49700	60.4
158	31300	62.2
168.8	16500	63.7

Asphalt General: Volumetric Properties as Built

Effective Binder Content (%)	11.6
Air Voids (%)	5.5
Total Unit Weight (pcf)	145

Level 2

Asphalt Mix: Aggregate Gradation

	Cumulative Percent Retained	Percent Passing
3/4 Inch Sieve	5	95
3/8 Inch Sieve	11	89
#4 Sieve	27	73
#200 Sieve	94.2	5.8

Asphalt Mix: LVE Converted Creep Compliance

Loading Time (s)	D(t) (1/psi)
	Mid Temp (14 F)
1	1.06E-04
2	1.25E-04
5	1.49E-04
10	1.64E-04
20	1.86E-04
50	2.04E-04
100	2.04E-04

Asphalt Binder: Superpave Binder Test Data

Temperature	Angular Freq. = 10 rad/sec	
(°F)	G* (Pa)	Delta (degree)
147.2	49700	60.4
158	31300	62.2
168.8	16500	63.7

Asphalt General: Volumetric Properties as Built

Effective Binder Content (%)	11.6
Air Voids (%)	5.5
Total Unit Weight (pcf)	145

Level 3

Asphalt Mix: Aggregate Gradation

Cumulative % Retained on 3/4 Inch Sieve	5
Cumulative % Retained on 3/8 Inch Sieve	11
Cumulative % Retained on #4 Sieve	27
% Passing #200 Sieve	5.8

Asphalt General: Volumetric Properties as Built

Effective Binder Content (%)	11.6
Air Voids (%)	5.5
Total Unit Weight (pcf)	145

Asphalt Binder: Superpave Binder Grading:	PG 64-22

Table C.6

Mixture Type: A 19_64_N2	
XML File: L1_PG64_19_A_R1	

Level 1

Asphalt Mix: Dynamic Modulus Table

Temperature	Mixture |E*|, psi					
(°F)	**0.1 Hz**	**0.5 Hz**	**1 Hz**	**5 Hz**	**10 Hz**	**25 Hz**
39.2	1,604,374	1,905,957	2,067,163	2,321,134	2,449,785	2,560,126
68	419,108	668,293	765,958	1,100,487	1,223,621	1,409,156
104	88,175	155,884	191,065	327,445	394,311	500,186
130	54,060	91,967	115,782	198,940	247,199	343,452

Asphalt Binder: Superpave Binder Test Data

Temperature	Angular Freq. = 10 rad/sec	
(°F)	G* (Pa)	Delta (degree)

Asphalt General: Volumetric Properties as Built

Effective Binder Content (%)	10.1
Air Voids (%)	5
Total Unit Weight (pcf)	145

Level 2

Asphalt Mix: Aggregate Gradation

	Cumulative Percent Retained	Percent Passing
3/4 Inch Sieve	1	99
3/8 Inch Sieve	9	91
#4 Sieve	19	81
#200 Sieve	94.7	5.3

Asphalt Mix: LVE Converted Creep Compliance

Loading Time (s)	D(t) (1/psi)
	Mid Temp (14 F)
1	8.19E-05
2	8.92E-05
5	1.03E-04
10	1.10E-04
20	1.10E-04
50	1.10E-04
100	1.10E-04

Asphalt Binder: Superpave Binder Test Data

Temperature	Angular Freq. = 10 rad/sec	
(°F)	G* (Pa)	Delta (degree)

Asphalt General: Volumetric Properties as Built

Effective Binder Content (%)	10.1
Air Voids (%)	5
Total Unit Weight (pcf)	145

Level 3

Asphalt Mix: Aggregate Gradation

Cumulative % Retained on 3/4 Inch Sieve	1
Cumulative % Retained on 3/8 Inch Sieve	9
Cumulative % Retained on #4 Sieve	19
% Passing #200 Sieve	5.3

Asphalt General: Volumetric Properties as Built

Effective Binder Content (%)	10.1
Air Voids (%)	5
Total Unit Weight (pcf)	145

Asphalt Binder: Superpave Binder Grading:	PG 64-22

Table C.7

Mixture Type: A 25_64_N2

XML File: L1_PG64_25_A_R1

Level 1

Asphalt Mix: Dynamic Modulus Table

Temperature	Mixture |E*|, psi					
(°F)	**0.1 Hz**	**0.5 Hz**	**1 Hz**	**5 Hz**	**10 Hz**	**25 Hz**
39.2	1,556,596	1,890,369	2,066,300	2,351,759	2,486,870	2,625,608
68	381,566	628,307	729,361	1,081,872	1,216,166	1,414,382
104	68,568	108,719	140,700	229,344	297,634	381,114
130	34,913	50,039	62,015	97,443	125,624	167,944

Asphalt Binder: Superpave Binder Test Data

Temperature	Angular Freq. = 10 rad/sec	
(°F)	G* (Pa)	Delta (degree)

Asphalt General: Volumetric Properties as Built

Effective Binder Content (%)	9.8
Air Voids (%)	5.2
Total Unit Weight (pcf)	145

Level 2

Asphalt Mix: Aggregate Gradation

	Cumulative Percent Retained	Percent Passing
3/4 Inch Sieve	7	93
3/8 Inch Sieve	9	91
#4 Sieve	15	85
#200 Sieve	94.5	5.5

Asphalt Mix: LVE Converted Creep Compliance

Loading Time (s)	D(t) (1/psi)
	Mid Temp (14 F)
1	4.77E-05
2	5.24E-05
5	5.66E-05
10	6.01E-05
20	6.34E-05
50	6.46E-05
100	6.46E-05

Asphalt Binder: Superpave Binder Test Data

Temperature	Angular Freq. = 10 rad/sec	
(°F)	G* (Pa)	Delta (degree)

Asphalt General: Volumetric Properties as Built

Effective Binder Content (%)	9.8
Air Voids (%)	5.2
Total Unit Weight (pcf)	145

Level 3

Asphalt Mix: Aggregate Gradation

Cumulative % Retained on 3/4 Inch Sieve	9
Cumulative % Retained on 3/8 Inch Sieve	7
Cumulative % Retained on #4 Sieve	15
% Passing #200 Sieve	5.5

Asphalt General: Volumetric Properties as Built

Effective Binder Content (%)	9.8
Air Voids (%)	5.2
Total Unit Weight (pcf)	145

Asphalt Binder: Superpave Binder Grading:	PG 64-22

Table C.8

Mixture Type: B 9.5_64_M1	
XML File:	L1_PG64_9.5_B_R3-A

Level 1

Asphalt Mix: Dynamic Modulus Table

Temperature	Mixture |E*|, psi					
(°F)	**0.1 Hz**	**0.5 Hz**	**1 Hz**	**5 Hz**	**10 Hz**	**25 Hz**
39.2	707,903	1,004,842	1,143,469	1,491,896	1,631,093	1,857,805
68	135,249	244,567	293,579	492,606	573,874	723,054
104	26,470	47,501	58,462	108,497	133,205	186,318
130	14,879	24,650	30,313	54,053	67,772	98,849

Asphalt Binder: Superpave Binder Test Data

Temperature	Angular Freq. = 10 rad/sec	
(°F)	G* (Pa)	Delta (degree)
147.2	24300	73.6
158	1170	76.6
168.8	6800	79.2

Asphalt General: Volumetric Properties as Built

Effective Binder Content (%)	12.6
Air Voids (%)	6.5
Total Unit Weight (pcf)	145

Level 2

Asphalt Mix: Aggregate Gradation

	Cumulative Percent Retained	Percent Passing
3/4 Inch Sieve	0	100
3/8 Inch Sieve	1	99
#4 Sieve	28	72
#200 Sieve	94	6

Asphalt Mix: LVE Converted Creep Compliance

Loading Time (s)	D(t) (1/psi)
	Mid Temp (14 F)
1	1.56E-04
2	1.72E-04
5	2.00E-04
10	2.16E-04
20	2.31E-04
50	2.55E-04
100	2.62E-04

Asphalt Binder: Superpave Binder Test Data

Temperature	Angular Freq. = 10 rad/sec	
(°F)	G* (Pa)	Delta (degree)
147.2	24300	73.6
158	1170	76.6
168.8	6800	79.2

Asphalt General: Volumetric Properties as Built

Effective Binder Content (%)	12.6
Air Voids (%)	6.5
Total Unit Weight (pcf)	145

Level 3

Asphalt Mix: Aggregate Gradation

Cumulative % Retained on 3/4 Inch Sieve	0
Cumulative % Retained on 3/8 Inch Sieve	1
Cumulative % Retained on #4 Sieve	28
% Passing #200 Sieve	6

Asphalt General: Volumetric Properties as Built

Effective Binder Content (%)	12.6
Air Voids (%)	6.5
Total Unit Weight (pcf)	145

Asphalt Binder: Superpave Binder Grading:	PG 64-22

Table C.9

Mixture Type: B 9.5_64_M2
XML File: L1_PG64_9.5_B_R3-V

Level 1

Asphalt Mix: Dynamic Modulus Table

Temperature	Mixture |E*|, psi					
(°F)	**0.1 Hz**	**0.5 Hz**	**1 Hz**	**5 Hz**	**10 Hz**	**25 Hz**
39.2	726,463	1,059,151	1,180,868	1,560,876	1,682,118	1,905,371
68	151,093	273,425	328,405	548,293	638,450	796,580
104	29,619	52,882	65,149	121,003	148,834	207,462
130	15,871	26,004	31,375	56,328	69,451	100,315

Asphalt Binder: Superpave Binder Test Data

Temperature	Angular Freq. = 10 rad/sec	
(°F)	G* (Pa)	Delta (degree)
147.2	5780	80.8
158	11500	78.4
168.8	19600	75.4

Asphalt General: Volumetric Properties as Built

Effective Binder Content (%)	11.6
Air Voids (%)	6.5
Total Unit Weight (pcf)	145

Level 2

Asphalt Mix: Aggregate Gradation

	Cumulative Percent Retained	Percent Passing
3/4 Inch Sieve	0	100
3/8 Inch Sieve	6	94
#4 Sieve	27	73
#200 Sieve	93.5	6.5

Asphalt Mix: LVE Converted Creep Compliance

Loading Time (s)	D(t) (1/psi)
	Mid Temp (14 F)
1	1.17E-04
2	1.30E-04
5	1.47E-04
10	1.64E-04
20	1.75E-04
50	1.91E-04
100	2.04E-04

Asphalt Binder: Superpave Binder Test Data

Temperature	Angular Freq. = 10 rad/sec	
(°F)	G* (Pa)	Delta (degree)
147.2	5780	80.8
158	11500	78.4
168.8	19600	75.4

Asphalt General: Volumetric Properties as Built

Effective Binder Content (%)	11.6
Air Voids (%)	6.5
Total Unit Weight (pcf)	145

Level 3

Asphalt Mix: Aggregate Gradation

Cumulative % Retained on 3/4 Inch Sieve	0
Cumulative % Retained on 3/8 Inch Sieve	6
Cumulative % Retained on #4 Sieve	27
% Passing #200 Sieve	6.5

Asphalt General: Volumetric Properties as Built

Effective Binder Content (%)	11.6
Air Voids (%)	6.5
Total Unit Weight (pcf)	145

Asphalt Binder: Superpave Binder Grading:	PG 64-22

Table C.10

Mixture Type: B 9.5_67_S
XML File: L1_PG67_9.5_B_R4

Level 1

Asphalt Mix: Dynamic Modulus Table

Temperature	Mixture |E*|, psi					
(ºF)	**0.1 Hz**	**0.5 Hz**	**1 Hz**	**5 Hz**	**10 Hz**	**25 Hz**
39.2	778,386	1,050,892	1,189,409	1,493,084	1,629,393	1,824,386
68	154,455	275,617	328,315	530,523	612,484	750,601
104	24,939	49,370	62,359	119,532	148,018	202,299
130	11,980	23,189	29,765	58,146	73,784	109,831

Asphalt Binder: Superpave Binder Test Data

Temperature	Angular Freq. = 10 rad/sec	
(ºF)	G* (Pa)	Delta (degree)
147.2	23600	72.2
158	10600	75.6
168.8	4910	78.6

Asphalt General: Volumetric Properties as Built

Effective Binder Content (%)	12.8
Air Voids (%)	5.5
Total Unit Weight (pcf)	145

Level 2

Asphalt Mix: Aggregate Gradation

	Cumulative Percent Retained	Percent Passing
3/4 Inch Sieve	0	100
3/8 Inch Sieve	3	97
#4 Sieve	28	72
#200 Sieve	94.7	5.3

Asphalt Mix: LVE Converted Creep Compliance

Loading Time (s)	D(t) (1/psi)
	Mid Temp (14 F)
1	3.31E-04
2	4.01E-04
5	5.35E-04
10	6.04E-04
20	7.07E-04
50	8.51E-04
100	8.51E-04

Asphalt Binder: Superpave Binder Test Data

Temperature	Angular Freq. = 10 rad/sec	
(ºF)	G* (Pa)	Delta (degree)
147.2	23600	72.2
158	10600	75.6
168.8	4910	78.6

Asphalt General: Volumetric Properties as Built

Effective Binder Content (%)	12.8
Air Voids (%)	5.5
Total Unit Weight (pcf)	145

Level 3

Asphalt Mix: Aggregate Gradation

Cumulative % Retained on 3/4 Inch Sieve	0
Cumulative % Retained on 3/8 Inch Sieve	3
Cumulative % Retained on #4 Sieve	28
% Passing #200 Sieve	5.3

Asphalt General: Volumetric Properties as Built

Effective Binder Content (%)	12.8
Air Voids (%)	5.5
Total Unit Weight (pcf)	145

Asphalt Binder: Superpave Binder Grading: PG 67-22

Table C.11

Mixture Type: B 12.5_64_M
XML File: L1_PG64_12.5_B_R3

Level 1

Asphalt Mix: Dynamic Modulus Table

Temperature	Mixture |E*|, psi					
(°F)	**0.1 Hz**	**0.5 Hz**	**1 Hz**	**5 Hz**	**10 Hz**	**25 Hz**
39.2	713,383	1,077,654	1,200,054	1,606,245	1,729,371	1,937,672
68	139,056	263,348	321,364	555,823	654,698	822,028
104	24,366	43,769	54,864	105,353	132,701	187,020
130	12,516	19,494	23,735	42,183	53,201	74,579

Asphalt Binder: Superpave Binder Test Data

Temperature	Angular Freq. = 10 rad/sec	
(°F)	G* (Pa)	Delta (degree)
147.2	14300	76.7
158	9440	79.6
168.8	5170	81.9

Asphalt General: Volumetric Properties as Built

Effective Binder Content (%)	12.5
Air Voids (%)	5.6
Total Unit Weight (pcf)	145

Level 2

Asphalt Mix: Aggregate Gradation

	Cumulative Percent Retained	Percent Passing
3/4 Inch Sieve	0	100
3/8 Inch Sieve	13	87
#4 Sieve	25	75
#200 Sieve	94	6

Asphalt Mix: LVE Converted Creep Compliance

Loading Time (s)	D(t) (1/psi)
	Mid Temp (14 F)
1	1.14E-04
2	1.31E-04
5	1.45E-04
10	1.58E-04
20	1.71E-04
50	1.83E-04
100	1.93E-04

Asphalt Binder: Superpave Binder Test Data

Temperature	Angular Freq. = 10 rad/sec	
(°F)	G* (Pa)	Delta (degree)
147.2	14300	76.7
158	9440	79.6
168.8	5170	81.9

Asphalt General: Volumetric Properties as Built

Effective Binder Content (%)	12.5
Air Voids (%)	5.6
Total Unit Weight (pcf)	145

Level 3

Asphalt Mix: Aggregate Gradation

Cumulative % Retained on 3/4 Inch Sieve	0
Cumulative % Retained on 3/8 Inch Sieve	13
Cumulative % Retained on #4 Sieve	25
% Passing #200 Sieve	6

Asphalt General: Volumetric Properties as Built

Effective Binder Content (%)	12.5
Air Voids (%)	5.6
Total Unit Weight (pcf)	145

Asphalt Binder: Superpave Binder Grading:	PG 64-22

Table C.12

Mixture Type: B 12.5_67_S
XML File: L1_PG67_12.5_B_R4

Level 1

Asphalt Mix: Dynamic Modulus Table

Temperature	Mixture |E*|, psi					
(°F)	**0.1 Hz**	**0.5 Hz**	**1 Hz**	**5 Hz**	**10 Hz**	**25 Hz**
39.2	799,436	1,098,798	1,226,957	1,560,258	1,685,026	1,894,083
68	178,701	307,743	364,226	578,586	666,209	811,324
104	40,797	72,786	89,099	159,438	192,590	267,258
130	26,760	43,528	57,073	95,217	125,372	167,782

Asphalt Binder: Superpave Binder Test Data

Temperature	Angular Freq. = 10 rad/sec	
(°F)	G* (Pa)	Delta (degree)
147.2	26800	73.8
158	10800	77.3
168.8	5270	80.3

Asphalt General: Volumetric Properties as Built

Effective Binder Content (%)	12.1
Air Voids (%)	6
Total Unit Weight (pcf)	145

Level 2

Asphalt Mix: Aggregate Gradation

	Cumulative Percent Retained	Percent Passing
3/4 Inch Sieve	0	100
3/8 Inch Sieve	14	86
#4 Sieve	25	75
#200 Sieve	95	5

Asphalt Mix: LVE Converted Creep Compliance

Loading Time (s)	D(t) (1/psi)
	Mid Temp (14 F)
1	1.24E-04
2	1.39E-04
5	1.67E-04
10	1.81E-04
20	1.98E-04
50	2.23E-04
100	2.27E-04

Asphalt Binder: Superpave Binder Test Data

Temperature	Angular Freq. = 10 rad/sec	
(°F)	G* (Pa)	Delta (degree)
147.2	26800	73.8
158	10800	77.3
168.8	5270	80.3

Asphalt General: Volumetric Properties as Built

Effective Binder Content (%)	12.1
Air Voids (%)	6
Total Unit Weight (pcf)	145

Level 3

Asphalt Mix: Aggregate Gradation

Cumulative % Retained on 3/4 Inch Sieve	0
Cumulative % Retained on 3/8 Inch Sieve	14
Cumulative % Retained on #4 Sieve	25
% Passing #200 Sieve	5

Asphalt General: Volumetric Properties as Built

Effective Binder Content (%)	12.1
Air Voids (%)	6
Total Unit Weight (pcf)	145

Asphalt Binder: Superpave Binder Grading:	PG 67-22

Table C.13

Mixture Type: B 19_64_M
XML File: L1_PG64_19_B_R3

Level 1

Asphalt Mix: Dynamic Modulus Table

Temperature (°F)	Mixture |E*|, psi					
	0.1 Hz	**0.5 Hz**	**1 Hz**	**5 Hz**	**10 Hz**	**25 Hz**
39.2	1,328,492	1,666,382	1,844,406	2,154,559	2,300,147	2,463,630
68	280,235	496,408	584,651	912,001	1,034,218	1,232,022
104	21,279	41,131	54,178	106,296	137,938	206,862
130	5,605	8,689	11,188	19,543	26,533	38,301

Asphalt Binder: Superpave Binder Test Data

Temperature (°F)	Angular Freq. = 10 rad/sec	
	G* (Pa)	Delta (degree)

Asphalt General: Volumetric Properties as Built

Effective Binder Content (%)	10.5
Air Voids (%)	5.5
Total Unit Weight (pcf)	145

Level 2

Asphalt Mix: Aggregate Gradation

	Cumulative Percent Retained	Percent Passing
3/4 Inch Sieve	1	99
3/8 Inch Sieve	14	86
#4 Sieve	25	75
#200 Sieve	94	6

Asphalt Mix: LVE Converted Creep Compliance

Loading Time (s)	D(t) (1/psi)
	Mid Temp (14 F)
1	1.70E-04
2	1.94E-04
5	2.49E-04
10	2.81E-04
20	3.11E-04
50	3.66E-04
100	3.81E-04

Asphalt Binder: Superpave Binder Test Data

Temperature (°F)	Angular Freq. = 10 rad/sec	
	G* (Pa)	Delta (degree)

Asphalt General: Volumetric Properties as Built

Effective Binder Content (%)	10.5
Air Voids (%)	5.5
Total Unit Weight (pcf)	145

Level 3

Asphalt Mix: Aggregate Gradation

Cumulative % Retained on 3/4 Inch Sieve	1
Cumulative % Retained on 3/8 Inch Sieve	14
Cumulative % Retained on #4 Sieve	25
% Passing #200 Sieve	6

Asphalt General: Volumetric Properties as Built

Effective Binder Content (%)	10.5
Air Voids (%)	5.5
Total Unit Weight (pcf)	145

Asphalt Binder: Superpave Binder Grading: PG 64-22

Table C.14

Mixture Type: B 25_64_M
XML File: L1_PG64_25_B_R3

Level 1

Asphalt Mix: Dynamic Modulus Table

Temperature	Mixture |E*|, psi					
(°F)	**0.1 Hz**	**0.5 Hz**	**1 Hz**	**5 Hz**	**10 Hz**	**25 Hz**
39.2	1,155,865	1,551,697	1,677,457	2,059,318	2,169,615	2,361,791
68	312,972	521,710	611,119	924,418	1,050,408	1,234,732
104	65,957	113,107	139,266	241,927	295,964	383,009
130	33,987	53,689	65,279	111,491	137,751	182,596

Asphalt Binder: Superpave Binder Test Data

Temperature	Angular Freq. = 10 rad/sec	
(°F)	G* (Pa)	Delta (degree)
147.2	33500	72.6
158	17200	75.4
168.8	17700	76.1

Asphalt General: Volumetric Properties as Built

Effective Binder Content (%)	9.4
Air Voids (%)	5.9
Total Unit Weight (pcf)	145

Level 2

Asphalt Mix: Aggregate Gradation

	Cumulative Percent Retained	Percent Passing
3/4 Inch Sieve	8	92
3/8 Inch Sieve	10	90
#4 Sieve	17	83
#200 Sieve	95	5

Asphalt Mix: LVE Converted Creep Compliance

Loading Time (s)	D(t) (1/psi)
	Mid Temp (14 F)
1	4.87E-05
2	5.51E-05
5	6.22E-05
10	6.96E-05
20	7.53E-05
50	8.20E-05
100	8.80E-05

Asphalt Binder: Superpave Binder Test Data

Temperature	Angular Freq. = 10 rad/sec	
(°F)	G* (Pa)	Delta (degree)
147.2	33500	72.6
158	17200	75.4
168.8	17700	76.1

Asphalt General: Volumetric Properties as Built

Effective Binder Content (%)	9.4
Air Voids (%)	5.9
Total Unit Weight (pcf)	145

Level 3

Asphalt Mix: Aggregate Gradation

Cumulative % Retained on 3/4 Inch Sieve	10
Cumulative % Retained on 3/8 Inch Sieve	8
Cumulative % Retained on #4 Sieve	17
% Passing #200 Sieve	5

Asphalt General: Volumetric Properties as Built

Effective Binder Content (%)	9.4
Air Voids (%)	5.9
Total Unit Weight (pcf)	145

Asphalt Binder: Superpave Binder Grading:	PG 64-22

Table C.15

Mixture Type: C 9.5_67_M
XML File: L1_PG67_9.5_C_R3

Level 1

Asphalt Mix: Dynamic Modulus Table

Temperature	Mixture |E*|, psi					
(°F)	**0.1 Hz**	**0.5 Hz**	**1 Hz**	**5 Hz**	**10 Hz**	**25 Hz**
39.2	1,042,729	1,338,882	1,493,116	1,797,075	1,938,251	2,119,050
68	252,870	416,779	484,584	735,545	832,459	993,556
104	47,958	78,495	100,325	164,872	209,851	264,927
130	22,643	34,356	43,766	70,134	91,120	118,701

Asphalt Binder: Superpave Binder Test Data

Temperature	Angular Freq. = 10 rad/sec	
(°F)	G* (Pa)	Delta (degree)
147.2	15900	77.7
158	7850	80.2
168.8	3240	82.7

Asphalt General: Volumetric Properties as Built

Effective Binder Content (%)	12.9
Air Voids (%)	5
Total Unit Weight (pcf)	145

Level 2

Asphalt Mix: Aggregate Gradation

	Cumulative Percent Retained	Percent Passing
3/4 Inch Sieve	0	100
3/8 Inch Sieve	5	95
#4 Sieve	32	68
#200 Sieve	94.5	5.5

Asphalt Mix: LVE Converted Creep Compliance

Loading Time (s)	D(t) (1/psi)
	Mid Temp (14 F)
1	8.26E-05
2	9.40E-05
5	1.12E-04
10	1.21E-04
20	1.33E-04
50	1.49E-04
100	1.49E-04

Asphalt Binder: Superpave Binder Test Data

Temperature	Angular Freq. = 10 rad/sec	
(°F)	G* (Pa)	Delta (degree)
147.2	15900	77.7
158	7850	80.2
168.8	3240	82.7

Asphalt General: Volumetric Properties as Built

Effective Binder Content (%)	12.9
Air Voids (%)	5
Total Unit Weight (pcf)	145

Level 3

Asphalt Mix: Aggregate Gradation

Cumulative % Retained on 3/4 Inch Sieve	0
Cumulative % Retained on 3/8 Inch Sieve	5
Cumulative % Retained on #4 Sieve	32
% Passing #200 Sieve	5.5

Asphalt General: Volumetric Properties as Built

Effective Binder Content (%)	12.9
Air Voids (%)	5
Total Unit Weight (pcf)	145

Asphalt Binder: Superpave Binder Grading:	PG 67-22

Table C.16

Mixture Type: C 12.5_67_M
XML File: L1_PG67_12.5_C_R3

Level 1

Asphalt Mix: Dynamic Modulus Table

Temperature	Mixture |E*|, psi					
(°F)	**0.1 Hz**	**0.5 Hz**	**1 Hz**	**5 Hz**	**10 Hz**	**25 Hz**
39.2	869,851	1,189,925	1,322,964	1,667,244	1,791,974	2,000,302
68	192,115	337,801	400,017	639,995	734,224	895,946
104	34,875	64,822	80,557	149,572	183,594	249,302
130	17,203	30,483	37,530	70,132	86,785	125,192

Asphalt Binder: Superpave Binder Test Data

Temperature	Angular Freq. = 10 rad/sec	
(°F)	G* (Pa)	Delta (degree)

Asphalt General: Volumetric Properties as Built

Effective Binder Content (%)	11.5
Air Voids (%)	5.8
Total Unit Weight (pcf)	145

Level 2

Asphalt Mix: Aggregate Gradation

	Cumulative Percent Retained	Percent Passing
3/4 Inch Sieve	0	100
3/8 Inch Sieve	12	88
#4 Sieve	27	73
#200 Sieve	93.9	6.1

Asphalt Mix: LVE Converted Creep Compliance

Loading Time (s)	D(t) (1/psi)
	Mid Temp (14 F)
1	1.43E-04
2	1.60E-04
5	1.95E-04
10	2.18E-04
20	2.38E-04
50	2.73E-04
100	2.89E-04

Asphalt Binder: Superpave Binder Test Data

Temperature	Angular Freq. = 10 rad/sec	
(°F)	G* (Pa)	Delta (degree)

Asphalt General: Volumetric Properties as Built

Effective Binder Content (%)	11.5
Air Voids (%)	5.8
Total Unit Weight (pcf)	145

Level 3

Asphalt Mix: Aggregate Gradation

Cumulative % Retained on 3/4 Inch Sieve	0
Cumulative % Retained on 3/8 Inch Sieve	12
Cumulative % Retained on #4 Sieve	27
% Passing #200 Sieve	6.1

Asphalt General: Volumetric Properties as Built

Effective Binder Content (%)	11.5
Air Voids (%)	5.8
Total Unit Weight (pcf)	145

Asphalt Binder: Superpave Binder Grading: PG 67-22

Table C.17

Mixture Type: C 12.5_76_M
XML File: L1_PG76_12.5_C_R3

Level 1

Asphalt Mix: Dynamic Modulus Table

Temperature	Mixture |E*|, psi					
(°F)	**0.1 Hz**	**0.5 Hz**	**1 Hz**	**5 Hz**	**10 Hz**	**25 Hz**
39.2	565,772	851,214	953,092	1,301,342	1,417,104	1,608,734
68	133,118	233,060	278,933	459,431	536,563	668,467
104	27,968	46,100	56,895	98,431	122,377	161,150
130	14,093	20,212	24,970	39,117	50,048	64,680

Asphalt Binder: Superpave Binder Test Data

Temperature	Angular Freq. = 10 rad/sec	
(°F)	G* (Pa)	Delta (degree)

Asphalt General: Volumetric Properties as Built

Effective Binder Content (%)	11.5
Air Voids (%)	5.8
Total Unit Weight (pcf)	145

Level 2

Asphalt Mix: Aggregate Gradation

	Cumulative Percent Retained	Percent Passing
3/4 Inch Sieve	0	100
3/8 Inch Sieve	12	88
#4 Sieve	27	73
#200 Sieve	93.9	6.1

Asphalt Mix: LVE Converted Creep Compliance

Loading Time (s)	D(t) (1/psi)
	Mid Temp (14 F)
1	8.37E-05
2	9.68E-05
5	1.13E-04
10	1.23E-04
20	1.36E-04
50	1.51E-04
100	1.61E-04

Asphalt Binder: Superpave Binder Test Data

Temperature	Angular Freq. = 10 rad/sec	
(°F)	G* (Pa)	Delta (degree)

Asphalt General: Volumetric Properties as Built

Effective Binder Content (%)	11.5
Air Voids (%)	5.8
Total Unit Weight (pcf)	145

Level 3

Asphalt Mix: Aggregate Gradation

Cumulative % Retained on 3/4 Inch Sieve	0
Cumulative % Retained on 3/8 Inch Sieve	12
Cumulative % Retained on #4 Sieve	27
% Passing #200 Sieve	6.1

Asphalt General: Volumetric Properties as Built

Effective Binder Content (%)	11.5
Air Voids (%)	5.8
Total Unit Weight (pcf)	145

Asphalt Binder: Superpave Binder Grading:	PG 76-22

Appendix D

GDOT RP 17-18: Innovative & Effective Training Modules and Methods for Pavement Designers for Operation of MEPDG

GDOT MEPDG TRAINING WORKSHOP AGENDA

March 9-10, 2020
University of Georgia, Athens, Georgia
Coverdell Room 175, 500 D. W. Brooks Drive, Athens, GA 30602

DAY ONE- MARCH 9TH, 2020

Time	Topic
9:30 - 9:45 am	**Welcome & Introduction** *Dr. Stephan A. Durham, UGA* *Ms. Monica Flournoy, GDOT* Introduction and opening remarks
9:45 - 10:30 am	**Review of Training Agenda** *Mr. Steve Pahno, UGA* *Mr. Ian Rish, GDOT* GDOT's MEPDG Implementation Efforts *Dr. S. Sonny Kim, UGA* UGA's MEPDG Implementation Efforts Module 0- MEPDG Basics and Level Hierarchy Module 1A- MEPDG Traffic and Climate Inputs
10:30 - 11:00 am	**Design Walkthrough- Climate Inputs** *Dr. Stephan A. Durham, UGA* MERRA data and climate inputs for MEPDG.
11:00 - 11:30 am	**Design Walkthrough- Traffic Inputs** *Dr. Wouter Brink, ARA* Traffic input module and importing/exporting traffic data to minimize input errors. Topics to cover: Georgia DOT specific inputs for TTC, MAF, Axles per truck and axle load spectra
11:30 - 12:15 pm	**MEPDG Training Modules Screening** *Hampton Worthey, UGA MS Student* Discussion and screening of AASHTO Pavement ME training modules. MEPDG Inputs and Implementation for Level 1, 2 and 3 Designs
12:15 - 1:15 pm	**BREAK - Lunch**
1:15 - 3:15 pm	**Design Walkthrough- Flexible Pavement Inputs** *Hampton Worthey, UGA MS Student* Walkthrough of HMA mechanical property input for Pavement ME designs. Step-by-step procedure for xml file import and use of GDOT HMA materials input library.
3:15 - 3:30 pm	**BREAK**
3:30 - 5:30 pm	**Design Walkthrough- Rigid Pavement Inputs** *Chandler Banks, UGA MS Student* Walkthrough of JPCP and CRCP layer property inputs for Pavement ME designs. Step-by-step procedure for XML file import and use of GDOT concrete material property database.
5:30 - 6:00 pm	**Open Discussion** Comments and discussion

3

DAY TWO- MARCH 10TH, 2020

Time	Topic
8:30 - 9:00 am	**Laboratory Procedure Overview** *Hampton Worthey* Discussion and screening of laboratory testing procedures conducted to collect Level 1 input database.
9:00 - 10:30 am	**AASHTO Pavement ME Updates – Part 1: PMED over the years: v2.2 through 2.5.5: What changes have been made, why, and how they may affect GDOT pavement engineers** *Dr. Wouter Brink, ARA* A brief overview and reasoning behind the most recent changes and enhancements made to the Pavement ME Design software and how it may affect GDOT pavement engineers. Specific topics include: User interface changes, climate data updates, recalibration of the flexible performance prediction models, and other enhancements and improvements.
10:30 - 10:45 am	**BREAK**
10:45 - 12:15 pm	**AASHTO Pavement ME Updates – Part 2: Overview of various available tools include with a Pavement ME Design license and current features in development.** *Dr. Wouter Brink, ARA* A detailed overview of the tools developed to assist pavement engineers. Specific tools to be discussed include: Backcalculation tool, MapME, Calibration Assistance Tool, and others. An overview of current and future enhancements will be discussed.
12:15 - 1:15 pm	**LUNCH**
1:15 - 1:45 pm	**MEPDG Traffic Inputs from WIM Data** *Seyedehnarges Tahaei Yaghoubi, UGA PhD Student*
1:45 - 2:15 pm	**Use of FWD to Estimate Level 2 Dynamic Modulus Input** *Ryan Romeo, UGA PhD Student* Estimation of Asphalt Dynamic Modulus and Creep Compliance using FWD data
2:15 - 2:45 pm	**Open Discussion & Closing Remarks** *Dr. S. Sonny Kim* *Mr. Ian Rish, GDOT* *Dr. Wouter Brink, ARA* Comments and discussion regarding all topics presented in the workshop, future works, and closing remarks.

Modulue 0- MEPDG Basics and Input Level Hierarchy

Time	Script
00:00	This MEPDG Training series is produced by the University of Georgia for use by the Georgia Department of Transportation as a partial fulfillment of Research Project 17-18
00:11	This module will cover MEPDG Basics and Input Level Hierarchy in AASHTOWare PavementME Design
00:18	This is an introductory video for all module series discussing MEPDG Inputs and Implementation
00:26	The Pavement ME Design Software Manual, User Input Guide, and Train the Trainer Workshop manuals should be used in tandem with the contents of this training series
00:36	Pavement ME Design is a sophisticated platform for conducting mechanistic-empirical based pavement designs
00:43	As stated in the Software Manual, "The concepts of ME based methods allow the pavement design engineer to quantify the effect of changes in materials, load, climate, age, pavement geometry, and construction practices on pavement performance"
00:56	As a result, each project requires many inputs across a variety of processes and design levels
01:03	The concept of hierarchical input levels is a fundamental consideration of MEPDG practices and Pavement ME Design, specifically
01:10	The most influential design inputs are structured in three different tiers to provide you with flexibility over the accuracy and conservatism of your design
01:19	Level 3 inputs represent values determined by nationally accepted averages or global defaults. These inputs provide the lowest level of design accuracy and the highest level of uncertainty but are the most efficient to use
01:32	Level 2 inputs represent values determined through limited testing, correlation, or data-base selection. The values used in Level 2 designs are considered more accurate than Level 3, but generally require more time and resources to obtain
01:45	Level 1 inputs are values gathered from site-specific data or laboratory evaluations. These values are directly indicative of the in-situ conditions and, thus, contain the highest level of accuracy and the lowest level of uncertainty. However, these inputs require the most time and resources to collect
02:02	The objective of this training series is to highlight the steps required for generating the most accurate and advanced Georgia-specific pavement designs at each design level
02:12	Let's begin with a brief overview of the software interface
02:17	After launching the software, you will find some of the most important operational features and tools located in the Menu Ribbon
02:23	A summary of each feature's function can be found in the Software Manual
02:28	To begin a pavement design, select "Open" to launch an existing file from the GDOT library or select "New" to start from scratch
02:36	Once a project is generated, you should notice several windows appear on your screen
02:40	These include the Explorer Tab, Project Information Tab, and Project Identifiers Window
02:49	We'll take a look at the Explorer Tab to highlight some of the important MEPDG features included in the software
02:56	Your current design project should appear under the projects folder. This folder will be used to access the traffic, climate, pavement structure, and calibration factors for your design
03:07	The Project Specific Calibration Factors are very important considerations that will have significant impact on your performance output. These values will differ based on your pavement design type
03:18	Always refer to the calibration tables located in the User Input Guide to ensure your files contain the appropriate calibration coefficients (Section 9.1, pg. 98)
03:27	The first step for every design is to determine general project information in the Project Information Tab
03:33	Here you will define the design type and pavement type. The design type selections include New Pavement, Overlay, or Restoration Design. And the pavement types include Flexible, JPCP, CRCP, and Semi-Rigid. For now, we will select a new, flexible pavement

03:52	After selection, more windows become available--the Performance criteria Window, Pavement Materials Window, and the Layer Inputs Window. You may also notice some activity in the Error List
04:07	Before moving to those inputs, we will finish defining the project information
04:12	Section 3.3 of the User Input Guide states "the design life for all new pavement and rehabilitation designs is 20 years" so for most designs, this should remain unchanged (Section 3.3, pg. 14)
04:23	Construction date inputs are keyed to monthly traffic loadings and climate data and effect all layer moduli. The Construction and Traffic Opening Dates table in the User Input Guide suggests inputs based on your design (Table 3.1, Section 3.4.1, pg. 16)
04:35	We will input the recommended dates for a new, flexible pavement
04:41	The next step of the design process is to define the Performance Criteria
04:47	The Performance Criteria inputs are different for flexible and rigid pavements
04:51	The first input for both pavement types is the Initial IRI. Initial IRI values are based on the type of wearing surface and may be determined from the associated table in the User Input Guide (Table 4.1, section 4.1, pg. 17)
05:07	The Terminal IRI inputs for flexible and rigid pavements are based on route type and number of lanes. These values are gathered from the Terminal IRI and HRI Ratings Table of the User Input Guide (Table 4.6, Section 4.2.3, pg. 20)
05:23	The remaining Performance criteria inputs are specific to Flexible Pavement only
05:28	AC top-down fatigue cracking is not considered as a design input in version 2.5 of PavementME. Therefore, we will input a value above the standard threshold
05:40	AC bottom-up fatigue cracking, AC thermal cracking, and Permanent Deformation of the Total Pavement are all based on the project's Roadway Type. These values may be found in the Flexible Pavement Design Criteria Table in the User Input Guide (Tables 4.2-4.5, Section 4.2, pg. 19)
05:59	Permanent deformation of AC only is another currently unused input and may be left as the default value
06:07	In cases where a rigid-pavement design is selected, the remaining Performance Criteria inputs include JPCP Transverse Cracking and Mean Joint Faulting or CRCP Punchouts, based on your pavement type selection
06:19	These values are also determined by roadway type and are located in the Distress Criteria or Threshold Values Section of the User Input Guide (Tables 4.2-4.5, Section 4.2, pg. 19)
06:34	Finally, the appropriate reliability for each criterion must be determined
06:39	Reliability Levels are selected based on the type of roadway and may be found in the recommended table of the User Input Guide (Table 4.7, Section 4.3, pg. 22)
06:51	This concludes the topics discussed under MEPDG Basics and Input Level Hierarchy
06:57	Proceed to the first series of modules to learn about Level 3 MEPDG Inputs and Implementation

Modulue 1A- MEPDG Traffic and Climate Inputs

Time	Script
00:00	This module will cover Level 3 MEPDG Traffic and Climate Inputs in AASHTOWare PavementME Design
00:08	This is the first module in the Level 3 input series for MEPDG Inputs and Implementation
00:15	The GDOT User Input Guide and Train the Trainer Workshop manuals are considered necessary tools for this module
00:23	We will begin with the steps required for Traffic inputs. The input process for traffic data is the same for both Flexible and Rigid pavement designs.
00:31	To access the traffic inputs, double click the "Traffic" drop-down in the Explorer Tab
00:38	The first traffic inputs are located in the window on the left, beginning with the Average Annual Daily Truck Traffic

00:46	Inputs highlighted in this section are considered site specific and should be obtained from the Traffic Analysis Branch of the Office of Planning or the Office of Transportation Data within GDOT
00:55	However, if sufficient truck volume data is unavailable, the Lane Distribution Factor table in the User Input Guide should be used (Table 5.1, Section 5.1, pg. 26)
01:05	Moving down, the Traffic Capacity input does not have any impact on the predictions of the performance indicators and may be ignored in version 2.5 of the software
01:14	The Axle Configuration inputs correspond to the following definitions from the User Input Guide and may be left as default values unless otherwise specified (Section 5.3, pg. 26)
01:23	The Lateral Wander inputs are only required for rigid pavements and may be left as default values for most designs
01:30	Inputs located under Wheelbase are also only required for rigid pavements but a set of recommended values are found in the User Input Guide (Section 5.5, pg. 27)
01:40	Vehicle Class Distribution and Growth is also taken into account within PavementME. To access these inputs, select the "Load Default Distribution" button at the top right
01:52	Appropriate percentages are provided by the Traffic Analysis Branch of the Office of Planning and the Truck Traffic Classification table in the User Input Guide is recommended only when actual truck traffic data is unavailable (Table 5.2, Section 5.6, pg. 28)
02:07	The Growth Rate and Growth Function inputs can be changed in the Vehicle Class Distribution and Growth Window. The Growth Rate will be found alongside the data provided by the Traffic Analysis Branch of the Office of Planning, if available
02:18	The Growth Function is selected from a drop-down where the choices include None, Linear, and Compound
02:26	Finally, Monthly Distribution Factors may be imported into PavementME from the truck traffic data library established for GDOT. These values are also presented in the highlighted tables of the User Input Guide (Tables 5.3 & 5.4, Section 5.7, pg. 29-30)
02:41	To review and confirm all distribution factors, return to the Traffic drop-down in the Explorer Tab and right click on each of the inputs
02:57	This concludes the necessary steps for Level 3 Traffic inputs. Next, we will discuss the Climate Inputs
03:04	The climate input process differs slightly for Flexible and Rigid pavement designs. We will cover both processes, starting with a flexible pavement
03:12	To access the climate inputs, double click the "Climate" drop-down in the Explorer Tab
03:19	To begin, direct your attention to the map in the bottom right window
03:24	Use the search bar to search for your project location
03:31	Zoom in on the map until the climate stations surrounding your project are clearly visible
03:37	Climate stations with blue pins indicate inputs are available for that location. Stations with red pins indicate data is missing or unavailable
03:45	For generic projects, one may obtain climate data files by clicking red pins and downloading the appropriate HCD files from the infopave website
03:54	However, custom HCD files have been generated for Georgia climate stations and inputs for GDOT roadway designs should be generated from this data
04:03	To access the custom climate data, click the "Options" drop down and select "Use custom HCD folder and station file"
04:12	Press the "refresh markers" button to regenerate the available climate stations
04:17	From the new set of stations, select the climate data pin most appropriate for your project location. Once selected, the pin will turn green
04:25	To import the data from the selected station, press the "Select Climate" button
04:31	If the import was successful, the data will appear under Project Climate
04:35	You will know the climate has been input correctly if the Climate icon in the Explorer Tab has turned green
04:43	Now we will discuss the same process for Rigid pavements
04:47	Beginning with a Rigid pavement design, once again double click the "Climate" drop-down in the Explorer Tab

04:55	Follow the same procedure as before, noticing the different locations for each climate data pin
05:02	Similar to the flexible pavement climate inputs, generic climate files for rigid pavements may be obtained online from the ME Design website. However, pre-generated custom Georgia climate files should be used for all projects
05:15	These are the same custom files used for flexible designs
05:20	As before, check the "Use custom HCD option" and press the refresh markers button to update the available stations
05:28	Select the most appropriate climate station for your project and press the "Select Climate" button
05:36	Finally, ensure the inputs were imported correctly by checking the Climate icon for confirmation
05:43	All climate inputs have now been defined for the project
05:47	This concludes the topics discussed in this module and the steps required for Level 3 Traffic and Climate inputs
05:54	Proceed to the next module to learn about Level 3 MEPDG Inputs and Implementation for Subgrade and Base Materials

Modulue 2A- MEPDG Inputs and Implementation for Subgrade and Base Materials

Time	**Script**
00:00	This module will cover the Level 3 Inputs and Implementation of Subgrade and Base Materials in AASHTOWare PavementME Design
00:08	This is the second module in the Level 3 input series for MEPDG Inputs and Implementation
00:15	As before, the GDOT User Input Guide and Train the Trainer Workshop manuals are considered necessary tools for this module
00:23	We will begin at the pavement structure process. At this point, the project information, performance criteria, traffic, and climate inputs have already been determined. If you are unsure how to reach this point in the design, revisit the previous modules in which the steps are fully discussed
00:39	In this module, we will discuss the inputs for the highlighted pavement layers of the New Pavement Structures Figure in the User Input Guide. These include the Subgrade, Granular Aggregate Base, and Stabilized Base Layers (Fig 8.1, Section 8.1, pg. 58)
00:52	Because Section 8.9 of the User Input Guide states "Do not enter a bedrock layer for locations where the depth to bedrock exceeds 100 inches or has more than 100 inches of soil above it", the first layer added to the structure will be the subgrade embankment (Section 8.9, pg. 95)
01:08	To add the first layer to the pavement structure, click the "Add Layer" button above the pavement figure or right click within in the window
01:16	In the "Material Layer Selection" Box, select the appropriate layer in the "Insert Layer Below" drop-down. For now, we will select the only existing layer.
01:24	Next, ensure that Subgrade is selected in the "Layer Type" drop down
01:29	In addition to the default list of subgrade classifications, you should see GDOT classified subgrade materials. These materials are imported from pre-generated files that already include the preferred properties for a GDOT design
01:41	Some counties have available data that warrant specific material files. For projects in the remaining counties, consult the Subgrade Classification Map in the User Input Guide to identify an appropriate subgrade selection (Figure 8.4, Section 8.6.2, pg. 86)
01:54	For the purpose of this video, we will select a IIB4 soil for the embankment and discuss the selection process for each material property input. After pressing "OK", the properites and inputs for the new layer will be highlighted on the right
02:08	The first input to be defined is the coefficient of lateral earth pressure. However, version 2.5 of the software does not integrate this input, so leaving it as the default value is recommended

02:19	Because this is the bottom-most layer of the structure, the layer thickness is considered Semi-Infinite. Therefore, a thickness input is not required for the embankment. If an additional subgrade layer is included in the design, the appropriate thickness will be defined here
02:33	The poisson's ratio for subgrade soil is an input that may be determined from the Poisson's Ratio Table in the User Input Guide. Using this table, we see the suggested value for a IIB4 soil is already defined appropriately (Table 8.22, Section 8.6.3, pg. 89)
02:47	Resilient modulus values for certain counties may be found in the Subgrade Resilient Modulus table in the User Input Guide (Table 8.18, Section 8.6.2, pg. 85)
02:55	However, for most counties, it is preferred to define the resilient modulus using the suggested ranges in the Soil Classification Figure. The preferred range for a IIB4 soil is between 6,000 and 10,000 psi (Figure 8.4, Section 8.6.2, pg. 86)
03:08	Click the drop-down arrow and type the new resilient modulus in the space provided at the bottom
03:16	Finally, the gradation input for GDOT materials is predefined based on Georgia soils of the same classification. If necessary, click on the drop-down to adjust these inputs based on availabe project data
03:29	If your resilient modulus was selected from the Resilient Modulus Table, verify the maximum dry unit weight and water content inputs are consistent with you resilient modulus value
03:40	All input properties have now been discussed for the embankment layer
03:43	The next base layer to discuss is the Granular Aggregate Base or GAB layer
03:49	Once again, click the "Add Layer" button and select the topmost layer in the "insert layer below" dropdown
03:55	For GAB layers, select the Non-Stabilized Base option in the Layer Type dropdown
04:01	As before, you may select your material from the list of default options or those custom generated for GDOT designs
04:07	If a specific material file is not available for your project, select the Default Values_All Gneiss GAB option
04:16	Like the subgrade, the GAB coefficient of lateral earth pressure is left as its default value
04:22	The layer thickness can be determined from the Minimum and Maximum Layer Thicknesses Table in the User Input Guide. For GAB layers, a minimum thickness of 12-in is suggested (Table 8.1, Section 8.1, pg 59)
04:35	The poisson's ratio for Level 3 GAB layers is found in same Poisson's Ratio table as before. The suggested input is 0.30 (Table 8.22, Section 8.6.3, pg. 89)
04:46	As with the subgrade, the GAB resilient modulus values are listed in the associated table in the User Input Guide. The appropriate value should already be defined for GDOT materials (Table 8.17, Section 8.6.2, pg. 84)
04:58	If necessary, type the value in the resilient modulus drop-down
05:03	Finally, select the gradation drop down and verify the maximum dry unit weight and water content values are consistent with the resilient modulus input selected from the table
05:14	Before proceeding, it is important to note that all GAB layers must be defined as a "Crushed Stone". If designing a GAB layer from scratch, begin with a Crushed Stone material from the Unbound Layers list
05:25	All input properties have now been discussed for the GAB
05:31	If a Stabilized Subgrade or Cement Treated Base layer is included in the design, the input process is similar to that of a subgrade soil
05:39	Once more, click the "Add Layer" button, select the appropriate layer in the "insert layer below" dropdown, and select the Subgrade "Layer Type"
05:49	All layer properties for a stabilized subgrade layer are default for an A-1-b soil with exception of Poisson's Ratio and Resilient Modulus, so an A-1-b material is recommended
06:02	As before, the coefficient of lateral earth pressure will remain as the default value
06:08	The default layer thickness for stablized base layers is defined as 10-in
06:15	The Level 3 poisson's ratio and resilient modulus values for stabilized subgrade are found in the highlighted table in the User Input Guide (Table 8.24, Section 8.8, pg. 93)

06:23	For this example, we will assume a cement stabilized soil is used
06:38	Gradation inputs for stabilized subgrade may be left as the default values for an A-1-b material
06:45	All input properties have now been discussed for the Stablized Subgrade
06:50	If your project is to include Asphalt Stabilized or Cement Treated Base layers, the inputs for these layers are the same as the Asphalt Conrete or Portland Cement Concrete layers, which will be discussed at a later time
07:02	This concludes the topics discussed in this module, procede to the next module to learn about Level 3 MEPDG Inputs and Implementation for AC Pavement

Module 3A- MEPDG Inputs and Implementation for AC Pavement

Time	**Script**
00:00	This module will cover the Level 3 Inputs and Implementation of Asphalt Pavement Layers in AASHTOWare PavementME Design
00:08	This is the third module in the Level 3 input series for MEPDG Inputs and Implementation
00:15	As before, the GDOT User Input Guide and Train the Trainer Workshop manuals are considered necessary tools for this module
00:23	We will continue with the pavement structure process, focusing on the asphalt layers of a flexible pavement design
00:29	At this point, project information, performance criteria, traffic, climate, and subbase material inputs have already been determined. If you are unsure how to reach this point in the design, revisit the previous modules in which the steps are fully discussed
00:42	In this module, we will discuss the inputs for the highlighted pavement layers in the New Pavement Structures figure in the User Input Guide. This includes asphalt surface, binder, base, and interlayers (Fig 8.1, Section 8.1, pg. 58)
00:55	Before inputting any flexible pavement layers please review section 8.1 of the User Input Guide. Highlights from this section include limiting your design to 3 HMA layers and how to combine thin surface layers, if necessary (Section 8.1, pg. 57)
01:11	To begin, open the asphalt layer properties by navigating to the Explorer Window and selecting the "AC Layer Properties" dropdown
01:22	Verify these inputs are set as the default values as defined in Chapter 7.1 of the User Input Guide (pg. 44)
01:28	This includes a surface shortwave absorptivity of 0.85, Full friction between layer interface, no applied endurance limit, and no multi-layer rutting calibration
01:41	The next steps will discuss the input process for asphalt base layers
01:46	Add a flexible pavement layer by clicking the "Add Layer" button in the pavement layers window
01:53	In the "Layer Type" dropdown, select "Flexible," and begin with the Default_asphalt concrete material for a Level 3 design
02:03	After pressing "OK", the properties and inputs for this new layer are highlighted on the right
02:09	The first input to determine is the asphalt thickness. Referencing the Minimum and Maximum Layer Thicknesses Table in the User Input Guide, the 25mm base layer thickness is project specific but should be no less than 3-in (Table 8.1, Section 8.1, pg. 59)
02:22	For the purpose of this example, a 4-in thickness will be assumed
02:29	The air voids, effective binder content, and unit weight inputs are all determined from the Volumetric Properties Table in the User Input Guide (Table 8.3, Section 8.3.2, pg. 64)
02:36	Therefore, we will input the appropriate values for the 25mm, base mixture, leaving Poisson's ratio as its default value
02:49	Continuing to the mechanical properties, asphalt binder grade for Level 3 designs is input through the dropdown selection
02:56	As suggested from the highlighted table in the User Input Guide, your selection will most often include PG 64 or PG 67-22 (Table 8.5, Section 8.3.3, pg. 66)

03:10	Creep compliance inputs are tied to the selected asphalt binder and are not necessary for Level 3 designs. The input process for this property will be discussed in the Level 1 and Level 2 modules
03:22	Dynamic Modulus inputs require four percent passing values for Level 3 designs. Refer to the Gradation for Georgia's Dense-Graded Mixtures Table in the User Input Guide and input the appropriate values for the 25mm Base Mix (Table 8.6, Section 8.3.3, pg. 67)
03:38	Further inputs are only required for higher level designs and will be discussed in later modules
03:48	The HMA Estar predictive model input should remain as the default selection, using the preferred viscosity-based model, NCHRP 1-37A
03:59	The reference temperature should remain at the default 70 deg-F, as all GDOT calibration factors are tied to this value
04:08	Moving to the thermal properties, the heat capacity and thermal conductivity inputs are also sensitive to the GDOT calibration factors and should be left as default values
04:18	Finally, the thermal contraction input is a calculated value that should not be changed
04:24	All input properties have now been discussed for the asphalt base layer
04:28	The next layer to discuss is the asphalt binder layer
04:33	Same as before, the new layer is added by selecting the default_asphalt concrete material under the Flexible layer type
04:49	All inputs for asphalt binder layers follow the same procedure as the asphalt base layer
04:55	A thickness range for asphalt binder layers is provided in the Minimum and Maximum Layer Thickness table in the User Input Guide (Table 8.1, Section 8.1, pg. 59)
05:06	The volumetric property inputs are provided in the same table as before. This time, using the values recommended for the Binder layer
05:23	The binder grade is selected from the dropdown
05:30	The Dynamic Modulus inputs are selected based on the Dense Graded Mixtures Table
05:45	And the remaining inputs are self-generated or left as default values
05:51	The next layer to discuss is the asphalt surface layer. The input process for this layer is identical to those of the base and binder layers, with the exception of asphalt thickness and indirect tensile strength
06:01	The surface layer will be added by selecting the top-most HMA layer in the pavement figure
06:07	From the Layer Thicknesses Table in the User Input Guide, the surface thickness is determined from the Average Daily Traffic
06:15	Assuming a project ADT of 4,000, a thickness of 1.25 inches is recommended
06:23	In cases where an additional layer is required for design, or the surface layer is less than 1 in thick, an equivalent layer thickness should be calculated
06:31	This is accomplished using the highlighted Equation from Section 8.1 in the User Input Guide (Equation 2, Section 8.1, pg. 57)
06:36	A Layer Thickness Ratio from the below table is combined with the equation to develop an equivalent dense-graded layer thickness (Table 8.2, Section 8.1, pg. 59)
06:45	Surface layers also require an input for indirect tensile strength at 14 deg F
06:51	IDT inputs are estimated using other volumetric and mechanical properties and are not necessary for Level 3 designs. The input process for this property will be discussed in the Level 1 and Level 2 modules
07:04	The remaining inputs are selected following the same procedures as before
07:13	Finally, an asphalt interlayer may be included in rigid pavement designs by following the same steps outlined for flexible designs
07:21	Asphalt interlayers should be inserted below the existing PCC layer
07:36	A layer thickness of 3-in is recommended from the Layer Thicknesses Table in the User Input Guide
07:48	And the remaining inputs are identical to those of a standard 19mm Superpave mixture
07:53	Therefore, all input properties have already been discussed for the asphalt interlayer
07:59	This concludes the content discussed in this module and the steps required to develop a Level 3 flexible pavement design

08:06	Proceed to the next module to learn about Level 3 MEPDG Inputs and Implementation for JPCP

Module 4A- MEPDG Inputs and Implementation for JPCP

Time	Script
00:00	This module will cover the Level 3 Inputs and Implementation of Jointed Plane Concrete Pavement in AASHTOWare PavementME Design
00:08	This is the fourth module in the Level 3 input series for MEPDG Inputs and Implementation
00:15	As before, the GDOT User Input Guide and Train the Trainer Workshop manuals are considered necessary tools for this module
00:23	We will continue with the pavement structure process, focusing on the PCC layers of a JPCP design as shown in the highlighted figure
00:33	First, a brief overview of the Rigid Pavement Design Structure
00:39	Rigid pavement designs are limited to one PCC layer for new pavements and two PCC layers for rehabilitation designs
00:47	Typically, only one of the following base layer types are used for rigid pavements & no more than one stabilized subgrade layer should be used
00:56	The subgrade for rigid pavement designs is limited to 2 layers-- compacted embankment and natural or undisturbed soil. If you are unfamiliar with the input processes for the subgrade or base layers, please review Module 2 of this series
01:11	Next, we will disucss the Design Property Inputs. Navigate to the Explorer Window and select "JPCP Design Properties" in the project dropdown
01:25	Unlike the flexible pavement design properties, some JPCP properties may differ based on your project specifications
01:32	The first design input is surface shortwave absorptivity. In which the default value of 0.85 should be used for all new and rehabilitation designs
01:42	Under the Doweled Joints drop-down, you'll find inputs for the dowel diameter and dowel spacing. The Dowel Diameter Table in the User Input Guide provides recommended diameters based on slab thickness, while a dowel spacing of 12-in is suggested for most designs (Table 7.3, Section 7.2.4, pg. 49)
02:00	The Erodibility Index for JPCP is defined by the type of base material for the project and is classified by categories presented in the highlighted table of the User Input Guide (Table 7.4, Section 7.2.8, pg. 50)
02:16	Under the PCC-Base Contact Friction dropdown, JPCP design should always use full friction between the slab and base course, while the months until friction loss is based on the type of base course used in the design. Reference the appropriate section of the User Input Guide for the suggested input (Section 7.2.8, pg. 50)
02:34	Under the Joint Spacing dropdown, PavementME allows for two spacing options- constant and random. GDOT only permits the use of constant joint spacing, with recommended values between 15-20 feet. For most JPCP designs, 15-ft is reccomended
02:51	The Permanent Curl/Warp Effective Temperature Difference input should be left as the default value of -10 degF for all new and rehabilitation designs
03:01	The Seleant Type input permits two available options for the transverse joint sealant-- preformed and other. Georgia currently seals joints with a silicone sealant, so selecting the "other" option is recommended
03:14	Both the Tied Shoulders and Widened Slab inputs are design based and may change depending on the project. If the shoulders are to be tied, a logitudinal joint load tranfer efficieny of 40% is recommended per the User Input Guide (Section 7.2.6, pg. 50)
03:28	Widened slabs are generally only used when reducing edge stresses from wheel loads is necessary. If this is the case, a maximum of 1-ft widening is to be used.
03:44	After adjusting all design properties, you may begin defining the Level 3 JPCP layer inputs
03:52	Navigate back to the materials window by selecting the JPCP layer at the top of the figure
03:59	The first layer property input is the Poisson's ratio. This input should not be changed as all relavent calibration factors are tied to the default Poisson's ratio value of 0.2

04:11	To determine the thickness of the concrete layer, first input a trial thickness using recommended values from the Minimum and Maximum Thicknesses Table in the User Input Guide. Then adjust the value in subsequent designs based on the performance output (Table 8.1, Section 8.1, pg. 59)
04:25	Unit weight inputs should be selected based on average values from construction records if a particular PCC mixture is to be used. Otherwise, use the default value of 150 pcf
04:38	For Level 3 designs, the PCC coefficient of thermal expansion input is recommended based on the concrete's coarse aggregate geological class. Designers must determine the coarse aggregate type, then use the highlighted table to select the appropriate input from the User Input Guide. If the coarse aggregate is unknown, use a CTE value of 5.1 (Table 8.11, Section 8.4.2, pg. 73)
05:01	The PCC heat capacity and thermal conductivity inputs are tied to the GDOT calibration factors and should remain as the default values
05:10	Under Mix Design properties the aggregate type may be determined from mixture design sheets or by locating your project location in the highlighted figure of the User Input Guide (Figure 8.3, Section 8.4.3, pg. 74)
05:25	Inputs for cement content and water cement ratio should be available from historial construction records, but if data is unavailable, use the recommended values of 660 and 0.45 respectively
05:41	For most Level 3 designs, the Cement type input should remain as Type I unless otherwise specified
05:49	Under the curing method dropdown, the choices include Wet Curing and Curing Compound. Curing compound is recommended for most GDOT PCC designs and wet curing is only to be used if the project specifically documents its use
06:04	The reversible shrinkage and time to develop 50% of ultimate strength inputs are tied to calibration factors and should be left as default values
06:14	The PCC zero-stress temperature input is calculated as a function of monthly ambient temperatures and cement content. This value may be input directly by the user, but calculation is preferred for most designs
06:28	The same is true for the ultimate shrinkage input, in which the value is calculated internally
06:35	For Level 3 designs, the strength property inputs for PCC layers are limited to the 28-day compressive strength or modulus of rupture and the elastic modulus. The median values from GDOT historical construction records are suggested. These values are 6,097 psi for compressive strength, 705 psi for MOR, and 4,500 ksi for elastic modulus
07:02	All input properties have now been discussed for a JPCP surface layer
07:08	This concludes the content discussed in this module and the steps required to develop a Level 3 JPCP design
07:15	Proceed to the next module to learn about Level 3 MEPDG Inputs and Implementation for CRCP

Module 5A- MEPDG Inputs and Implementation for CRCP

00:00	This module will cover the Level 3 Inputs and Implementation of Continuously Reinforced Concrete Pavement in AASHTOWare PavementME Design
00:08	This is the fifth and final module in the Level 3 input series for MEPDG Inputs and Implementation
00:15	As before, the GDOT User Input Guide and Train the Trainer Workshop manuals are considered necessary tools for this module
00:23	We will continue with the pavement structure process, focusing on the PCC layers of a CRCP design as shown in the highlighted figure in the User Input Guide
00:33	Once again, the first step in the design is to input the CRCP Design Properties
00:40	Open the properties by navigating to the Explorer Tab and selecting "CRCP Design Properties" from the project dropdown
00:49	Similar to the JPCP design properties, some CRCP properties may differ based on your project specifications

00:57	The first design input is surface shortwave absorptivity. As before, the default value of 0.85 should be used for all new and rehabilitation designs
01:07	The Bar Diameter input refers to the diameter of the longitudinal reinforcement and is a project-specific design value
01:15	The base/slab friction coefficient value represents the coefficient of friction at the interface of the CRCP and the supporting layer. A set of recommended design values based on the base course type is found in the highlighted table in the User Input Guide (Table 7.5, Section 7.3.1, pg. 56)
01:29	The crack spacing input is generated internally using a prediction model and should be left as the default setting
01:36	The Steel % input refers to the percent of longitudinal steel and should be determined from project-specific design criteria. Typical values for this input may range between 0.65 and 0.80
01:49	As discussed in the previous module, The Permanent curl/warp Effective Temperature Difference input should remain as the default value of negative 10 degF
01:59	Shoulder Type is an input based on project design. PavementME provides four available shoulder types: Tied PCC (separate), Tied PCC (monolithic), Asphalt, and Gravel. The User Input Guide states a roller-compacted concrete can be assumed as an asphalt shoulder since it is not tied into the PCC slab
02:18	Finally, the steel depth input is a project-specific design value. Generally, the steel is placed at mid-depth or higher in PCC slabs, but a minimum cover depth of 3.5 inches is required
02:30	After adjusting all CRCP design inputs, navigate back to the materials layer window to finish designing the pavement structure
02:39	All inputs for CRCP layers follow the same procedure as JPCP layers. If you are unfamiliar with JPCP design, please return to Module 4A where it is discussed in further detail
02:49	Therefore, only a brief review will be provided in this module
02:55	Under PCC properties, Poisson's ratio should remain as the default value of 0.2
03:01	Layer thickness is determined using a trial and error process beginning with minimum values found in the Layer Thicknesses Table in the User Input Guide
03:09	Unit Weight is selected based on average values from construction records. If unknown, a unit weight of 150 pcf is recommended
03:17	Under thermal properties, the PCC coefficient of thermal expansion is determined based on the concrete's coarse aggregate type and the associated Table in the User Input Guide
03:27	The PCC heat capacity and thermal conductivity inputs are default values that should not be changed.
03:33	Under Mix design properties, Aggregate Type is selected based on mixture design specifications or aggregate sources local to your project
03:42	Cementitious material content and water cement ratio inputs are based on historical construction records, but if data is unavailable, use standard values of 660 and 0.45 respectively
03:54	For most designs, Type I cement is used for the Cement Type and "Curing Compound" is selected for the Curing Method
04:01	The reversible shrinkage and time to develop 50% of ultimate strength inputs should remain as the default values
04:08	PCC zero-stress temperature and ultimate shrinkage values are calculated by the software and require no input
04:15	Finally, the PCC strength and modulus property is determined from 28-day compressive strength or modulus of rupture and the elastic modulus. The recommended values are 6,097 psi for compressive strength, 705 psi for MOR, and 4,200 ksi for elastic modulus
04:37	All input properties have now been discussed for a CRCP surface layer
04:42	This concludes the content discussed in this module and the steps required to develop a Level 3 CRCP design
04:48	This is the final module in the Level 3 AASHTOWare Pavement ME Design Video Series. For a continued discussion of Level 1 and Level 2 designs, proceed to the next series of training modules

Module 1B- MEPDG Calibration Factors & Baseline Files

Time	Script
00:00	This module will cover Level 1 and 2 MEPDG Calibration Factors in AASHTOWare PavementME Design
00:08	This is the first module in the Level 1 and 2 input series for MEPDG Inputs and Implementation
00:15	The GDOT User Input Guide and Software Design Manual are considered necessary tools for this module
00:23	The previous module series discussed the basic concepts and inputs for routine or Level 3 designs in Pavement ME
00:31	The topics in this series will focus on the more in-depth processes required for Level 1 and 2 designs
00:38	As mentioned in the introductory module, Level 1 and 2 designs are more accurate and effective at predicting the long-term pavement performance as they require the use of local databases or laboratory-tested values
00:49	Therefore, the focus of this series is to highlight the Level 1 and 2 inputs available in Pavement ME and the steps required to integrate them using the GDOT input library
01:00	The first topic to discuss is the GDOT Calibration Factors
01:05	All higher-level designs will require the most up-to-date Georgia-specific calibration coefficients in order to accurately predict the performance indicators
01:14	Calibration settings are specific to the design type and pavement type you are generating in the software
01:21	After defining the general information for your project, you may access the calibration settings by navigating to the Explorer Window and selecting the appropriate option under the "Project Specific Calibration Factors" dropdown
01:35	In the window on the right, you will see all the Calibration coefficients and equations necessary for your design
01:42	Here you will notice the variety of transfer function and prediction methodology inputs required to generate the pavement performance indicators
01:50	These coefficients should reflect the results from the Long-Term Pavement Performance program test sections in Georgia
01:57	A summary of the most recent Georgia calibration factors is listed in Chapter 9 of the User Input Guide (Section 9.2, pg. 98). You may refer to this section to ensure your calibration settings are up-to-date with the most recent coefficients
02:10	To streamline this process, a set of baseline project files have been pre-generated using the latest calibration factors
02:18	Baseline files were created for a variety of both new and rehabilitation pavement types. As a result, the first step for every project will require you to launch the appropriate baseline file before defining any project specific information
02:32	This is done by simply selecting the "Open" button in the Menu Bar and locating the appropriate DGPX file for your design
02:44	Once opened, navigate back to the Project Specific Calibration Factors dropdown and select the relevant calibration factors for your pavement type
02:54	If the files are properly updated, you will see the calibration settings are already congruent with the values presented in the User Input Guide
03:02	It is important to remember that calibration settings are updated continually and may change with new versions of the software. Always make sure the baseline files are generated using the same software version in which you are conducting your design. If this is not the case, some factors may be incorrectly defined and result in fatal errors for your project output
03:23	If used correctly, these baseline files will ensure every project is evaluated using the most accurate pavement performance indicators
03:32	This concludes the topics discussed in this module and the steps required for beginning a higher-level pavement design
03:39	Proceed to the next module to learn about Level 1 and 2 MEPDG Traffic Inputs

Module 2B- MEPDG Traffic Inputs

Time	Script
00:00	This module will cover Level 1 and 2 MEPDG Traffic Inputs in AASHTOWare PavementME Design
00:08	This is the second module in the Level 1 and 2 input series for MEPDG Inputs and Implementation
00:15	The GDOT User Input Guide and Software Design Manual are considered necessary tools for this module
00:23	Higher level Traffic inputs in Pavement ME Design involve the use of regional truck class volume and axle load distribution factors
00:31	For the purpose of this example, we will focus on the traffic inputs for a standard JPCP pavement design
00:38	Traffic inputs for a flexible pavement involve identical processes but do not incorporate Wheelbase or Hourly Distribution Factor inputs
00:47	To access the traffic inputs, navigate to the Explorer Tab and select "Traffic" in the Project dropdown
00:56	As discussed in previous modules, inputs in the left-hand column are project-specific and should be acquired from the Traffic Analysis Branch of the Office of Planning or the Office of Transportation Data within GDOT
01:07	The input processes for these properties will not change based on your design level. If you are unfamiliar with this process, return to the Level 3 Traffic and Climate module where the steps are fully discussed
01:19	We will begin with the Truck Volume Distribution Factors
01:24	Truck volume inputs effect the vehicle class distribution and growth rates, the monthly adjustment, and number of axles per truck
01:31	For Level 1 and 2 designs, these inputs are defined using the MEPDG Traffic Library established for GDOT
01:38	To import the appropriate data, return to the Explorer tab and right click the "Traffic" folder
01:46	Select the "Import Traffic.." feature and navigate to the folder where the truck traffic files are located
01:55	Currently, the selections include global default files, a Georgia default file with the number of Axles per Truck, and two Georgia-specific roadway files developed for the database
02:06	The seasonally independent data is recommended for freight route designs and the seasonally dependent data is recommended for non-freight route designs. These files may be used when sufficient truck volume data are unavailable
02:18	For the purpose of this example, we will select the seasonally independent file and press "Open"
02:25	You should notice all truck volume input windows have been updated with the imported values. An additional column for Hourly Adjustment inputs will be shown for rigid pavements
02:36	If truck volume is selected from the GDOT library, the Monthly Adjustment Inputs should be consistent with those values listed in the MDF Table of the User Input Guide (Table 5.4, Section 5.7, pg. 30)
02:47	The Axles Per Truck Class inputs should reflect those found in the Axles per Truck Class Table of the User Input Guide (Table 5.6, Section 5.9, pg. 31)
02:55	And for rigid pavements, the Hourly Adjustment inputs should compare to the Recommended Hourly Distribution Factors Table of the User Input Guide (Table 5.5, Section 5.8, pg. 31)
03:04	Check the inputs in each of the imported fields to ensure the values are representative of your design project. You may manually adjust each input by selecting the cell and typing a new value

03:16	All relevant truck Volume Distribution Factors have now been defined for higher level designs
03:21	Next, we will discuss the Axle Load Distribution Factors
03:26	Axle Load inputs effect the Single, Tandem, Tridem, and Quad Axle distribution factors
03:33	Once again, for Level 1 and 2 designs, these inputs are defined using the MEPDG Traffic Library established for GDOT
03:42	As before, locate the "Traffic" folder in the Explorer Tab and right click to import the data files
03:49	This time, navigate to the "Axle Load Distributions" option and select the "Import XML…" feature
03:57	Navigate to the folder where the axle load destruction files are located
04:02	Currently, selections include options for global default and Georgia specific axle load distributions for Heavy 1, Heavy 2, and Moderate categories
04:11	The NALS Database table in the User Input Guide should be used to select the most appropriate file for you project (Table 5.7, Section 5.10, pg. 32)
04:20	For the purpose of this video, we will assume an AADTT greater than 2,000, select the GDOT_H2 file, and press "Open"
04:31	To ensure the import was successful, return to the Explorer Tab, Navigate to the Traffic folder, and double click the Axle Distributions to view their input values
04:46	If necessary, you may manually adjust each input by selecting the cell and typing the new value
04:54	All higher-level properties have now been defined for the traffic inputs
04:59	This concludes the topics discussed in this module and the steps required to integrate Traffic inputs
05:06	Proceed to the next module to learn about Level 1 and 2 MEPDG Inputs and Implementation for Subgrade and Base Materials

Module 3B- MEPDG Inputs and Implementation for Subgrade and Base Materials

Time	**Script**
00:00	This module will cover Level 1 and 2 MEPDG Inputs and Implementation for Subgrade and Base Materials in AASHTOWare PavementME Design
00:08	This is the third module in the Level 1 and 2 input series for MEPDG Inputs and Implementation
00:15	The GDOT User Input Guide and Software Design Manual are considered necessary tools for this module
00:23	Higher level design inputs for subgrade and base layers are found in the material's resilient modulus, gradation, and related engineering properties inputs
00:32	The processes required for these inputs are identical across all design types and pavement types
00:39	For the purpose of this example, we will focus only on the subgrade layer of a standard flexible pavement design
00:46	The first input to discuss is the Resilient Modulus
00:51	Navigate to the subgrade or GAB material properties window and click on the resilient modulus dropdown arrow
00:58	Where previously, an approximate resilient modulus value was directly input in the highlighted cell, we will now use the Input Level dropdown to select Level 2
01:08	You may notice there is no option for Level 1 inputs. As of version 2.5 of the software, Level 1 inputs are not yet permitted for resilient modulus of soils or unbound materials, so our selection is limited to Level 2 and 3
01:23	The first notable difference between Level 2 and 3 inputs is the 3rd available analysis type
01:29	If "Modify Input Value by Temperature/Moisture" is selected, the modulus values are varied by temperature/moisture predicted by the enhanced climatic model used in the ME Design software

01:41	If "Monthly Representative Values" is selected, the modulus is varied only by the 12-indepent values input by the user
01:49	And if "Annual Representative Value" is selected, the modulus will remain as a singular value throughout the design period
01:57	For most designs, using the enhanced climatic model is recommended
02:02	The other notable difference between Level 2 and 3 inputs is the available options in the "Method" dropdown
02:09	These options include CBR, R-Value, Layer Coefficient-AI, DCP Penetration, and Based on PI and Gradation
02:20	The recommended method for your design will be based on the available data in the GDOT Materials Library
02:27	Currently, all available Level 2 resilient modulus data for subgrade soils is presented in the highlighted table of the User Input Guide (Section 8.6.2, Table 8.18, pg. 85).
02:38	A similar table is also available for GAB materials (Section 8.6.2, Table 8.17, pg. 84)
02:46	These tables present a set of typical mean modulus values, so "Resilient Modulus" will remain our input method
02:55	As before, the modulus is input by simply typing the value in the highlighted cell
03:04	The next set of inputs with Level 2 capabilities are the gradation and related engineering properties
03:10	These properties are found by clicking the dropdown arrow next to the Gradation input
03:17	If particle size distribution data is available for your material, you may improve the accuracy of the performance indicators by individually inputting the percent passing values in the table on the left
03:28	However, for most GDOT classified materials, the gradation has been pre-defined using typical values from existing records
03:36	The recommended values for GDOT classified soils are found in the highlighted table of the User Input Guide (Table 8.19, Section 8.6.2, pg. 87)
03:45	The same approach is used for the engineering properties on the right. These values may be improved by clicking the check-box and inserting project-specific data as necessary. For most Level 2 designs, using those values found in the associated property tables is recommended
04:05	All higher-level input properties have now been discussed for the subgrade and base layers
04:11	If your project is located in a county with existing Level 2 resilient modulus data, you may bypass most of these processes and simply insert the specialized subgrade or GAB material type into your pavement structure
04:27	In these cases, the Level 2 input properties have already been defined and no additional inputs are required, except for layer thickness
04:37	Alternatively, you may import the material properties to an existing subgrade or base layer using the import function
04:44	To do this, navigate to the pavement structure figure and right click on the appropriate pavement material layer
04:51	Select the "Import" feature and navigate to the folder where material XML files are located
04:59	After locating the desired material, click on the file and press "Open"
05:06	The layer properties should update with the newly defined material inputs
05:12	A final note: If higher level inputs are used for a single layer of your pavement design, you are not required to use higher level inputs for the remaining layers. For example, Level 2 inputs may be used for the subgrade layer of a design where Level 3 inputs are used elsewhere. Always consider this dynamic when trying to generate the most accurate pavement design
05:35	This concludes the topics discussed in this module and the steps required to develop Level 1 and 2 subgrade and base layers
05:43	Proceed to the next module to learn about Level 1 and 2 MEPDG Inputs and Implementation for AC Pavement

Module 4B- MEPDG Inputs and Implementation for AC Pavement

Time	Script
00:00	This module will cover Level 1 and 2 MEPDG Inputs and Implementation for AC Pavement in AASHTOWare PavementME Design
00:08	This is the fourth module in the Level 1 and 2 input series for MEPDG Inputs and Implementation
00:15	The GDOT User Input Guide and Software Design Manual are considered necessary tools for this module
00:23	Higher level design inputs for AC pavement layers are found in the asphalt mechanical property inputs
00:29	These include the asphalt binder, creep compliance, dynamic modulus, and indirect tensile strength
00:36	The processes required for these inputs are identical for all asphalt base, binder, surface, and interlayers.
00:43	For the purpose of this example, we will focus on the asphalt surface layer of a standard flexible pavement design
00:50	First, we will discuss the processes for Level 2 AC Layer Inputs
00:55	For higher level designs, it is important to begin with the dynamic modulus as the design level input for dynamic modulus is directly tied to the design level input of the asphalt binder
01:05	Navigate to the asphalt material properties window and click the dynamic modulus dropdown arrow
01:12	Use the Dynamic Modulus Input Level dropdown to select Level 2
01:17	You will notice that the required inputs are no different than that of Level 3
01:22	As a result, the Gradation of Georgia's Dense Graded Mixtures Table from the User Input Guide may be used to determine Level 2 Dynamic Modulus inputs (Table 8.6, Section 8.3.3, pg 67)
01:31	Assuming a 9.5 mm Type II surface mix is used, we will input the percent passing for the appropriate sieves
01:45	Although this input process is identical to Level 3, selecting Level 2 dynamic modulus inputs will also require the use of Level 2 Binder Grade inputs
01:54	To input the Level 2 asphalt binder, click on the input dropdown arrow
01:59	Where previously the binder grade was simply selected using a dropdown list, now the required inputs include temperature, Gstar, and phase angle values
02:09	Currently, Level 2 binder inputs are not recommended for default asphalt materials until a regional database has been established for the GDOT Library
02:18	When an established database is available, the require inputs may be inserted directly into the table
02:25	The next input to discuss is the creep compliance
02:29	To access Level 2 creep compliance inputs, click on the dropdown arrow and change the input to Level 2
02:36	Currently, the GDOT Materials Library does not contain a database at any level for creep compliance inputs
02:42	Therefore, for most designs, Level 3 inputs are recommended in which creep compliance is estimated using the available binder data
02:49	When an established database is available, Level 2 inputs will require 1/psi values at specific loading times for a single mid-range temperature. The values may be inserted directly into the table
03:03	The final Level 2 input for asphalt layers is the Indirect Tensile Strength
03:09	Indirect Tensile Strength inputs are only available for the asphalt material on the surface layer of the pavement
03:15	Like creep compliance, an established IDT database has not yet been developed for the GDOT Materials Library

03:22	As a result, Level 3 inputs are recommended for most designs where IDT strength is estimated using other volumetric and mechanical properties
03:31	In the case of future implementation, the Level 2 inputs require individual strength values at four different temperatures. The values may be inserted directly into the table
03:42	All inputs have now been defined for a Level 2 design
03:46	Next, we will discuss the processes for Level 1 AC Layer Inputs
03:51	Once again, we will start with the Dynamic Modulus
03:55	Navigate to the modulus input and click on the dropdown arrow
03:59	Use the Dynamic Modulus Input Level dropdown to select Level 1
04:04	Inputs at this level require Estar values measured at multiple temperatures and frequencies
04:09	The number of temperature and frequency levels may be changed by using the associated dropdowns
04:15	Inputs of this type may only be determined from the GDOT Materials Library. A catalog of existing Dynamic Modulus data is found in the Appendix of the User Input Guide
04:25	Here you will find Estar values at four temperatures and six frequencies for a variety of Georgia asphalt mixtures
04:32	Use the HMA Database figure and the associated table in the User Input Guide to determine if Level 1 data is available for your project
04:41	If so, the Estar values may be inserted directly into the table
04:47	With dynamic modulus defined, you may now determine the Level 1 inputs for the asphalt binder
04:53	The process for Level 1 asphalt binder inputs is identical to Level 2, where once again, the Temperature, Gstar, and phase angle are required
05:02	Using the GDOT Materials Library, all asphalt mixtures with Level 1 dynamic modulus data will also contain Level 1 binder data
05:11	Referencing the same tables in the Appendix of the User Input Guide, locate the asphalt binder test data and insert it directly into the table
05:21	In the event that Creep Compliance test data is available, Level 1 inputs may be selected using the same approach as Level 2
05:28	The only difference between the two design levels are the additional creep compliance inputs at Low and High temperatures
05:35	If applicable, the values may be inserted directly into the table
05:41	Finally, Level 1 indirect tensile strength inputs may be selected for the asphalt surface layer
05:47	If IDT test data is available, up to 7 strength measurements may be inserted at a range of temperatures
05:54	Otherwise, using the default Level 3 inputs is suggested
06:00	All higher-level inputs have now been discussed for the AC pavement layers
06:05	If your project contains one of the available mixtures in the GDOT Materials Library, you may bypass most of these processes and simply insert the specialized HMA material type into your pavement structure
06:20	In these cases, the Level 1 and 2 input properties have already been defined and no additional inputs are required, except for layer thickness
06:30	Alternatively, you may import the material properties to an existing AC pavement layer using the import function
06:37	To do this, navigate to the pavement structure figure and right click on the appropriate asphalt material layer
06:44	Select the "Import" feature and navigate to the folder where material XML files are located
06:52	After locating the desired material, click on the file and press "Open"
06:58	The layer properties should update with the newly defined material inputs
07:04	This concludes the content discussed in this module and the steps required to develop Level 1 and 2 flexible pavement layers
07:15	Proceed to the next module to learn about Level 1 and 2 MEPDG Inputs and Implementation for Concrete Pavement

Module 5B- MEPDG Inputs and Implementation for PCC Pavement

Time	Script
00:00	This module will cover Level 1 and 2 MEPDG Inputs and Implementation for Concrete Pavements in AASHTOWare PavementME Design
00:08	This is the final module in the Level 1 and 2 input series for MEPDG Inputs and Implementation
00:15	The GDOT User Input Guide and Software Design Manual are considered necessary tools for this module
00:23	Higher level design inputs for concrete pavement layers are primarily found in the strength and modulus inputs
00:29	These include the compressive strength, modulus of rupture, and modulus of elasticity
00:35	Inputs such as unit weight, CTE, cement content, and water cement ratio are also relevant, but the input process will not change based on design level
00:46	All higher-level inputs are identical for both JPCP and CRCP pavement layers
00:51	For the purpose of this example, we will focus on the JPCP layer of a standard rigid pavement design
00:58	Although a catalog of Georgia concrete mixtures has been established through recent research efforts, A design approach has not yet been developed for the concrete properties in the GDOT Materials Library
01:09	In the meantime, the existing database may be referenced in the PCC Properties Section of the Layer/Material Property Inputs Chapter of the User Input Guide (Section 8.4, pg. 70)
01:19	Here you will find all relevant Level 1 and 2 input properties for a diverse set of Georgia concrete mixtures
01:26	With that said, we will now discuss the processes for Level 2 concrete layer inputs
01:32	Navigate to the concrete material properties window and click the PCC Strength and Modulus dropdown arrow
01:39	Use the input level dropdown to select Level 2
01:44	Where previously, a single 28-day compressive strength or MOR value was satisfactory, now the required inputs include compressive strength values recorded at 7, 14, 28, and 90 days and the 20-year/28-day ratio
02:00	This data is contained in the GDOT Materials Library and may currently be accessed through the Time Dependent Compressive Strength Tables in the User Input Guide (Table 8.12, Section 8.4.4, pg. 76)
02:09	After selecting the most appropriate mixture from the collection of unique Georgia concrete mixtures, the properties may be inserted directly into the table
02:17	For the purpose of this example, we will use the values associated with Mix No. 4
02:25	With the strength properties defined, the remaining PCC inputs must be updated to reflect the selected concrete mixture
02:33	The Concrete Fresh Mixture Properties Table in the User Input Guide may be used to determine the appropriate Unit Weight (Table 8.8, Section 8.4.1, pg. 71)
02:42	The PCC coefficient of thermal expansion is listed in the CTE for Georgia Concrete Mixtures Table of the User Input Guide (Table 8.10, Section 8.4.2, pg. 73)
02:52	And finally, the Georgia Concrete Mixture Properties Table in the User Input Guide may be used for the aggregate type, cementitious material content, and water cement ratio (Table 8.7, Section 8.4, pg. 71)
03:09	All inputs have now been defined for a Level 2 design
03:14	Next, we will discuss the processes for Level 1 concrete layer inputs
03:19	Once again, open the PCC strength and modulus inputs by clicking the dropdown arrow
03:25	Use the input level dropdown to select Level 1
03:29	Inputs at this level require both the Modulus of Rupture and Elastic Modulus recorded at 7, 14, 28, and 90 days and the 20-year/28-day ratio
03:41	Modulus of rupture inputs are recorded in the GDOT Materials Library and may be located in the Time Dependent Elastic Modulus Table of the User Input Guide (Table 8.14, Section 8.4.4, pg. 76)

03:52	The same is true for elastic modulus inputs which may be found in the Time Dependent Elastic Modulus Table of the User Input Guide (Table 8.13, Section 8.4.4, pg. 76)
04:00	For the purpose of this example, we will once again select the values associated with Mix No. 4 and insert them directly into the tables
04:12	As with the Level 2 design, the remaining PCC inputs must be updated to reflect the selected concrete mixture for Level 1
04:21	This procedure is identical to that of the Level 2, as inputs are gathered from the same database
04:27	Once the properties are updated, all inputs have been defined for a Level 1 design and all higher-level inputs have been discussed for concrete pavement layers
04:36	If your project contains one of the available mixtures in the GDOT Materials Library, you may bypass most of these processes and simply insert the specialized concrete material property inputs
04:49	You may import the material properties to an existing concrete pavement layer using the import function
04:56	To do this, navigate to the pavement structure figure and right click on the appropriate concrete material layer
05:03	Select the "Import" feature and navigate to the folder where material XML files are located
05:11	After locating the desired material, click on the file and press "Open"
05:17	The layer properties should update with the newly defined material inputs
05:23	This concludes the content discussed in this module and the steps required to develop Level 1 and 2 flexible pavement layers
05:34	This is the final module in the Level 1 and 2 AASHTOWare Pavement ME Design Video Series. For a complete overview of the MEPDG pavement design process, make sure to visit each of the 5 modules discussed in this series.